

Complex Interpretation of Core and Log Data for Pore Fluid Characterisation

Thesis by Nwosu Basil Chukwuemeka

Submitted at the Institute of Geophysics, University of Leoben Austria

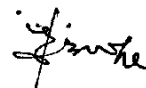
May, 2015

AFFIDAVIT

I declare in lieu of oath, that I wrote this thesis and performed the associated research myself, using only literature cited in this volume.

May, 2015

Date

A handwritten signature in black ink, appearing to read "J. Linde", written above a horizontal line.

Signature

ACKNOWLEDGEMENTS

I like to acknowledge the special help received from a number of individuals, without which this tome could not have been achieved.

Therefore I owe my thanks to:

Univ. Prof. Dr. Jürgen Schön for critically reviewing drafts of the manuscript, pointing out errors of fact or emphasis, and suggesting improvements.

Dipl.-Ing. Dr. mont. Marcellus Schreilechner for the provision of workstation, core and log data and the opportunity of an MSc thesis within Joanneum Research Leoben, Austria.

DI Johannes Amtmann for his invaluable and dedicated assistance with Interactive Petrophysics (IP) software programme. He took time off his own duties to help me.

All staff of Joanneum Research Leoben, Austria. You provided me with a conducive and friendly working environment. I have very fond memories of my time there.

Jude Ogbunugha and family - No one has ever been given more loving and unconditional support than I have been given by you. You are rare and priceless. I am very grateful.

For my parents and family who stood by me and for their great patience and support, it could not have been possible without you. I owe you plenty.

TABLE OF CONTENTS

ACKNOWLEDGEMENTS	I
TABLE OF CONTENTS.....	II
LIST OF TABLES	IV
LIST OF FIGURES.....	V
NOMENCLATURE	VII
SYMBOLS	XI
ABSTRACT.....	XII
ABSTRACT - ENGLISH	XII
ABSTRACT – GERMAN (ZUSAMMENFASSUNG)	XIII
1 INTRODUCTION.....	1
2 METHODOLOGY.....	2
2.1 METHODOLOGY CORE ANALYSIS	2
2.1.1 <i>Used Standard and Special Core Analysis Methods</i>	2
2.1.1.1 Porosity data determination.....	2
2.1.1.2 Permeability data determination.....	5
2.1.1.3 Air-brine capillary pressure data determination	8
2.1.1.4 Formation factor and resistivity index data determination.....	12
2.1.1.5 Cementation exponent (m) and saturation exponent (n) data determination.....	13
2.2 METHODOLOGY LOG ANALYSIS	14
2.2.1 <i>Compilation of measured logs and derived parameters</i>	14
2.2.1.1 Caliper log.....	14
2.2.1.2 Compensated formation density log.....	16
2.2.1.3 Neutron porosity log	18
2.2.1.4 Gamma-ray log	20
2.2.1.5 Electrical measurements with Inductionlogs (for deep reading, Rt) and Microdevices for Rxo	23
3 DATABASE	26
3.1 CORE DATABASE	26
3.2 LOG DATABASE	26
4 CORE DATA ANALYSIS	28
4.1 POROSITY-RESISTIVITY-WATER SATURATION: DERIVATION OF ARCHIE PARAMETERS	28
4.1.1 <i>Well plots</i>	29
4.1.1.1 Plots of formation resistivity factor FF versus porosity ϕ fraction on a logarithmic scale.....	29
4.1.1.2 Plots of logarithm of formation resistivity factor FF versus logarithm of porosity ϕ fraction	33
4.2 PORO-PERM CORRELATION	39
4.2.1 <i>Individual well plots</i>	39
4.2.1.1 Plot of Kair versus ϕ on a logarithmic scale	39
4.2.1.2 Plot of Kair versus S_{wi} on a logarithmic scale.....	43
4.3 DETAILED CAPILLARY PRESSURE EVALUATION COMBINED WITH PERMEABILITY	49
4.4 SUMMARY	56
5 LOG DATA ANALYSIS.....	58

5.1	PRINCIPLES	58
5.1.1	<i>Volume of shale</i>	58
5.1.2	<i>Porosity</i>	58
5.1.3	<i>Water saturation</i>	59
5.1.4	<i>Permeability</i>	59
5.2	LOG ANALYSIS USING INTERACTIVE PETROPHYSICS (IP)	59
5.2.1	<i>Volume of shale calculation</i>	59
5.2.2	<i>Porosity and water saturation calculations</i>	59
5.2.3	<i>Resistivity R_w calculations</i>	60
6	CONVENTIONAL ANALYSIS	61
6.1	POROSITY	61
6.1.1	<i>Calculation with Interactive Petrophysics (IP)</i>	61
6.1.2	<i>Comparison with core data</i>	61
6.2	WATER SATURATION.....	61
6.2.1	<i>Default parameters</i>	61
7	REPROCESSING WITH CORE DATA	62
7.1	IMPLEMENTING CORE DATA FOR REPROCESSING WATER SATURATION USING OUTPUT PARAMETER SET RB2.....	62
7.2	PERMEABILITY ESTIMATE FROM PORO-PERM REGRESSION AND COMPARISON WITH CORE DATA.....	65
8	DISCUSSION.....	66
8.1	LOG PLOTS	66
8.2	CROSSPLOTS.....	66
9	CONCLUSION	72
10	REFERENCES	73
	APPENDIXES	74
	APPENDIX A [SEE CD-ROM FOR DATABASE/LOG PLOTS REAL-SCALE]	74
	APPENDIX B [SEE ATTACHED FILE JACKET ON INSIDE BACK COVER FOR LOG PLOTS REAL- SCALE (HARD COPIES)].....	74

LIST OF TABLES

TABLE 2.1: MEAN VALUES FOR DENSITY, ELECTRON DENSITY, RATIO Z/A , AND PHOTOELECTRIC ABSORPTION INDEX PE , BAKER ATLAS DOCUMENT	18
TABLE 2.2 RADIOACTIVITY OF ROCKS - GENERAL TENDENCY.....	20
TABLE 4.1: RESISTIVITY OF SATURANT BRINE OF CORE SAMPLES OF INDIVIDUAL WELLS.....	28
TABLE 4.2: AVERAGE SATURATION EXPONENT VALUES OF DIFFERENT CORE SAMPLES FOR THE INDIVIDUAL WELLS.....	29
TABLE 4.3: ARCHIE PARAMETERS OF THE INDIVIDUAL AND COMPOSITE WELLS (FIGURES 4.1 – 4.12).....	38
TABLE 4.4: PETROPHYSICAL PARAMETERS OF THE INDIVIDUAL AND COMPOSITE WELLS (FIGURES 4.13 – 4.23)	48
TABLE 4.5: COMPARISON OF SPLIT WELLS.....	52
TABLE 4.6: WELL B5-NC-74A.....	53
TABLE 4.7: WELL B6-NC-74A.....	54
TABLE 4.8: WELL B8-NC-74A.....	55
TABLE 7.1: AVERAGED ARCHIE PARAMETER SET OF INDIVIDUAL WELLS	62

LIST OF FIGURES

FIGURE 2.1: AUTOPORE IV 9520 MERCURY INJECTION POROSIMETER [PETERS, 2012]	4
FIGURE 2.2: HASSLER-SLEEVE CORE HOLDER USED FOR FLUID FLOW EXPERIMENTS (FRACTIONS OF OIL AND WATER FLOWING, ABSOLUTE PERMEABILITY, AND RELATIVE PERMEABILITY [TIAB ET AL., 2004]	5
FIGURE 2.3: RUSKA GAS PERMEAMETER [TIAB ET AL, 2004]	6
FIGURE 2.4: POROUS DIAPHRAGM CAPILLARY PRESSURE DEVICE [TIAB ET AL., 2004].....	9
FIGURE 2.5: TYPICAL METHOD FOR PLOTTING CAPILLARY-PRESSURE VERSUS SATURATION FOR A WATER-WET SYSTEM [TIAB ET AL., 2004].....	10
FIGURE 2.6: CAPILLARY-PRESSURE CELL FOR MERCURY INJECTION [AMYX ET AL., 1960]	10
FIGURE 2.7: POSITIONS OF CORE AND GRADUATED TUBE IN A CENTRIFUGE FOR MEASUREMENT OF OIL-DISPLACING-WATER CAPILLARY PRESSURE CURVE [PETERS, 2012].....	11
FIGURE 2.8: POSITIONS OF CORE AND GRADUATED TUBE IN A CENTRIFUGE FOR MEASUREMENT OF WATER-DISPLACING-OIL CAPILLARY PRESSURE CURVE [PETERS, 2012]	11
FIGURE 2.9: CORE SAMPLE RESISTIVITY CELL [AMYX ET AL., 1960].....	12
FIGURE 2.10: SCHEMA EXPLAINING THE MEASUREMENT OF THE BOREHOLE DIAMETER. THE CURSOR OF A POTENTIOMETER IS LINKED TO THE ARM OF THE TOOL [SERRA, 2008].....	15
FIGURE 2.11: FOUR-ARM CALIPER LOGGING TOOL [HTTPS://WWW.GOOGLE.AT/SEARCH FEBRUARY, 2015].....	15
FIGURE 2.12: SCHEMATIC REPRESENTATION OF CALIPER LOG IN DIFFERENT FORMATIONS [SCHÖN, J. BOREHOLE GEOPHYSICS STUDY MATERIAL MONTANUNIVERSITÄT, LEOBEN (UNPUBLISHED)]	16
FIGURE 2.13: FORMATION DENSITY TOOL [ELLIS ET AL, 2007]	17
FIGURE 2.14: SCHEMATIC OF A GENERIC NEUTRON LOGGING TOOL [ELLIS ET AL, 2007]	19
FIGURE 2.15: GAMMA MEASUREMENTS - PRINCIPLES [SCHÖN, J. BOREHOLE GEOPHYSICS STUDY MATERIAL MONTANUNIVERSITÄT, LEOBEN (UNPUBLISHED)].....	21
FIGURE 2.16: GAMMA RAY RESPONSE FOR EVALUATING <i>IGR</i> [SCHÖN, J. BOREHOLE GEOPHYSICS STUDY MATERIAL MONTANUNIVERSITÄT, LEOBEN (UNPUBLISHED)].....	22
FIGURE 2.17: CHART FOR CORRECTING THE GAMMA RAY INDEX <i>IRA</i> TO THE SHALE VOLUME <i>V_{shale}</i> [SCHÖN, J. PETROPHYSICS OF RESERVOIR ROCKS STUDY MATERIAL MONTANUNIVERSITÄT, LEOBEN (UNPUBLISHED)]	23
FIGURE 2.18: INDUCTION TOOL PRINCIPLE [ELLIS ET AL, 2007].....	24
FIGURE 2.19: SCHLUMBERGER, 2000, LOG INTERPRETATION CHARTS. SCHLUMBERGER ED.SERV.	25
FIGURE 4.1: <i>FF</i> VERSUS ϕ FOR WELL B2-NC-74A.....	30
FIGURE 4.2: <i>FF</i> VERSUS ϕ FOR WELL B5-NC-74A	31
FIGURE 4.3: <i>FF</i> VERSUS ϕ FOR WELL B6-NC-74A.....	31
FIGURE 4.4: <i>FF</i> VERSUS ϕ FOR WELL B8-NC-74A	32
FIGURE 4.5: <i>FF</i> VERSUS ϕ FOR WELL B8-NC-74A (DATA POINT 0.106, 147 ABSENT).....	33
FIGURE 4.6: LOG <i>FF</i> VERSUS LOG ϕ FOR WELL B2-NC-74A	34
FIGURE 4.7: LOG <i>FF</i> VERSUS LOG ϕ FOR WELL B5-NC-74A.....	34
FIGURE 4.8: LOG <i>FF</i> VERSUS LOG ϕ FOR WELL B6-NC-74A.....	35
FIGURE 4.9: LOG <i>FF</i> VERSUS LOG ϕ FOR WELL B8-NC-74.....	36
FIGURE 4.10: LOG <i>FF</i> VERSUS LOG ϕ FOR WELL B8-NC-74A (DATA POINT -0.9747, 2.167 ABSENT).....	36
FIGURE 4.11: <i>FF</i> VERSUS ϕ FOR ALL WELLS	37
FIGURE 4.12: LOG <i>FF</i> VERSUS ϕ FOR COMBINED WELLS.....	38
FIGURE 4.13: <i>Kair</i> VERSUS ϕ FOR WELL B2-NC-74A	40
FIGURE 4.14: <i>Kair</i> VERSUS ϕ FOR WELL B5-NC-74A.....	41
FIGURE 4.15: <i>Kair</i> VERSUS ϕ FOR WELL B6-NC-74A.....	41
FIGURE 4.16: <i>Kair</i> VERSUS ϕ FOR WELL B8-NC-74A.....	42
FIGURE 4.17: <i>Kair</i> VERSUS ϕ FOR WELL B8-NC-74A (SPLIT PLOT)	43
FIGURE 4.18: <i>Kair</i> VERSUS <i>Swi</i> FOR WELL B2-NC-74A.....	44
FIGURE 4.19: <i>Kair</i> VERSUS <i>Swi</i> FOR WELL B5-NC-74A.....	45

FIGURE 4.20: <i>K_{air}</i> VERSUS <i>S_{wi}</i> FOR WELL B6-NC-74A.....	45
FIGURE 4.21: <i>K_{air}</i> VERSUS <i>S_{wi}</i> FOR WELL B8-NC-74A	46
FIGURE 4.22: <i>K_{air}</i> VERSUS ϕ FOR ALL WELLS	47
FIGURE 4.23: <i>K_{air}</i> VERSUS <i>S_{wi}</i> FOR ALL WELLS	47
FIGURE 4.24: A SCHEMATIC REPRESENTATION OF THE RELATIONSHIP BETWEEN A CAPILLARY PRESSURE CURVE AND OIL ACCUMULATION [HOLMES, 2002]	49
FIGURE 4.25: CAPILLARY PRESSURE CURVE FOR WELL B2-NC-74A	50
FIGURE 4.26: CAPILLARY PRESSURE CURVE FOR WELL B2-NC-74A(1) HOMOGENEOUS	51
FIGURE 4.27: CAPILLARY PRESSURE CURVE FOR WELL B2-NC-74A(2) HETEROGENEOUS	51
FIGURE 4.28: CAPILLARY PRESSURE CURVE FOR WELL B5-NC-74A	53
FIGURE 4.29: CAPILLARY PRESSURE CURVE FOR WELL B6-NC-74A	54
FIGURE 4.30: CAPILLARY PRESSURE CURVE FOR WELL B8-NC-74A	55
FIGURE 7.1: LOG PLOT FOR WELL B2-NC-74A (IMAGE PLOT NOT TO SCALE).....	63
FIGURE 7.2: LOG PLOT FOR WELL B5-NC-74A (IMAGE PLOT NOT TO SCALE).....	63
FIGURE 7.3: LOG PLOT FOR WELL B6-NC-74A (IMAGE PLOT NOT TO SCALE).....	64
FIGURE 7.4: LOG PLOT FOR WELL B8-NC-74A (IMAGE PLOT NOT TO SCALE).....	65
FIGURE 8.1: (BVO2-BVO1) - RB1:PHIE - CROSSPLOT FOR WELL B2-NC-74A	68
FIGURE 8.2: (BVO2-BVO1) - RB1: PHIE – CROSSPLOT FOR WELL B5-NC-74A.....	69
FIGURE 8.3: (BVO2-BVO1) - RB1: PHIE - CROSSPLOT FOR WELL B6-NC-74A	70
FIGURE 8.4: (BVO2-BVO1) - RB1: PHIE - CROSSPLOT FOR WELL B8-NC-74A	71

NOMENCLATURE

RCAL	Routine Core Analysis
SCAL	Special Core Analysis
DEPT	Depth
VCL	Volume of clay
DD	Bit size
SPI-CPX	Secondary porosity indicator
SWP-CPX	Formation water saturation
PHIE-CPX	Effective porosity
K_{air}	Permeability to air
S	Fluid saturation
FF	Formation resistivity factor
P_c	Capillary pressure
V_b	Bulk volume
V_g	Grain volume
V_p	Pore volume
M_{dry}	Mass of dry core sample in air
M_{sat}	Mass of saturated core sample
M_l	Mass of core sample immersed in fluid
P_1	Inlet pressure
P_2	Outlet pressure
V	Volume of fluid through core sample
Q	Volume rate of flow through core sample
t	Time of passage of fluid through core sample
K	Permeability
A	Cross-sectional area of core sample

L	Length of core sample
Q_{av}	Average flow rate
P_{av}	Average pressure
Q_1	Entrance gas flow rate
Q_2	Exit gas flow rate
P_{ct}	Threshold capillary pressure
S_{or}	Residual oil saturation
S_{wor}	Residual oil and water saturation
R_o	Resistivity of a fully water saturated rock
R_w	Resistivity of the water in the rock
I	Resistivity index
R_t	Resistivity of a partially water saturated rock
RES	Resistance of core sample
R	Resistivity of core sample
S_w	Water saturation
R_{xo}	Flushed zone resistivity
ρ_b	Formation bulk density
ρ_e	Electron density
ρ_{ma}	Matrix density
ρ_{fl}	Fluid density
ρ_l	Density of saturating fluid
V_{shale}	Volume of shale
API	American Petroleum Institute
I_{GR}	Gamma ray index
GR	Gamma ray reading
GR_{cn}	Gamma ray minimum
GR_{sh}	Gamma ray maximum

R_{mc}	Mudcake resistivity
R^2	Correlation coefficient
a	Grain size coefficient
b	Cementation-compaction coefficient
S_{wi}	Irreducible water saturation
$n ; b$	Saturation exponent
a	Archie's parameter
m	Cementation exponent
P_{ce}	Pore entry capillary pressure
SN	Sample number
ASCII	American Standard Code for Information Interchange
VCL_{min}	Clay volume minimum
VCLAV	Average clay volume
VCLGR	Gamma ray clay volume
PHI	Porosity
RB1	Result-Basil 1
RB2	Result-Basil 2
S_w1	Water saturation RB1
S_w2	Water saturation RB2
IP	Interactive Petrophysics
NMR	Nuclear Magnetic Resonance
CAL	Caliper
KLOG	Permeability log
BVO1	RB1: Bulk Volume Oil
BVO2	RB2: Bulk Volume Oil
BVO2-BVO1	Difference in Bulk Volume Oil RB1 & RB2
BVW1	RB1: Bulk Volume Water

BVW2	RB2: Bulk Volume Water
PHIE	Effective porosity
SW1-SW2	Difference in water saturation RB1 & RB2

SYMBOLS

μ	Fluid viscosity
ΔP	Pressure gradient across core sample
Z	Atomic number
A	Molecular weight of compound
ϕ_D	Density derived porosity
$\phi_{N,fluid}$	Neutron response of fluid
$\phi_{N,shale}$	Neutron response of shale
ϕ_N	Neutron porosity
$\phi_{N,matrix}$	Neutron response of matrix
ϕ_{core}	Core porosity
ϕ	Porosity

ABSTRACT

Abstract - English

This study presents interpretation results of core and log data measurements of four wells (B2-NC-74A, B5-NC-74A, B6-NC-74A and B8-NC-74A) situated in Sirte Basin of Libya. Measured data were analysed for log calculated water saturation essential for proper evaluation of oil volumes. It illustrates the effect of true core derived exact formation properties, such as saturation exponent(n), cementation exponent(m), and Archie parameter (a) on water saturations and reservoir bulk volumes calculated from default parameters and formation log data. An initial conventional analysis using Interactive Petrophysics (IP) software programme for saturation with default values “ a ”, “ m ” and “ n ” of 1, 2 and 2 presented standard water saturation and bulk volume oil results. Working data is later reprocessed with true formation average “ a ”, “ m ” and “ n ” values from core data measurements for comparative analysis.

Following reprocessing and complex interpretation of working data, result interpretation demonstrates that proper and accurate evaluation of initial water saturation is significantly influenced and controlled by deviation of formation values “ a ”, “ m ” and “ n ” from the standard assumed default values of 1, 2 and 2. Average “ a ”, “ m ” and “ n ” values of core data provided water saturation and oil volume results that differed from those of default parameter set. Oil volume calculations showed strong relationships with saturations as demonstrated by applicable crossplots. Wells with decreased “ n ” values showed increase in oil volumes while wells with higher “ n ” values had much water and less oil in them.

Abstract – German (Zusammenfassung)

Die Studie beinhaltet Ergebnisse aus Kern und Log Daten von vier Bohrungen ((B2-NC-74A, B5-NC-74A, B6-NC-74A und B8-NC-74A) aus dem Sirte Becken (Libyen). Die Studie behandelt insbesondere den Einfluss von Formationsparametern (Sättigungsexponent (n), Zementationsexponent (m) und Archie Parameter (a)) auf die Wassersättigung und auf das Ölvolumen in der Lagerstätte. Hierfür wurden zuerst Literaturwerte (a=1; m=2; n=3) für diese Formationsparameter eingesetzt und als weiterer Schritt wurden die Parameter durch die Ergebnisse aus der detaillierten Kernanalyse ersetzt.

Eine mehrmalige Loganalyse beziehungsweise eine Interpretation einer bestehenden Analyse kommt zum Ergebnis, dass diese Parameter einen signifikanten Einfluss auf die Wassersättigung und schließlich auf das Ölvolumen in der Lagerstätte haben. Bohrungen mit niedrigerem “n” Werten zeigen höhere reale Ölvolumen während Bohrungen mit höherem “n” Werten viel geringere Ölvorkommen zeigen.

1 INTRODUCTION

Coring and logging program is brought into play early in the field development stage. Core and log data analysis are special techniques in petrophysics used for reservoir and fluid characterisation. Their interpretation and use are very fundamental in the determination of initial fluid saturations and in-place hydrocarbon reserves and their most efficient recovery. Improper saturation determinations may result in under or over estimation of hydrocarbons in-place and a bypassing of potentially productive pay zones/significant loss in reserves.

This work involved Routine Core Analysis (RCAL) and Special Core Analysis (SCAL) on four major wells namely B2-NC-74A; B5-NC-74A; B6-NC-74A; and B8-NC-74A. Time is a major factor that differentiates RCAL from SCAL. While the former is completed within hours after core recovery, the later could span six to eight weeks because of the slow rate of investigation. Routine Core Analysis data implemented in this work include porosity, permeability and fluid saturation data. Special Core Analysis is more sophisticated and uses specialized equipment. SCAL measurements yielded critical petrophysical parameters such as capillary pressure, water-oil relative permeability, formation factor, cementation exponent and saturation exponent. Implemented log data from the above four wells include depth (DEPT), volume of clay (VCL), bit size (DD), secondary porosity indicator (SPI-CPX), formation water saturation (SWP-CPX), effective porosity (PHIE-CPX) and product (PHIE * SW).

Following conventional analysis using Interactive Petrophysics (IP) software programme, core data was used for the reprocessing of log saturations and bulk volumes estimations to enable optimum evaluation of initial hydrocarbons in-place. Results show dissimilarity. Find in this report the causative reasons and how they were clearly isolated to be responsible.

2 METHODOLOGY

2.1 Methodology Core Analysis

2.1.1 Used Standard and Special Core Analysis Methods

Standard and special core analysis methods are used to quantitatively describe important parameters of the petroleum reservoir rock. Some of the important petrophysical parameters used in this work include porosity(ϕ), permeability to air(K_{air}), fluid saturation(S), formation resistivity factor(FF), capillary pressure(P_c), cementation exponent(m) and saturation exponent(n). The following describes in detail how these fundamental properties of petroleum reservoir rocks can be determined.

All used data are from measurements of an external laboratory (CORE LABORATORIES UK LTD). Therefore the description of methods is more general.

2.1.1.1 Porosity data determination

Porosity is one of the most important reservoir rock properties which provide a measure of the space available for storage of petroleum hydrocarbons. It is the ratio of the void space in a rock multiplied by 100 to express it in percent (Amyx, J.W., et al 1960). Porosity can be **absolute** or **effective**. Absolute porosity is summation of all the pore space (connected and isolated) in the rock. Effective porosity is the summation of all the interconnected pore spaces involved in fluid transmission through the rock and it is numerically equal or less than the absolute porosity. The effective porosity is exclusive of the pores containing irreducible fluid saturations since they are not involved in the flow process. From petrophysics standpoint, effective porosity is the quantitative value desired, as this represents the space which is occupied by mobile fluids. For direct quantitative measurement of porosity, reliance must be placed on formation samples obtained by coring.

Equipment and procedures

We require three basic parameters in order to determine porosity. They are bulk volume(V_b), rock matrix, or solids volume(V_{grain}) and pore volume(V_p). During the laboratory measurement of porosity, only two out of the three basic parameters are required. They are the bulk volume and grain volume. Laboratory measurements are usually performed on extracted cores, which have been cleaned and dried.

Bulk volume

Bulk volume can be determined by:

- i. Caliper
- ii. Fluid displacement

Caliper method will require well machined samples with easily measured dimensions from which the bulk volume is easily calculated.

Fluid displacement is of two types. One requires fluids (e.g. mercury) that cannot penetrate the pore spaces at atmospheric pressure. Mercury has poor tendency to permeate the pore spaces of intergranular materials due to its wetting and surface tension characteristics. A pycnometer measures the volume of the displaced mercury which is equal to the volume of the bulk sample. The other requires fluids (e.g. brine, kerosene or toluene) that do penetrate the pore spaces. In the second fluid displacement method, the sample is weighed in air, evacuated, and then saturated with the liquid. Weight of the saturated sample is measured in air and also when fully immersed in the saturating liquid. The volume equivalent of the lost weight (Archimedes principle) is equal to the bulk volume of the sample.

Grain volume

The grain volume can be determined by fluid displacement and gas expansion using Boyle's law porosimeter. The loss in weight of the dry sample and the sample fully immersed in a liquid is proportional to the grain volume.

Pore volume

Pore volume can be determined by (1) fluid saturation and (2) mercury injection. The difference in the weight of the saturated sample and the dry sample is proportional to the pore volume. In mercury injection, mercury at a relatively high pressure is forced into the pores of an evacuated sample using a mercury porosimeter (**FIGURE 2.1**). The injected mercury volume is equal to the connected pore volume of the sample. This method is destructive because the sample is no longer suitable for other measurements after the test.



FIGURE 2.1: Autopore IV 9520 mercury injection porosimeter [Peters, 2012]

The results of core analysis are used to calibrate well logs. Application of routine core analysis on consolidated samples is generally expected to yield values of true fractional porosity plus or minus 0.005.

The following steps are applied in the calculation of core porosity:

1. Mass of dry core sample in air = M_{dry}
2. Mass of saturated core sample = M_{sat}
3. Mass of sample immersed in fluid = M_l
4. Density of saturating fluid = ρ_l
5. Pore volume (V_p) = $\frac{(M_{sat} - M_{dry})}{\rho_l}$
6. Bulk volume (V_b) = $\frac{(M_{sat} - M_l)}{\rho_l}$
7. Porosity (ϕ) = $\frac{V_p}{V_b}$

Remarks about porosity and specific conditions of its determination

Vugular materials like carbonates have less than true values when porosity methods are applied because of the effect of vugs, solution cavities, etc.

2.1.1.2 Permeability data determination

The rock's ability to conduct fluids is termed as permeability (Tiab et al, 2004, p.100). It is the inverse of the resistance to flow. We therefore determine the permeability of a sample by measuring the rate at which a liquid will flow through a porous medium of specific dimensions with a given pressure gradient across the length of the porous medium. Non-reactive liquid or gas is used for absolute permeability measurements.

Equipment and procedures

Using a non- reactive liquid

- Cores are cleaned and dried in oven at a given temperature.
- Dried cores are evacuated in a vacuum chamber to remove air.
- Cores are then inserted into a core holder with an air pressure source.
- Record the inlet and outlet pressures, P_1 and P_2 respectively, volume of fluid passed through the cores (V), and the time of passage through the cores (t).

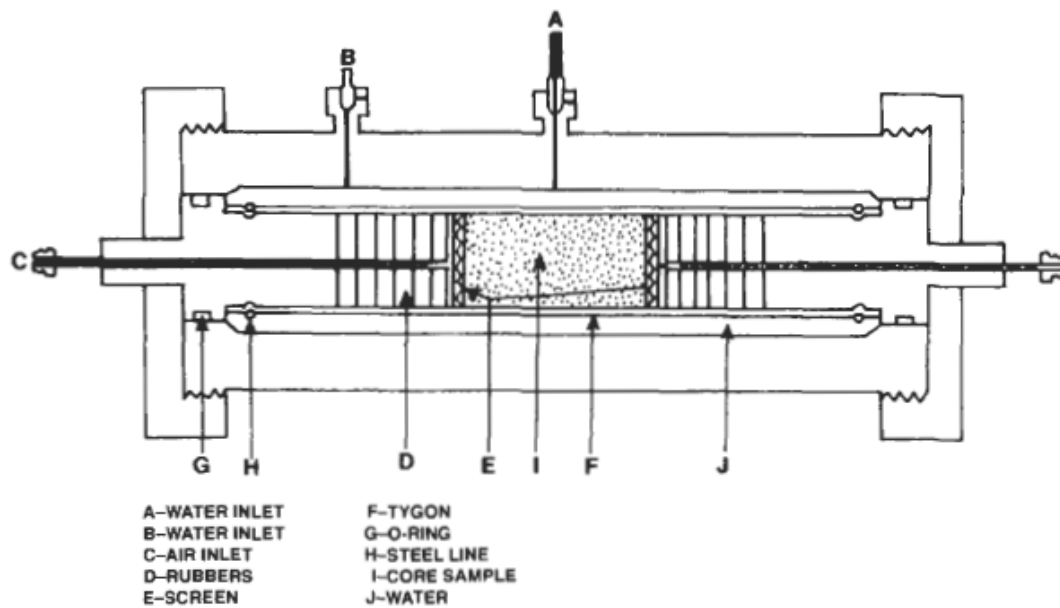


FIGURE 2.2: Hassler-sleeve core holder used for fluid flow experiments (fractions of oil and water flowing, absolute permeability, and relative permeability [Tiab et al., 2004])

The absolute permeability is then calculated as follows:

$$Q(\text{cm}^3/\text{s}) = \frac{K(\text{darcy}) * A(\text{cm}^2)}{\mu(\text{cP})} * \frac{\Delta P(\text{atm})}{L(\text{cm})} \quad (2.1)$$

$$K = \frac{\mu * V * L}{A * \Delta p * t} \quad (2.2)$$

where:

Q : volume rate of flow, cm^3/s ,

K : permeability of the medium, darcies,

A : average cross-sectional area perpendicular to the lines of flow, cm^2 ,

V : volume of fluid, cm^3 ,

t : time required for passage of $V cm^3$ of fluid, seconds,

μ : viscosity of the fluid, cP , at the observed temperature,

ΔP : pressure gradient across the cores ($P_1 - P_2$), atm ,

L : core sample length, cm .

Generally, permeability is expressed in millidarcies (mD). This is because darcy is a fairly large unit and mD is more convenient to use.

1 darcy is expressed as micrometers squared (μm^2) in SI units.

$$\text{Darcy} = 0.987 \times 10^{-8} cm^2 = 0.987 \mu m^2$$

Using a gas

Gas as a test fluid is more convenient to determine the permeability of a core sample. To account for gas expansion, only the average flow rate (Q_{av}) and average pressure (P_{av}) values are considered.

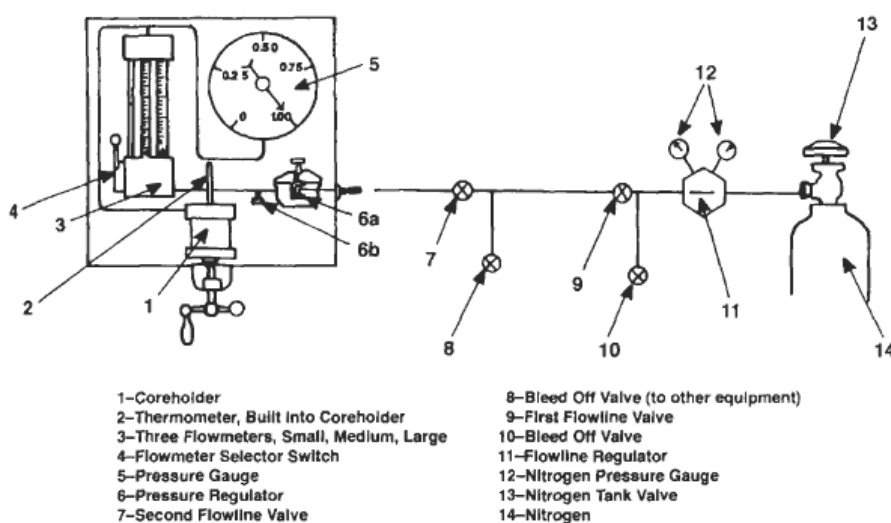


FIGURE 2.3: Ruska gas permeameter [Tiab et al, 2004]

where:

Q_1 : entrance gas flow rate (cm^3/s),

Q_2 : exit gas flow rate (cm^3/s),

$Q_1 < Q_2$; Reason is expansion of gas.

P_1 : inlet pressure,

P_2 : outlet pressure,

$P_1 \times Q_1 = P_2 \times Q_2 = P_{av} \times Q_{av}$

$$P_{av} = \frac{(P_1 + P_2)}{2}$$

$$Q_{av} = \frac{(P_2 \times Q_2)}{P_{av}}$$

t : time required to collect a specific volume of gas at the exit, seconds,

μ : viscosity of the gas (cP),

L : length of core sample (cm).

Permeability is therefore determined as follows:

$$K \text{ (Darcy)} = \frac{Q_{av} \mu L}{A(P_2 - P_1)} \quad (2.3)$$

Remarks about permeability and specific conditions of its determination

- Mobile phase must be non-reactive fluid.
- If gas is used as the measuring fluid, corrections must be made for gas slippage-Klinkenberg effect.
- Corrections must be applied for change in permeability due to reduction in confining pressure of the sample at the surface.
- Conductivity of samples with natural planes of weakness should be excluded in the laboratory data.
- When using liquids for example water to evaluate permeability, the salinity of the water must correspond to that of the formation water.
- Samples that differed in forward and reverse oil permeability are indicative of mobile fines and as such should not be prescribed for further analysis.

2.1.1.3 *Air-brine capillary pressure data determination*

Capillary pressure is the difference in pressure between two immiscible fluids across a curved interface at equilibrium. Hydrocarbon reservoirs are initially saturated with water but later displaced by migrating hydrocarbons. This process is repeated in the laboratory by displacing water from a core with a gas or oil. The pressure required for the equilibrium displacement of the wetting phase (water) with the non-wetting gas or oil is the water drainage capillary pressure, which is recorded as a function of the water saturation.

Some of the methods of measuring capillary pressure on small core samples include:

- i. Porous diaphragm (Displacement cell).
- ii. Mercury injection.
- iii. Centrifuge Method.

Porous diaphragm

The essential requirement of the diaphragm method is a permeable membrane i.e. a porous disk. Various materials like fritted glass, porcelain, cellophane, etc. can be used successfully as diaphragms. The porous disk has finer pores than does the rock sample (the permeability of the disk should be at least 10 times lower than the permeability of the core). A core is cleaned, dried, evacuated and pressure saturated with simulated formation brine and synthesized according to information provided for use in the analysis to stabilize the clay minerals which tend to swell and dislodge when in contact with fresh water. The saturated core is then placed on a porous disk, which is also saturated with water (**FIGURE 2.4**). The pore sizes of the porous disk should be small enough to prevent penetration of the displacing fluid until the water saturation in the core has reached its irreducible value.

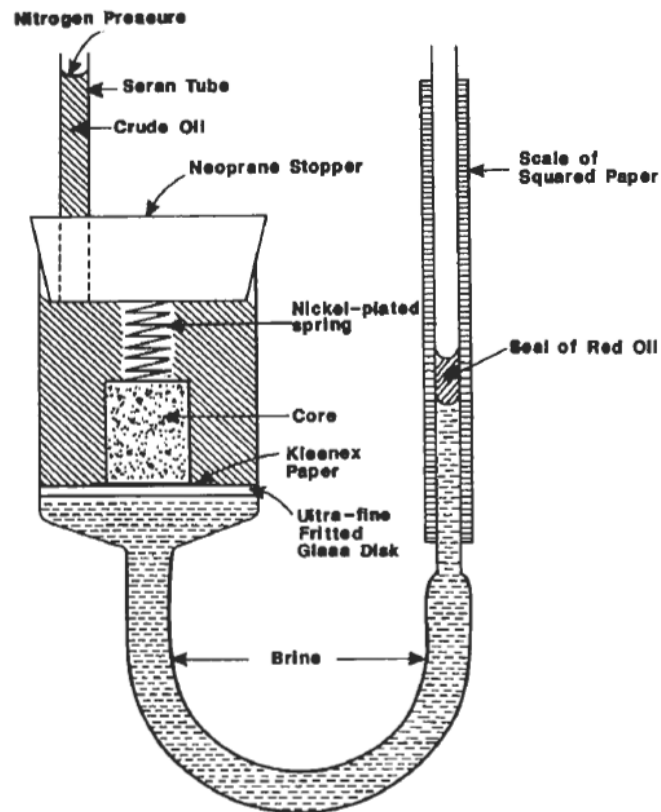


FIGURE 2.4: Porous diaphragm capillary pressure device [Tiab et al., 2004]

The pressure of the displacing fluid is increased in a stepwise fashion and by small increments. After each increase of pressure, the amount of water displaced is monitored until it reaches static equilibrium. The capillary pressure is plotted as a function of water saturation (**FIGURE 2.5**). P_{ct} is the threshold pressure if the pore surfaces are preferentially wet by water. If the analysis is reversed by placing the core on another porous disk which is saturated with oil and the core is covered with water, for a core preferentially wet by water, water will imbibe into the core and displace the oil toward residual oil saturation ($S_{or} = 1 - S_{wor}$), following the path of curve 2. Diaphragm method is time consuming and can vary from 10 to 40 days for a single sample owing to the vanishing pressure differentials causing flow as the core approaches equilibrium at each imposed pressure.

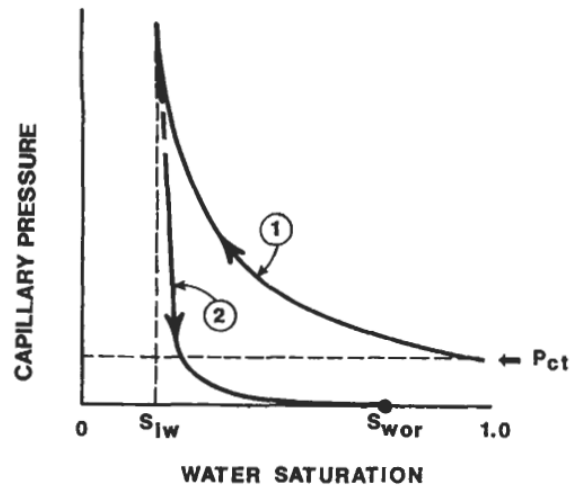


FIGURE 2.5: Typical method for plotting capillary-pressure versus saturation for a water-wet system [Tiab et al., 2004]

Mercury Injection

This method uses a mercury capillary-pressure apparatus designed to accelerate the determination of the capillary-pressure-saturations relationship (**FIGURE 2.6**).

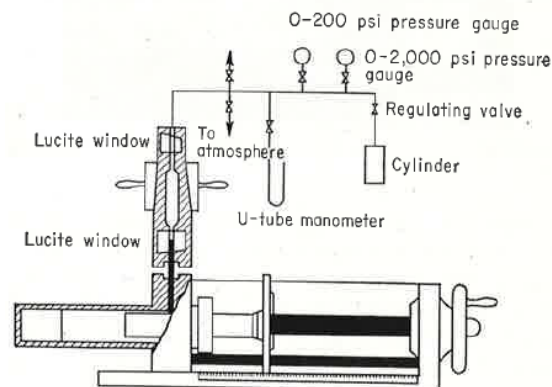


FIGURE 2.6: Capillary-pressure cell for mercury injection [Amyx et al., 1960]

Mercury is non-wetting and the volume of mercury injected in the evacuated core sample at each pressure determines the non-wetting phase saturation. The process is stopped after the core sample is filled with mercury or pressure reaches some predetermined value. The mercury injection method is faster and only in few minutes and large pressure range can be applied. Unfortunately core sample is lost permanently and there is a difference in mercury wetting properties.

Centrifuge method

In this method, the sample is saturated with a wetting fluid and is placed in a centrifuge cup containing the nonwetting fluid as shown in **FIGURES 2.7** and **2.8**. The sample is rotated at a series of constant angular velocities and the amount of wetting fluid displaced at each velocity is measured with the aid of a stroboscopic light. The only data measured directly in this method are the volume of wetting fluid displaced and the corresponding rotational speed of the centrifuge. These data can be used to derive the capillary pressure versus saturation relationship of the porous medium.

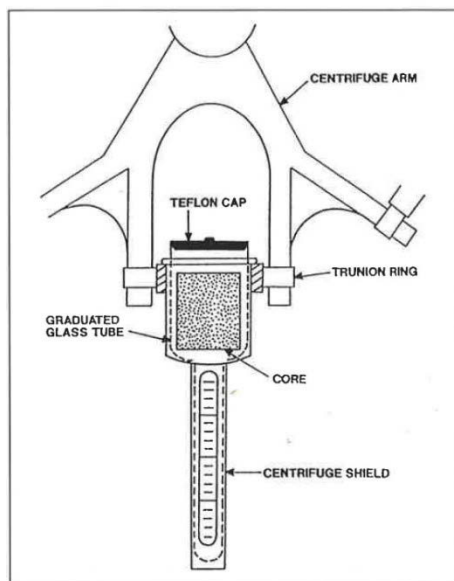


FIGURE 2.7: Positions of core and graduated tube in a centrifuge for measurement of oil-displacing-water capillary pressure curve [Peters, 2012]

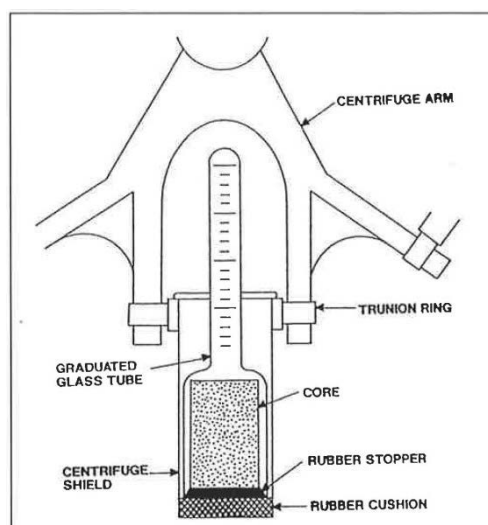


FIGURE 2.8: Positions of core and graduated tube in a centrifuge for measurement of water-displacing-oil capillary pressure curve [Peters, 2012]

Remarks about capillary pressure and specific conditions of its determination

- Ensure core sample is saturated with simulated brine to avoid the possibility of clay swelling.
- In the case of the diaphragm method capillary pressure is only correct when the volume of water displaced is said to be at equilibrium.

2.1.1.4 Formation factor and resistivity index data determination

Formation factor is the most fundamental factor in considering the electrical properties of porous rocks.

$$FF = \frac{R_o}{R_w} \quad (\text{Archie}) \quad (2.4)$$

R_o : Resistivity of a fully water-saturated rock,

R_w : Resistivity of the water in the rock.

The second fundamental factor of electrical properties of porous rocks is that of the resistivity index I :

$$I = \frac{R_t}{R_o} \quad (2.5)$$

R_t : Resistivity of a partially water-saturated rock,

R_o : Resistivity of a fully water-saturated rock.

Equipment and procedures

Core sample resistivity cell device is required (**FIGURE 2.9**).

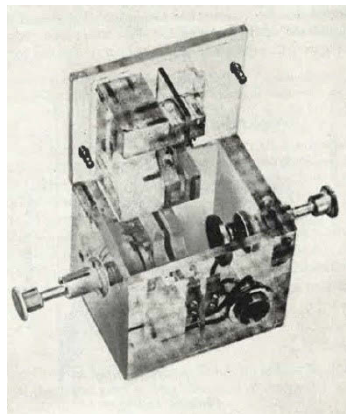


FIGURE 2.9: Core sample resistivity cell [Amyx et al., 1960]

A sample cut to a suitable size is clamped between electrodes in the cell. Current I is then flown through the sample, and the potential difference U is measured. Using Ohm's law, the resistance of the sample is computed as follows:

$$RES = \frac{U}{I} \quad (2.6)$$

and R (the resistivity) is computed from

$$R = RES \cdot \frac{A}{L} \quad (2.7)$$

where:

A : cross-sectional area of the sample,

L : Length of the sample.

Remarks about formation factor, resistivity index and specific conditions of its determination

- Reliable electrical resistivity of the fully saturated samples and saturant brine can only be obtained when ionic equilibrium within the core samples is achieved and stabilized.
- No Resistivity Index data is available for samples that failed to desaturate at maximum pressure.

2.1.1.5 Cementation exponent (m) and saturation exponent (n) data determination

The cementation exponent (m) is determined from a graphical plot of formation resistivity factor (FF) against porosity (ϕ) based on the petrophysical relationship $FF = \frac{1}{\phi^m}$. Similarly the saturation exponent (n) is determined from a graphical plot of formation resistivity index against brine saturation fraction based on the petrophysical relationship:

$$\frac{R_t}{R_o} = \frac{1}{S_w^n} \quad (2.8)$$

where:

R_t : resistivity of the rock filled with water and hydrocarbon (ohm-m),

R_o : resistivity of the rock filled with water (ohm-m),

S_w : water saturation (fractional),

n : saturation exponent.

Remarks about cementation and saturation exponents, and specific conditions of its determination

- Since cementation exponent (m) depends on formation resistivity factor (FF) and porosity (ϕ), care should be taken in their measurements. Similarly, the same measures should be applied during the measurement of resistivity R and water saturation values (S_w) as saturation exponent (n) also depends on them.

2.2 METHODOLOGY LOG ANALYSIS

2.2.1 Compilation of measured logs and derived parameters

Well logging is used in the derivation of important reservoir and wellbore parameters useful for pore fluid characterisation. Different log types measure various properties in the wellbore and surrounding formations. During this investigation, logging data was used to determine parameters such as porosity, volume of clay, water saturation, hole-size, and depth. Here is a list of log types used in the determination of these parameters:

- Caliper log.
- Compensated formation density log.
- Neutron porosity log.
- Gamma ray log.
- Electrical measurements with Laterologs and Inductionlogs (for deep reading, R_t) and microdevices for R_{xo} .

2.2.1.1 Caliper log

The size of a borehole is determined by the outside diameter of the drill bit. A uniform borehole size is necessary for reliable measurements downhole. However, this is often affected by washout and/or collapse of shale and poorly cemented porous rocks. It can be affected by a build-up of mud cake on porous and permeable formations. Consequently, it is important to know precisely the borehole diameter at each sampling level i.e. as a function of depth.

Measurement principle

Borehole diameter can be determined through three different ways:

- Mechanical measurement.**

The borehole diameter is measured by means of symmetric articulated arms connected with the cursor of a potentiometer (**FIGURE 2.10**). The caliper tool could be two, three, four or six arms. The more the number of arms, the more precise is the measurement of the hole shape and the hole volume. Variations in the hole diameter with depth cause the arms to close or open and the movement is reflected in resistance changes in potentiometer. A simple calibration allows the changes in resistances to be scaled to changes in diameters.

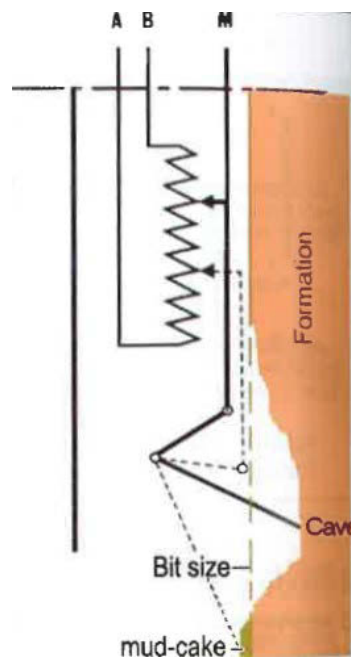


FIGURE 2.10: Schema explaining the measurement of the borehole diameter. The cursor of a potentiometer is linked to the arm of the tool [Serra, 2008]



FIGURE 2.11: Four-arm caliper logging tool [https://www.google.at/search February, 2015]

b. Acoustic measurement.

The diameter of the borehole is determined by means of an ultrasonic tool. Measurement of the transit time of an acoustic wave going to and fro, the transmitter and the receiver being aligned with the axis of the hole is made. Transit time and velocity is later converted to borehole diameter measurement.

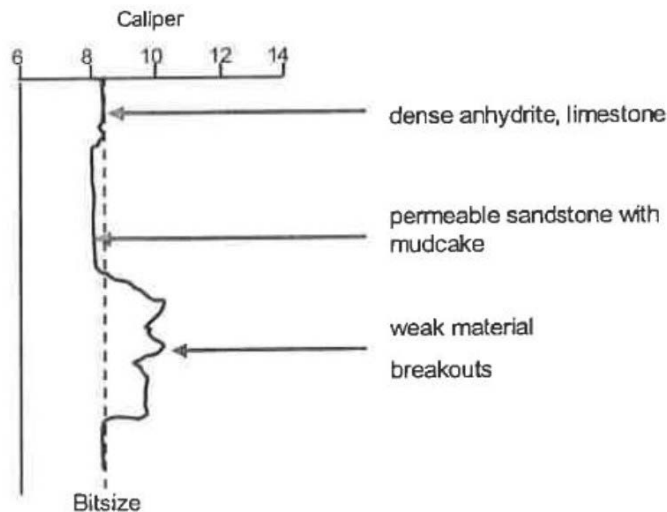


FIGURE 2.12: Schematic representation of caliper log in different formations [Schön, J. Borehole geophysics study material Montanuniversität, Leoben (unpublished)]

2.2.1.2 Compensated formation density log

Density logging provides a continuous record of a formation's bulk density along the length of a borehole. Bulk density is a function of the density of the minerals forming the rock (i.e. matrix) and the fluid enclosed in the pore spaces. The tool itself originally consisted of a radioactive source and a single detector but because of the effect of drilling fluid on the measurement, that configuration had to be modified to the compensated formation density log tool. This improvement is to compensate for borehole effects (primarily mudcake thickness). Compensated formation density log tool uses two or more detectors. In the two detector configuration (**FIGURE 2.13**), the short-spaced detector has a much shallower depth of investigation than the long-spaced detector so it is used to measure the effect that the drilling fluid has on the scattered gamma ray detection. The result is used to correct the long-spaced detector.

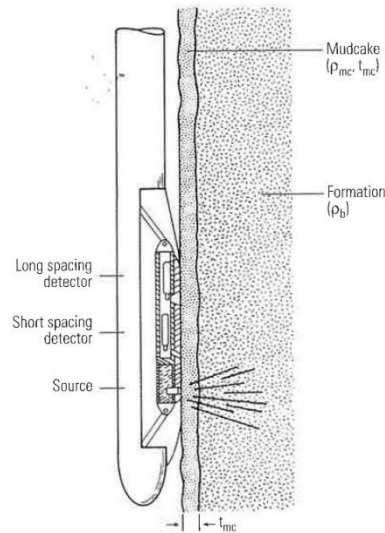


FIGURE 2.13: Formation density tool [Ellis et al, 2007]

Measurement principle

The density logging tool has a relatively shallow level of investigation, and as a result, is held against the side of the borehole during logging to maximize its response to the formation. The tool has a radioactive source (gamma source) and a detector (gamma detector). When lowered down the borehole, the source emits medium-energy gamma rays into the formation. Radioactive sources are typically a directional Caesium-137 source. These gamma rays interact with electrons in the formation and are scattered in an interaction known as Compton scattering. The number of scattered gamma rays that reach the detector, placed at a set distance from the emitter, is related to the formation's electron density, which itself is related to the formation's bulk density (ρ_b or RHOB) by

$$\rho_e = 2 \rho_b \frac{Z}{A} \quad (2.9)$$

where:

Z : atomic number,

A : molecular weight of the compound.

The electron density (ρ_e) determines the response of the density tool.

The measured bulk density (ρ_b) only depends on the matrix density (ρ_{ma}) and fluid density (ρ_{fl}) and assuming that these values are known along the wellbore, porosity (ϕ) can be inferred by the formula:

$$\phi_D = \frac{\rho_{ma} - \rho_b}{\rho_{ma} - \rho_{fl}} \quad (2.10)$$

where:

ϕ_D : density derived porosity,

ρ_{ma} : matrix density (sandstone = 2.56g/cm³; limestone = 2.71g/cm³; dolomite = 2.87g/cm³),

ρ_b : formation bulk density (the log reading),

ρ_{fl} : fluid density (For normal invasion the tool reads invaded zone. Therefore fluid density approximates to density of mud filtrate).

Some specific notes

TABLE 2.1: Mean Values for Density, Electron Density, ratio Z/A , and Photoelectric Absorption Index Pe , Baker Atlas Document

Substance	ρ (g/cm ³)	ρ_e (g/cm ³)	Z/A	Pe (b/e)
quartz	2.654	2.650	0.499	1.806
calcite	2.710	2.708	0.500	5.084
dolomite	2.870	2.864	0.499	3.142
halite	2.165	2.074	0.479	4.65
gypsum	2.320	2.372	0.511	3.420
anhydrite	2.97	2.96	0.499	5.05
kaolinite	2.44	2.44	0.50	1.83
illite	2.64	2.63	0.499	3.45
barite	4.48	4.09	0.446	266.8
water (fresh)	1.000	1.110	0.555	0.358
oil	0.850	0.948	0.558	0.125

[Schön, J. Borehole geophysics study material Montanuniversität, Leoben (unpublished)]

2.2.1.3 Neutron porosity log

Neutron porosity logs measure the hydrogen concentration in a formation. Neutrons are created from a chemical source (mixture of americium and beryllium which continuously emit neutrons) in the neutron logging tool or a neutron generator. Neutrons as a function of their energy can interact with atoms in different ways. Hydrogen plays an important part for elastic scattering as dominant interaction. As hydrogen is present in both water and oil, an estimation of its amount in the porous formations will allow the estimation of the amount of

liquid-filled porosity. Therefore, an evaluation of the hydrogen index is directly associated to porosity.

Measurement principle

The measurement principle of the neutron porosity or hydrogen index is based on the fact that hydrogen is very efficient in the slowing down of fast neutrons based on elastic scattering. During elastic collisions, maximum energy is lost when the target nucleus has a mass equal to that of the incident neutron. Neutron slow-down is most strongly affected by hydrogen atoms (H), the single proton of a nucleus having very nearly the mass of a neutron. Because hydrogen in a porous formation is concentrated in the fluid-filled pores, energy loss can be related to the formation's porosity. The neutron porosity log is predominantly sensitive to the quantity of hydrogen atoms in a particular formation, which generally corresponds to rock porosity.

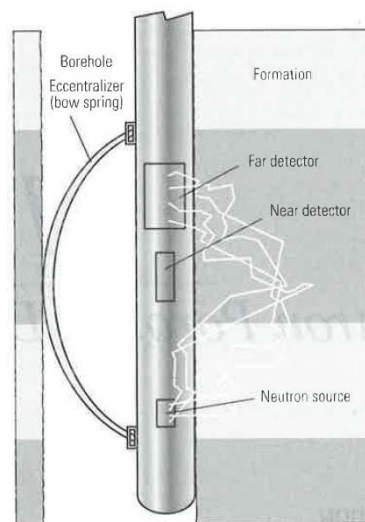


FIGURE 2.14: Schematic of a generic neutron logging tool [Ellis et al, 2007]

Most neutron tools are “limestone-calibrated” i.e. the calibration curve relates the neutron reading (response) to the porosity of a fresh water saturated limestone. Therefore different mineral composition and different pore fluid will result in a deviation from the porosity as defined by the ratio of volume of pore space to sample volume. Corrections are therefore necessary for any porous rock composed of different mineral components. For example, for a rock such as shale, and fluids, the porosity derived from a limestone-freshwater-calibrated device will result as:

$$\phi_N = \phi \cdot \phi_{N,fluid} + (1 - \phi) \cdot [(1 - V_{shale}) \cdot \phi_{N,matrix} + V_{shale} \cdot \phi_{N,shale}] \quad (2.11)$$

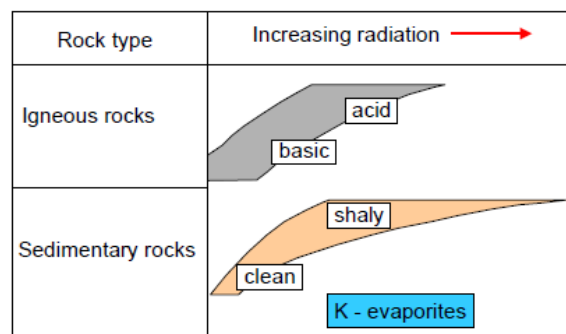
where:

- ϕ : rock porosity,
 $\phi_{N,fluid}$: neutron response of the fluid,
 $\phi_{N,shale}$: neutron response of the shale,
 ϕ_N : measured neutron porosity,
 $\phi_{N,matrix}$: neutron response of the matrix,
 V_{shale} : shale content.

2.2.1.4 Gamma-ray log

Gamma rays are electromagnetic radiations emitted from an atomic nucleus during radioactive decay; with the wavelength in the range of 10^{-9} to 10^{-11} cm. Gamma ray logs are lithology logs that measure the natural radioactivity of a formation. They are used to identify lithologies, correlate between formations, and calculate volume of shale. As shale content increases, the gamma ray log response increases because of the concentration of radioactive materials in shale (TABLE 2.1).

TABLE 2.2 Radioactivity of rocks - General tendency



[Schön, J. Petrophysics of Reservoir Rocks study material Montanuniversität, Leoben (unpublished)]

Measurement principle

The gamma ray logging is done by lowering an instrument down the drill hole and recording gamma radiation variation with depth. Natural gamma activity of minerals and rocks is originated from (1) Uranium-radium series (half-life time of $4.4 \cdot 10^9$ years), (2) Thorium series (half-life time of $1.4 \cdot 10^9$ years) and (3) Potassium K^{40} (half-life time of $1.3 \cdot 10^9$ years). Abundance of these elements or isotopes controls the intensity of natural radioactivity; the result is a spectrum of radiation. Spectral character leads to two types of measurement:

- Integral measurement
- Spectral measurement

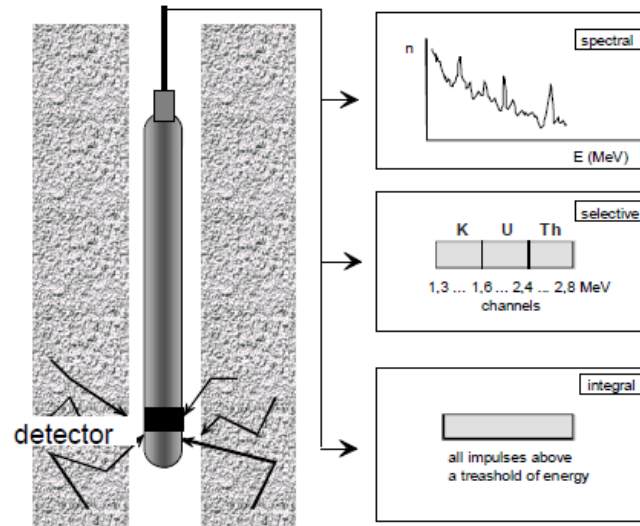


FIGURE 2.15: Gamma measurements - principles [Schön, J. Borehole geophysics study material Montanuniversität, Leoben (unpublished)]

Gamma radiation is usually recorded in API units. The integral measurement is the resultant effect of three contributors. $GR\ API = [(8 \times \text{Uranium concentration in ppm}) + (4 \times \text{Thorium concentration in ppm}) + (15 \times \text{Potassium concentration in percent})]$. Spectral measurement is the effect of a contributor only. An important use of the spectral gamma ray log is in determining shale (clay) volume (V_{shale}) in reservoirs that contain uranium minerals, potassium feldspars, micas, and/or glauconite otherwise we use a standard gamma ray log.

Volume of shale calculation

The basis is the correlation between shale content and gamma activity. The volume of shale expressed as a decimal fraction or percentage is called V_{shale} . A first step is to calculate the gamma ray index, I_{GR} .

$$I_{GR} = \frac{GR - GR_{cn}}{GR_{sh} - GR_{cn}} \quad (2.12)$$

where:

- I_{GR} : gamma ray index,
- GR : gamma ray reading of the formation,
- GR_{cn} : minimum gamma ray (clean sand or carbonate),
- GR_{sh} : maximum gamma ray (shale).

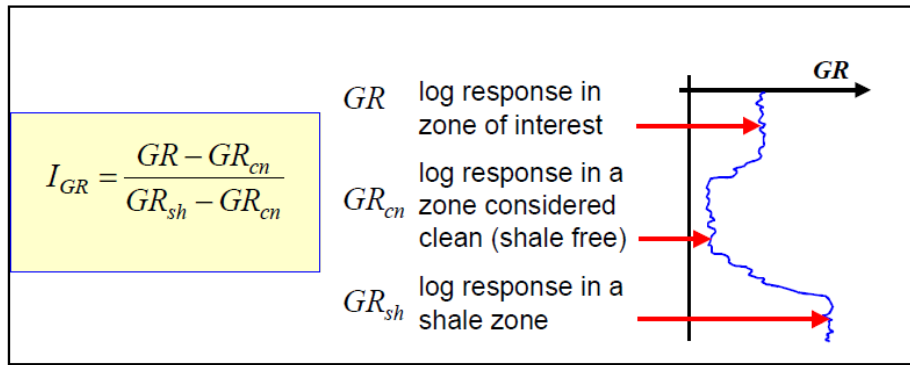


FIGURE 2.16: Gamma ray response for evaluating I_{GR} [Schön, J. Borehole geophysics study material Montanuniversität, Leoben (unpublished)]

Gamma ray response has linear as well several nonlinear empirical relationships with shale volume. The nonlinear responses are based on geographic area or formation age. All nonlinear responses produce a shale volume value that are lower than that from the linear equation i.e. they are more optimistic.

- Linear response.

Here we have the volume of shale as $V_{shale} = I_{GR}$

- Nonlinear response.

In the order of decreasing calculated shale volumes (increasing optimism), we have the respective volume of shale as:

- Larinov (1969) for Tertiary rocks: $V_{shale} = 0.083(2^{3.7 \cdot I_{GR}} - 1)$.
- Steiber (1970): $V_{shale} = \frac{I_{GR}}{3 - 2 \times I_{GR}}$.
- Clavier (1971): $V_{shale} = 1.7 - [3.38 - (I_{GR} - 0.7)^2]^{\frac{1}{2}}$.
- Larinov (1969) for older rocks: $V_{shale} = 0.33 \times (2^{2 \cdot I_{GR}} - 1)$.

FIGURE 2.17 shows how we can also determine the shale volume from radioactivity index using empirical relationships.

Procedure:

- Find the gamma ray index value (I_{RA}) on the horizontal scale.
- Follow the value vertically to where it intersects each of the curves.
- From the curve, move horizontally to the scale at the left and read the shale volume. This is the amount of shale in the formation expressed as a decimal fraction.

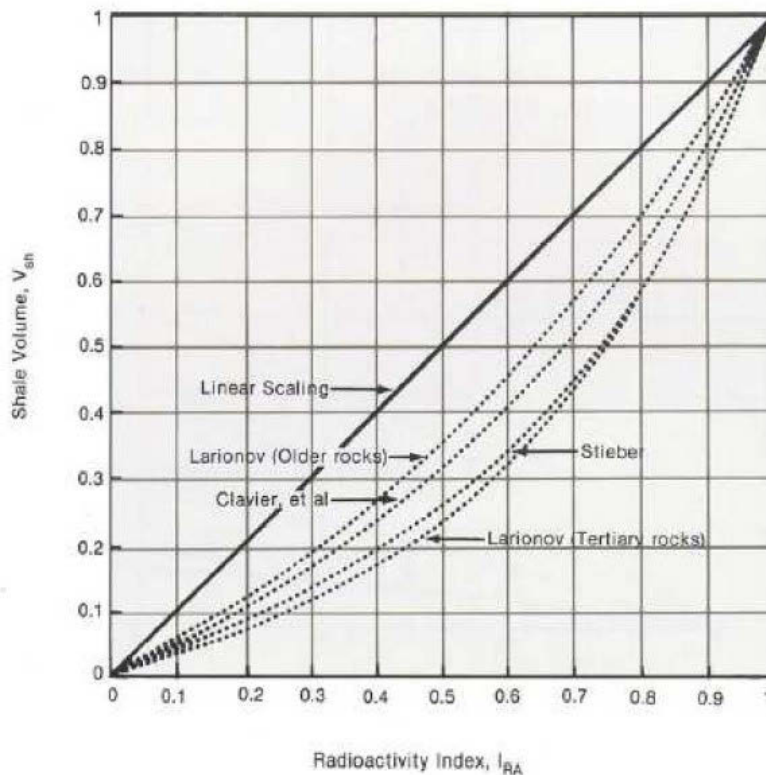


FIGURE 2.17: Chart for correcting the gamma ray index I_{RA} to the shale volume (V_{shale}) [Schön, J. *Petrophysics of Reservoir Rocks* study material Montanuniversität, Leoben (unpublished)]

2.2.1.5 Electrical measurements with Inductionlogs (for deep reading, R_t) and Microdevices for R_{xo}

The induction log measures conductivity (inverse of resistivity) deep within the formation with minimum disturbance by the invaded zone. Because the induction tool measures conductivity directly rather than resistivity, more reliable readings tend to be made within lower resistivity sections. Unlike other resistivity tools, the induction tool can be run in holes drilled with air, or with oil-base muds since it does not require electrical contact with the mud or formation. The tool has excellent operation in fresh muds but readings in salty muds are greatly affected, this is as a result of the contribution of the borehole to the total conductivity reading. Microdevices use electrode systems on a pad which is pressed at the borehole wall. This results in extreme high vertical resolution but extreme small depth of investigation (R_{mc} , R_{xo})

where:

R_{mc} : resistivity of the mudcake,

R_{xo} : resistivity of the flushed zone.

Measurement principle

Transmitter coils with a high frequency AC within the induction tool induces eddy currents in adjacent sections. Most of the eddy currents are focused beyond the diameter of the typical flushed zone and their magnitude is an approximation of the conductivity of the virgin formation. In turn, they induce voltages in the receiver coil which are translated to estimates of formation conductivity and, as a reciprocal of resistivity. Resistivity tools are used for saturation calculations.

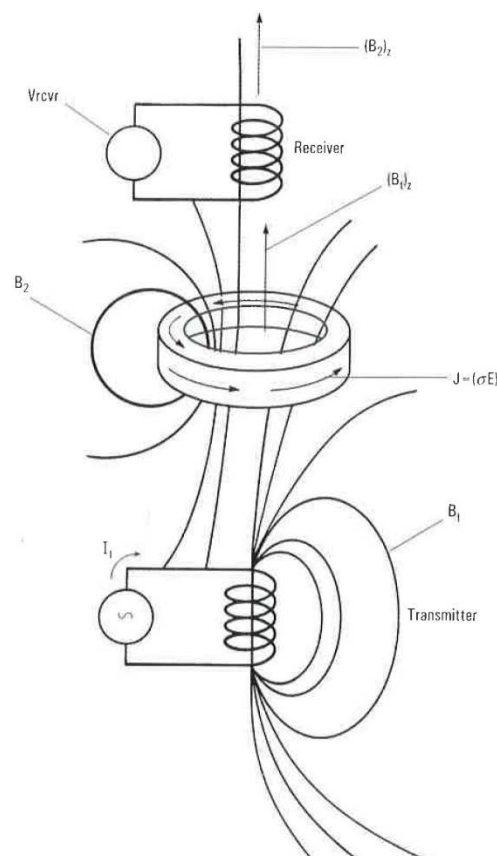


FIGURE 2.18: Induction tool principle [Ellis et al, 2007]

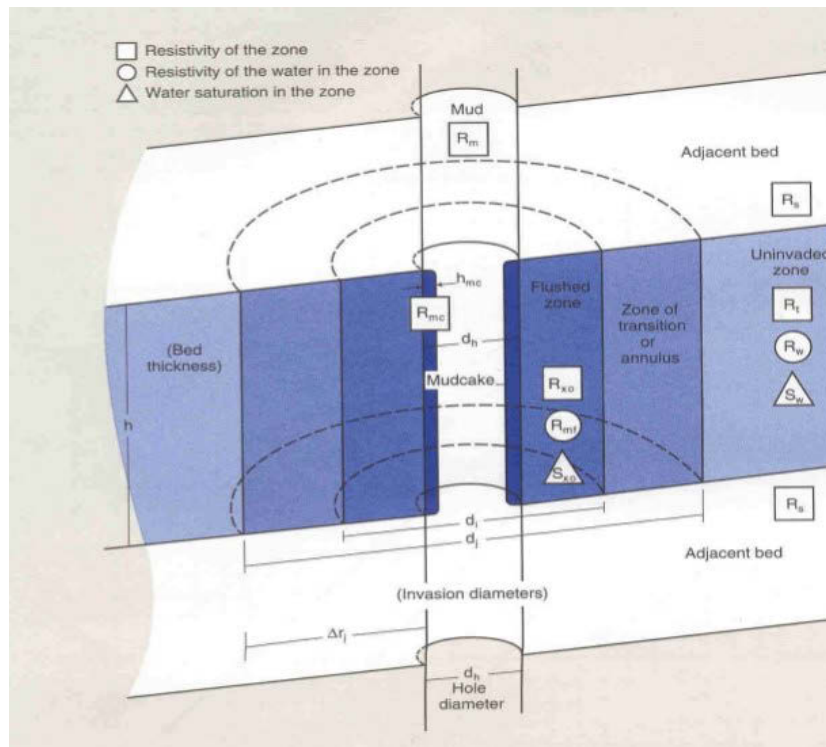


FIGURE 2.19: Schlumberger, 2000, Log interpretation charts. Schlumberger Ed.Serv.

$$S_w = \sqrt{\frac{R_o}{R_t}} \quad (2.13)$$

where:

R_o : resistivity of a fully water-saturated rock,

R_t : resistivity of a partially water-saturated rock,

S_w : water saturation of the rock.

3 DATABASE

A total of four (4) wells containing core and log data were provided for studies. They include wells B2-NC-74A; B5-NC-74A; B6-NC-74A and B8-NC-74A. Parameters relevant for core and log data interpretation were extracted to generate a core and log database. These parameters were later loaded into Interactive Petrophysics (IP) software programme for processing and reprocessing for accurate evaluation of reservoir hydrocarbon volumes.

3.1 Core Database

The core database contains the following petrophysical parameters:

(a) Porosity, (b) Permeability, (c) Relative permeability, (d) Capillary pressure, (e) Formation resistivity factor, (f) Cementation exponent, and (g) Saturation exponent.

NB: See Appendix A [**CD-ROM (TABLES 3.1 - 3.4)**] for detailed core data description.

3.2 Log Database

A list of the measured logs used in this study include Caliper logs, Compensated formation density log, Neutron porosity log, Gamma ray logs and Induction deep resistivity log. Depth sampling in each case was done at 0.5000ft intervals.

- Caliper logs: This log samples downhole the diameter of the borehole by means of symmetrical articulated arms. It could be two, three, four or six arm.
- Compensated formation density log: This log provides samples of the formation's bulk density downhole by means of a radioactive gamma source and one or more detectors. The bulk density is related to the number of scattered gamma rays that reach the detectors.
- Neutron porosity log: Hydrogen index in a formation is directly associated to porosity. This log estimates porosity by measuring the hydrogen concentration in a formation.
- Gamma ray logs: Gamma ray logs measure the natural radioactivity in a formation. It is used in the calculation of volume of shale given its response to the radioactive content in shale.
- Induction deep resistivity log: This log among other electrical measurements provides the resistivity of a formation indirectly by measuring the conductivity of the formation.

The following well log and petrophysical results are contained in the log database:

(a) Depth, (b) Volume of clay, (c) Calliper-bit size, (c) Secondary porosity indicator, (d) Formation water saturation, (f) Effective porosity and (e) PHIE*SW product.

NB: See appendix B (**CD-ROM TABLES 3.5 – 3.8**) for detailed log data description.

4 CORE DATA ANALYSIS

4.1 Porosity-resistivity-water saturation: Derivation of Archie parameters

Important petrophysical relationships exist among porosity, resistivity and water saturation.

These relationships are very useful in obtaining relevant Archie parameters.

$$FF = \frac{a}{\phi^m} = \frac{R_o}{R_w} \quad (4.1)$$

$$\frac{R_t}{R_o} = \frac{1}{S_w^n} \quad (4.2)$$

where:

FF : formation factor,

a : tortuosity factor (Archie parameter),

ϕ : porosity ,

m : cementation exponent,

n : saturation exponent,

R_o : resistivity of the rock filled with water only ($S_w = 1$),

R_t : resistivity of the rock partially saturated with water ($S_w < 1$),

R_w : resistivity of the water/brine,

S_w : water saturation.

Measured stable values of R_o and R_w from core analysis in the laboratory are indicative of the establishment of ionic equilibrium within the core samples. The resistivity of the various saturant brine (R_w) used for the core sample analysis of the individual wells are as shown in

TABLE 4.1.

TABLE 4.1: Resistivity of saturant brine of core samples of individual wells

Subject Well	Resistivity of saturant brine, R_w ($\Omega.m$)
B2-NC-74A	0.134
B5-NC-74A	0.086
B6-NC-74A	0.086
B8-NC-74A	0.086

From laboratory results, the saturation exponent (n) values of the various samples for each well vary. The average " n " values for each well are determined and are as shown in **TABLE 4.2**.

TABLE 4.2: Average saturation exponent values of different core samples for the individual wells

Subject Well	Average " n " value
B2-NC-74A	2.03
B5-NC-74A	1.99
B6-NC-74A	2.65
B8-NC-74A	2.16

In order to analyse required Archie parameters for the individual and composite wells, a log-log plot of formation factor versus porosity is created. Archie parameters " a " and " m " were extracted from these plots. Power law equation was used as a test for a straight line in good approximation. The quality of fit of the data points is described by the R^2 value. Where R^2 value is nearly equal to 1 (unity), this would mean a good fit for the plotted data points.

4.1.1 Well plots

4.1.1.1 Plots of formation resistivity factor (FF) versus porosity(ϕ) fraction on a logarithmic scale

Brines in the pore spaces of rocks are the main conductors of electricity through a rock material. Therefore the more pore spaces filled with brine, the lower the formation resistivity factor of such a rock material. By extension the porosity of a rock gives us an indication of its formation resistivity which implies that a certain form of relationship does exist between both.

We applied a regression (power law) which follows the equation

$$FF = \frac{a}{\phi^m} \quad (4.3)$$

where:

a : constant called Archie parameter,

m : cementation exponent.

Exponent " m " is believed to increase with cementation.

Well B2-NC-74A

There is a general decrease in formation resistivity factor with increase in porosity in this well (**FIGURE 4.1**). This confirms the strong influence of porosity on the formation resistivity factor of a formation. The accuracy in regression analysis is very good as shown by

the R^2 value of 0.9162. A great majority of the data points fits on the trendline generated by the power law equation, $FF = 1.2591 * \phi^{1.76}$ which has an empirical constant value "a" of 1.2591, and a cementation exponent value "m" of 1.76 (slope of the plot).

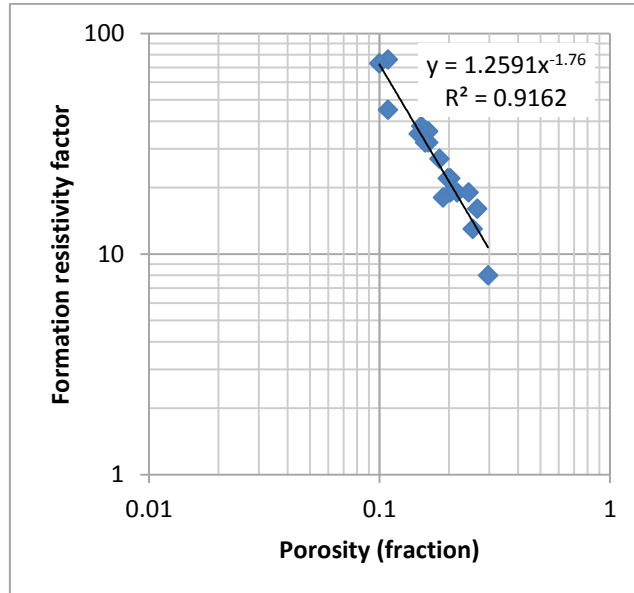


FIGURE 4.1: FF versus ϕ for Well B2-NC-74A

Well B5-NC-74A

Well B5-NC-74A has R^2 value of 0.9777 (**FIGURE 4.2**) and exhibits a similar trend as **FIGURE 4.1** except for its higher accuracy in the quality of fit of data points on the trendline. I found again a general decrease in formation resistivity factor as the porosity of the rock increases. The regression equation is given by $FF = 0.4129 * \phi^{2.497}$ and has an empirical constant value "a" of 0.4129, and a cementation exponent value "m" of 2.497 (slope of the plot).

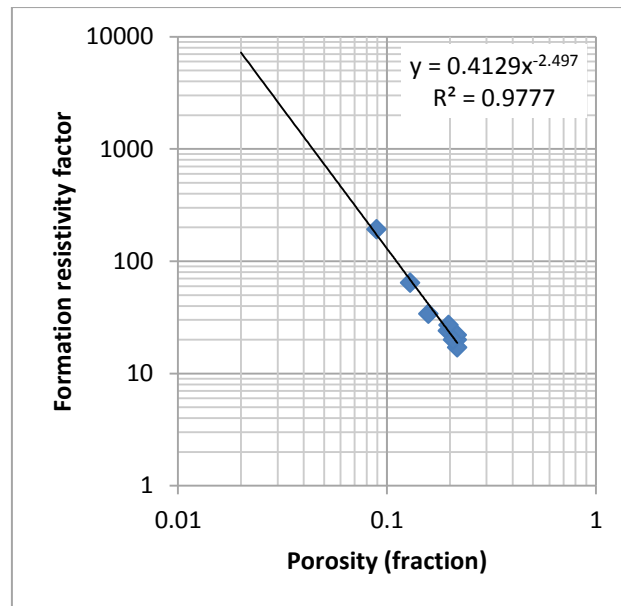


FIGURE 4.2: FF versus ϕ for Well B5-NC-74A

Well B6-NC-74A

This is the well (FIGURE 4.3) with the highest accuracy of regression as shown by its R^2 value of 0.9925. Nearly all the data points fit on the trendline and the plot describes a general decrease in formation resistivity factor as porosity increases. The regression equation is given by $FF = 1.5849 * \phi^{1.577}$ which has an empirical constant value "a" of 1.5849, and a cementation exponent value "m" of 1.577 (slope of the plot).

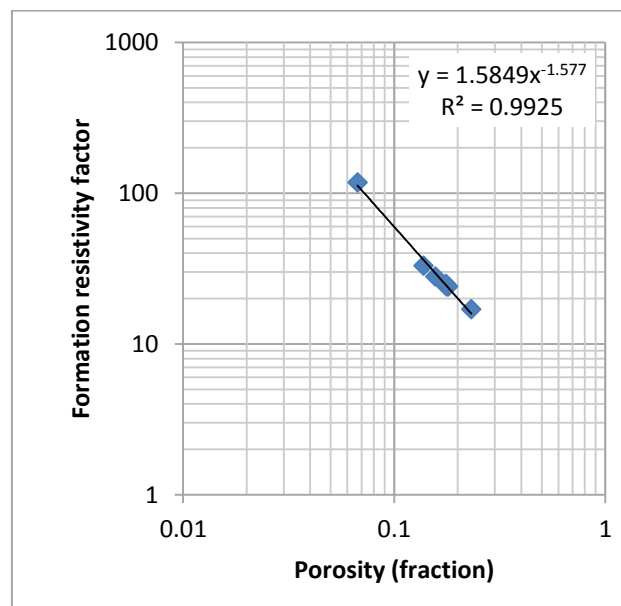


FIGURE 4.3: FF versus ϕ for Well B6-NC-74A

Well B8-NC-74A

This well (**FIGURE 4.4**) has the least accuracy of regression among all the wells compared as shown by its R^2 value of 0.8421. Few of the data points are away from the trendline; however, it also describes a general decrease in formation resistivity factor as porosity increases. The regression equation is given by $FF = 0.4037 * \phi^{2.412}$ and has an empirical constant value "a" of 0.4037 and a cementation exponent value "m" of 2.412 (slope of the plot).

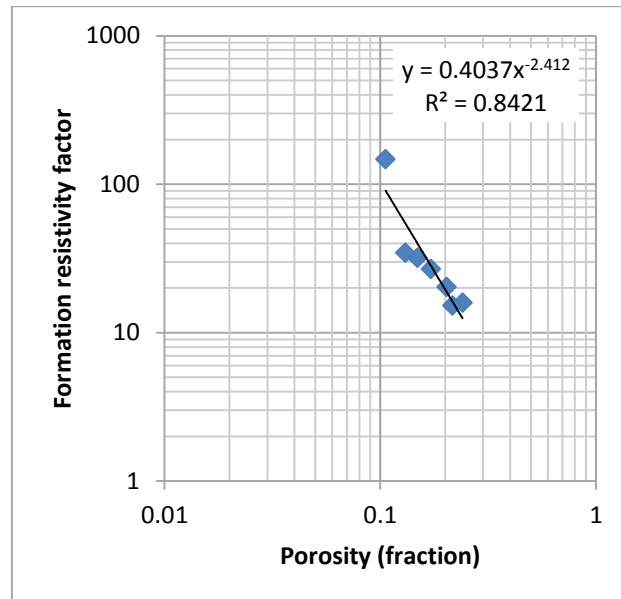


FIGURE 4.4: FF versus ϕ for Well B8-NC-74A

FIGURE 4.4 low quality of regression is originated mainly by one data point ($\phi = 0.106$, $FF = 147$). If we do not implement this point, the result is much better. This is demonstrated in **FIGURE 4.5**. In **FIGURE 4.5**, we notice a remarkable improvement in the quality of regression as shown by its R^2 value of 0.9331. Majority of the data points fit on the trendline and the formation resistivity factor decreases as the porosity increases. The regression equation is given by $FF = 1.9152 * \phi^{1.453}$ and has an empirical constant value "a" of 1.9152 and a cementation exponent value "m" of 1.453 (slope of the plot).

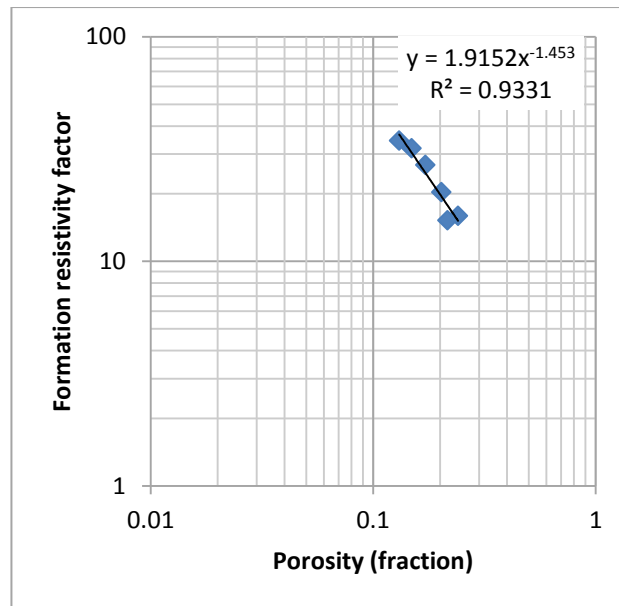


FIGURE 4.5: *FF* versus ϕ for Well B8-NC-74A (Data point 0.106, 147 absent)

4.1.1.2 Plots of logarithm of formation resistivity factor (*FF*) versus logarithm of porosity(ϕ) fraction

To further analyse Archie's parameters, a plot of the logarithm of the measured formation resistivity factor against the logarithm of the measured porosity is created. Applying regression (power law) following the frequently used simplified form of Archie's equation

$$FF = \frac{1}{\phi^m} \quad (4.4)$$

We set point $\log \phi = 0$ and $\log FF = 0$, the plot resulted into a straight line relationship indicating that the applied power law is in good approximation and has a slope "*m*" equal to the cementation exponent. Exponent "*m*" is believed to increase with cementation. The cementation exponent in this analysis is not constant but varied across the wells. It is likely to be the result of strong complex pore structures. The effect of assuming a precise "*m*" value for all the samples would mean that they all share similar diagenetic variations and complex pore structure.

Equation (4.4) shows that formation resistivity factor will decrease as "*m*" value increases. If we extrapolate the trendline to meet the vertical axis, we will have an intercept equal to the logarithm of the formation resistivity factor.

Regression analysis of well B6-NC-74A (**FIGURE 4.8**) still records the highest regression accuracy ($R^2 = 0.9695$) with majority of data points fitting on the trendline.

Well B2-NC-74A

This well (**FIGURE 4.6**) has a cementation exponent " m " value of 1.8894 and shows a general decrease in formation resistivity factor with increase in porosity. The regression accuracy ($R^2 = 0.911$) is third among the 4 (four) wells investigated.

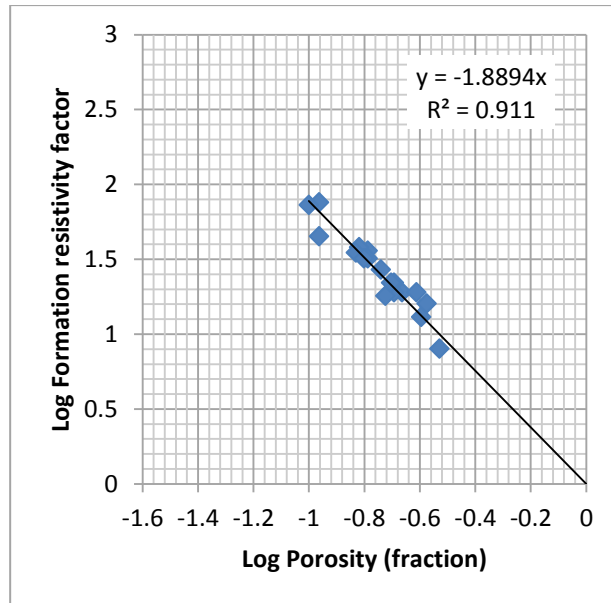


FIGURE 4.6: Log FF versus Log ϕ for Well B2-NC-74A

Well B5-NC-74A

This well (**FIGURE 4.7**) has a cementation exponent " m " value of 2.0104 and shows a general decrease in formation resistivity factor with increase in porosity. The regression accuracy ($R^2 = 0.9392$) is second among the 4 (four) wells investigated.

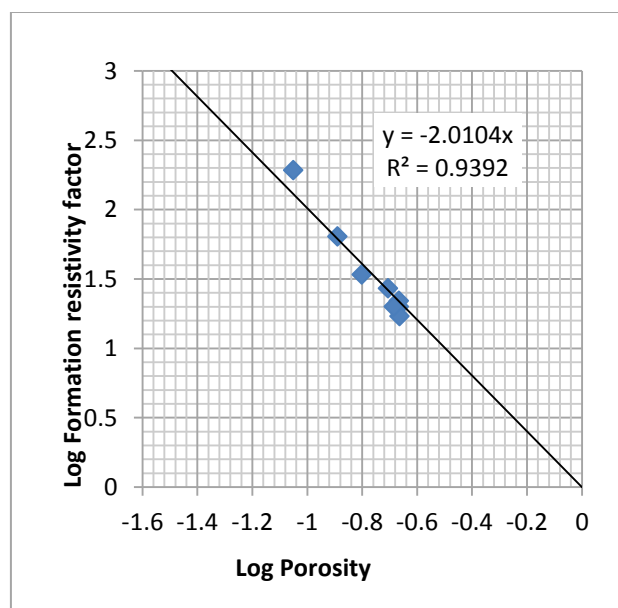


FIGURE 4.7: Log FF versus Log ϕ for Well B5-NC-74A

Well B6-NC-74A

This well (**FIGURE 4.8**) has a cementation exponent " m " value of 1.8127 and also shows a general decrease in formation resistivity factor with increase in porosity. The regression accuracy ($R^2 = 0.9695$) is the highest among the 4 (four) wells investigated.

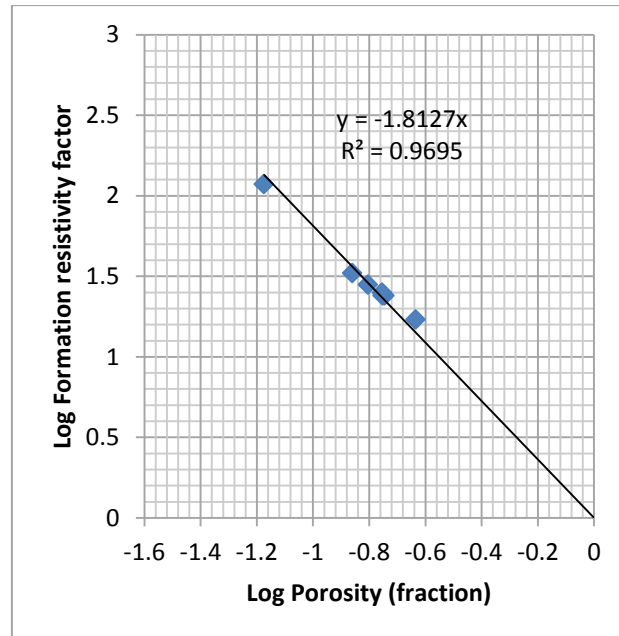


FIGURE 4.8: Log FF versus Log ϕ for Well B6-NC-74A

Well B8-NC-74A

This well (**FIGURE 4.9**) has a cementation exponent " m " value of 1.9149 and shows a general decrease in formation resistivity factor with increase in porosity. The regression accuracy ($R^2 = 0.8056$) is the least among the 4 (four) wells investigated.

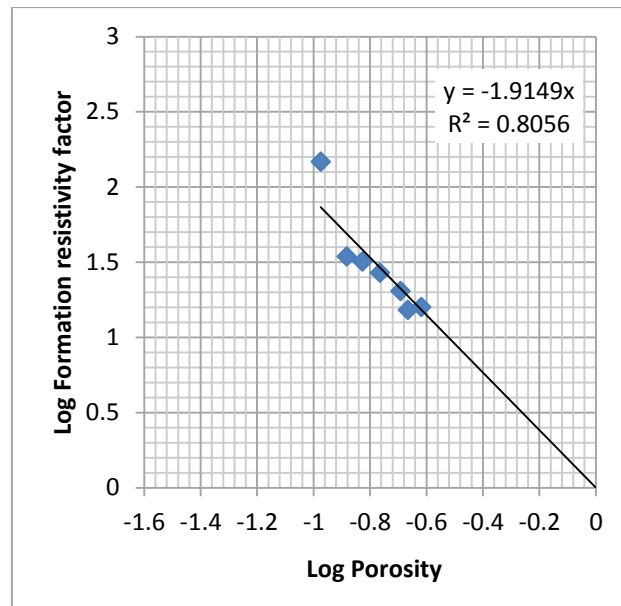


FIGURE 4.9: Log FF versus Log ϕ for Well B8-NC-74

As seen in **FIGURE 4.9** the low quality of regression is originated mainly by one data point (Log $\phi = -0.974694135$, Log $FF = 2.167317335$). If we do not implement this point, the result is much better. This is demonstrated in **FIGURE 4.10**. In **FIGURE 4.10**, there is a marked improvement in the quality of regression as shown by its R^2 value of 0.87. Majority of the data points now fit on the trendline and the formation resistivity factor decreases as the porosity increases.

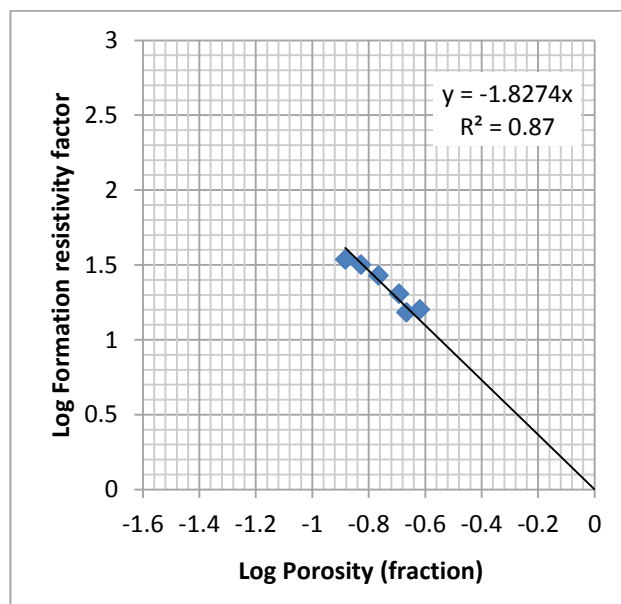


FIGURE 4.10: Log FF versus Log ϕ for Well B8-NC-74A (Data point -0.9747, 2.167 absent)

Compilation for all wells

To have an understanding of the general trend for all the wells under investigation, data from all 4 (four) wells are combined to create plots of (1) FF versus ϕ on log scale and (2) $\log FF$ versus $\log \phi$. Representative average petrophysical parameters are extracted using Archie's equations.

FIGURE 4.11 is a plot of FF versus ϕ on a logarithmic scale for all the wells. The straight line plot indicates that the power law is in good approximation and shows a general decrease in formation resistivity factor as porosity increases. This confirms the strong influence of porosity on the formation resistivity factor of a formation. The average accuracy in regression analysis is good as shown by R^2 value of 0.8737. A great majority of the data points fits on the trendline generated by the power law equation, $FF = 0.9854 * \phi^{1.911}$ which has an average empirical constant value "a" of 0.9854, and an average cementation exponent value "m" of 1.911 (slope of the plot).

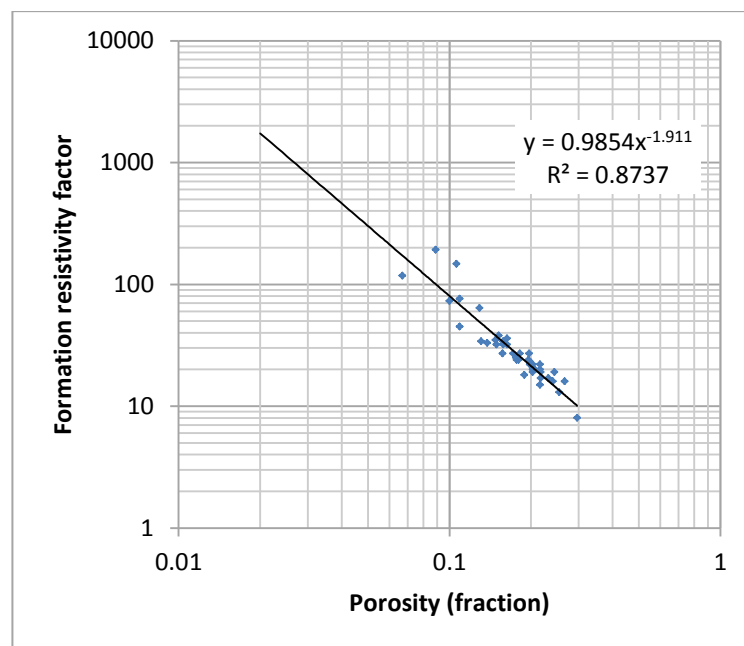


FIGURE 4.11: FF versus ϕ for all wells

FIGURE 4.12 is a plot of $\log FF$ versus $\log \phi$ for all the wells. This plot shows an average cementation exponent "m" value of 1.9018 and describes a general decrease in formation resistivity factor as porosity increases. The regression accuracy ($R^2 = 0.8755$) is the averaged value from a combination of the 4 (four) wells investigated.

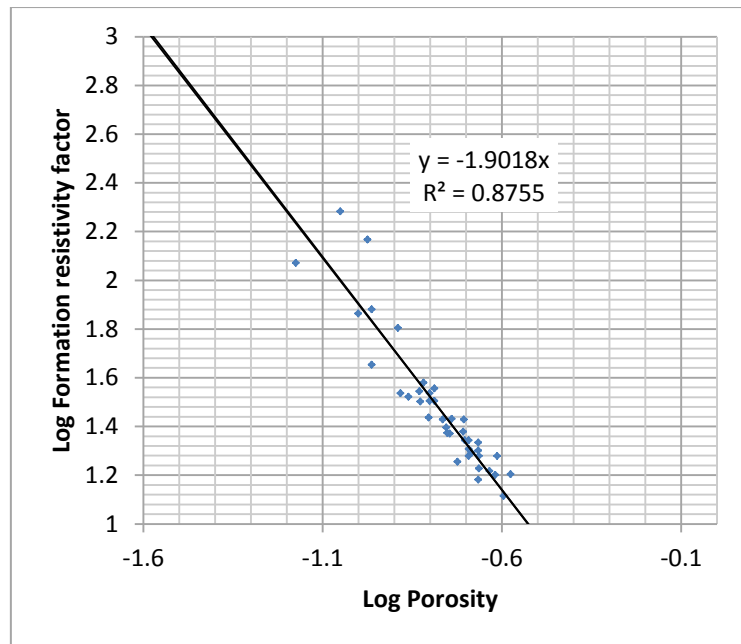


FIGURE 4.12: Log FF versus ϕ for combined wells

TABLE 4.3 is a summary of the petrophysical parameters obtained from the analysis of Archie equations of the individual and composite wells of preceding discussed plots (FIGURES 4.1 through 4.12).

TABLE 4.3: Archie parameters of the individual and composite wells (FIGURES 4.1 – 4.12)

Subject Well	Plot of FF versus ϕ on a logarithmic scale			Plot of Log FF versus Log ϕ	
	a	m	R^2	m	R^2
B2-NC-74A	1.2591	1.76	0.9162	1.8894	0.911
B5-NC-74A	0.4129	2.497	0.9777	2.0104	0.9392
B6-NC-74A	1.5849	1.577	0.9925	1.8127	0.9695
B8-NC-74A	1.4037	2.412	0.8421	1.9149	0.8056
ALL WELLS	0.9854	1.911	0.8737	1.9018	0.8755

Results show:

- Formation in the individual wells is characterised by a relatively small but clear visible difference in the Archie parameters,
- There is only a very small difference in the quality of regression between the two forms of Archie's equation. Therefore for the following analyses the more comfortable form

$$FF = \frac{1}{\phi^m}$$

is used with " m " = 1.813.....2.01 and an overall mean value of 1.90.

4.2 Poro-perm correlation

The correlation between permeability and porosity is of high practical importance for a permeability estimate from porosity logs. In order to derive the permeability versus porosity behaviour, regression, and other properties of the investigated core samples, a graphical plot of logarithmically scaled permeability as a function of logarithmically scaled porosity is created. The individual plots for the different wells indicate that there is a reasonably good relation between three petrophysical parameters and the permeability can be estimated from:

$$K = a \cdot \phi^b \quad (4.5)$$

where:

K : permeability in md,

a : grain size coefficient in md,

ϕ : matrix porosity, fraction,

b : cementation-compaction coefficient, dimensionless,

R^2 : quality of fit of plotted parameters.

4.2.1 Individual well plots

4.2.1.1 Plot of K_{air} versus ϕ on a logarithmic scale

Applied regression (power law) follows an equation

$$K = a \cdot \phi^b \quad (4.6)$$

Well B2-NC-74A

FIGURE 4.13 shows an increasing permeability with porosity trend for samples of Well B2-NC-74A. The trendline of permeability against porosity values is defined which implies that the power law is in good approximation. The quality of fit is defined by R^2 which has a value of 0.6303 and indicates a moderate correlation. Power law results in the equation, $K = 10223 * \phi^{4.61}$ with a grain size coefficient of 10223 and cementation-compaction coefficient of 4.6132. The permeability at any point on the plot can be predicted by simply inputting the matrix porosity fraction value at such a point, but scatter originates an uncertainty.

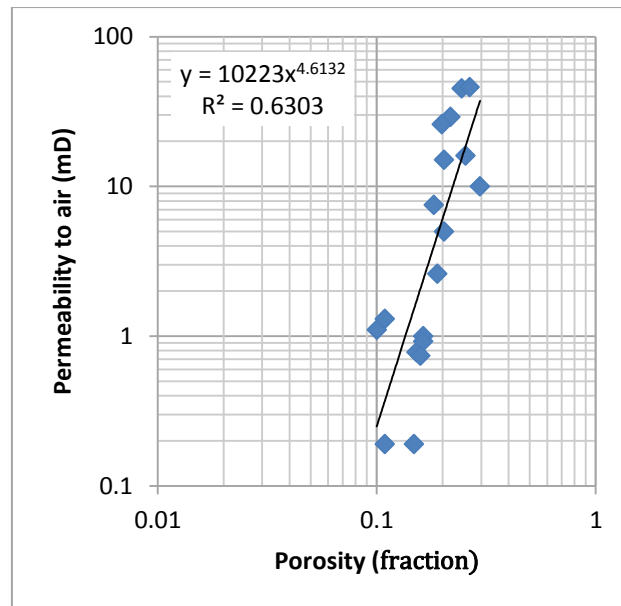


FIGURE 4.13: K_{air} versus ϕ for Well B2-NC-74A

Well B5-NC-74A

Among the four wells compared, porosity–permeability correlation for Well B5-NC-74A (**FIGURE 4.14**) shows the highest approximation according to power law and has R^2 value of 0.800. Therefore the relationship between permeability and porosity is highest in this well and is likely to be situated in a good reservoir. Regression results in the equation, $K = 713.09 * \phi^{2.9168}$ with a grain size coefficient of 713.09 and cementation-compaction coefficient of 2.9168. Similar to the preceding well, the permeability at any point on the plot can be predicted using the given matrix porosity fraction value.

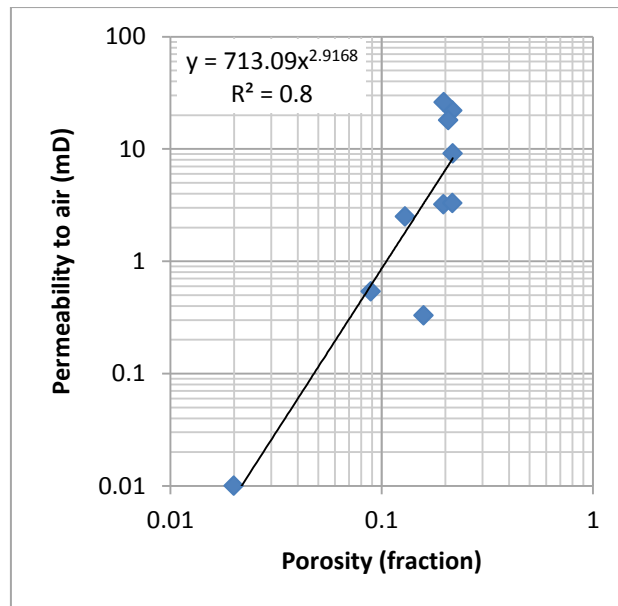


FIGURE 4.14: K_{air} versus ϕ for Well B5-NC-74A

Well B6-NC-74A

The quality of fit between permeability and porosity in this well (**FIGURE 4.15**) is less compared to the preceding wells under discussion as shown by the R^2 value of 0.5204.

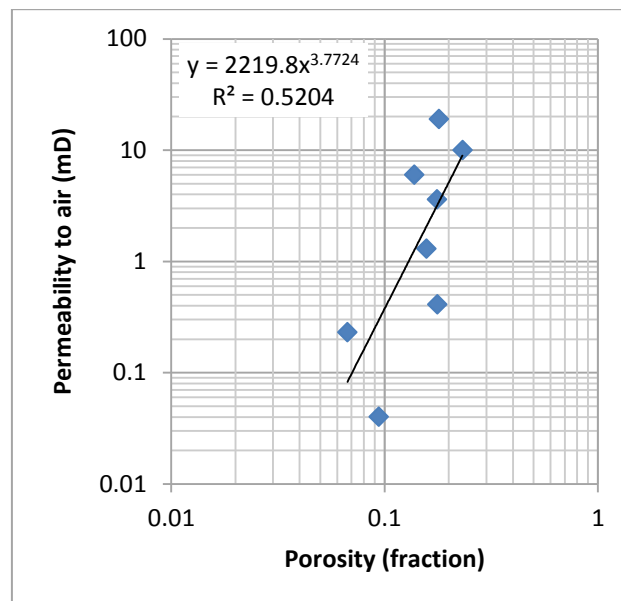


FIGURE 4.15: K_{air} versus ϕ for Well B6-NC-74A

Regression results in the equation, $K = 2219.8 * \phi^{3.7724}$ with a grain size coefficient of 2219.8 and cementation-compaction coefficient of 3.7724. Similar to the preceding wells, the permeability at any point on the plot can be predicted using the given matrix porosity fraction value.

Well B8-NC-74A

This is the well with the least relationship between permeability and porosity as evidenced by the poor R^2 value of 0.2750 (**FIGURE 4.16**). The relationship between permeability and porosity in this well is not very strong; consequently, permeability predictions using $K = 65.617 * \phi^{1.8919}$ might not be very reliable. It has a grain size coefficient of 65.617 and cementation-compaction coefficient of 1.8919.

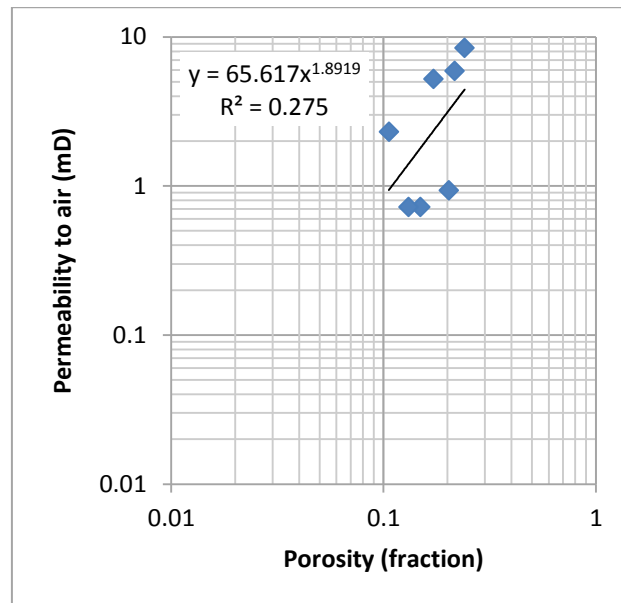


FIGURE 4.16: K_{air} versus ϕ for Well B8-NC-74A

The distribution of the data indicates that probably two different formations are present in this well. We can describe therefore the correlation by two different equations using higher and lower datasets as shown in **FIGURE 4.17**. Interestingly results show good correlation in the individual datasets given by their high R^2 values of 0.9694 and 0.9182 for higher dataset (red coloured) and lower dataset (blue coloured) respectively. The relationship between permeability and porosity in both cases is strong. Higher dataset has grain size coefficient of 64.841 and cementation compaction coefficient of 1.4803. The grain size coefficient and cementation compaction coefficient of lower dataset is 2.5003 and 0.629 respectively.

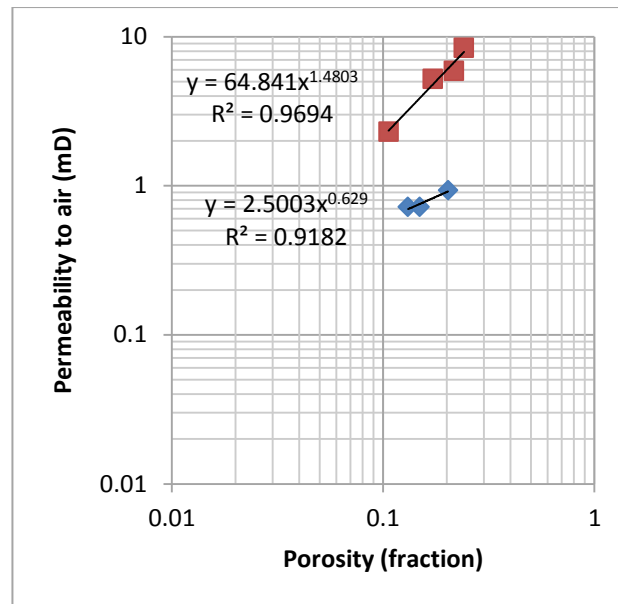


FIGURE 4.17: K_{air} versus ϕ for Well B8-NC-74A (split plot)

4.2.1.2 Plot of K_{air} versus S_{wi} on a logarithmic scale

In order to derive the permeability versus irreducible water saturation, regression, and other properties of the investigated core samples, a graphical plot of logarithmically scaled permeability as a function of logarithmically scaled irreducible water saturation is created. The general trend shows a decrease in permeability with increasing irreducible water saturation. Observation of the individual plots shows that a reasonably good relation between three petrophysical parameters exists. Therefore, if the particle size and the irreducible water saturation are known, the permeability can be estimated from

$$K = a \cdot S_{wi}^b \quad (4.7)$$

where:

K : permeability,

a : grain size coefficient,

S_{wi} : irreducible water saturation,

b : saturation exponent,

R^2 : quality of fit of plotted parameters.

Well B2-NC-74A

In **FIGURE 4.18**, Well B2-NC-74A has a defined trendline which demonstrates a general decrease in permeability with increasing irreducible water saturation. The power law is in good approximation as shown by the shape of the trendline. The accuracy of regression is moderate with R^2 value of 0.6592. Power law results in the equation, $K = 0.5843 * S_{wi}^{2.138}$ with a grain size coefficient of 0.5843 and saturation coefficient of 2.138. The permeability at any point on the plot is easily predicted by simply inputting the irreducible water saturation fraction value at such a point.

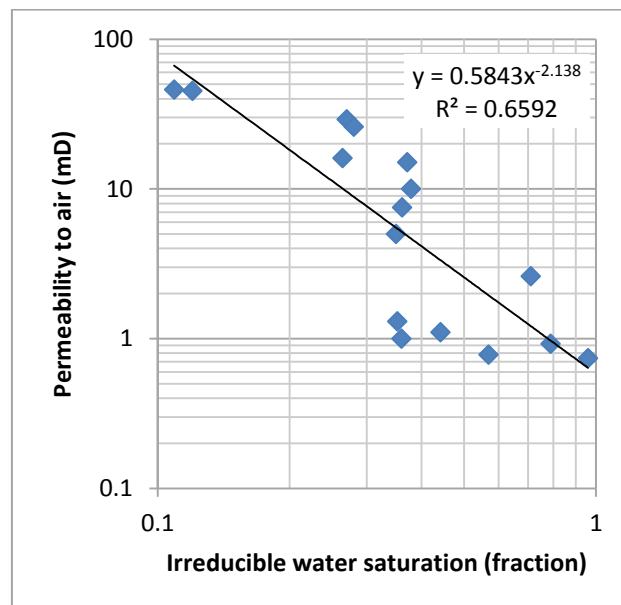


FIGURE 4.18: K_{air} versus S_{wi} for Well B2-NC-74A

Well B5-NC-74A

FIGURE 4.19 shows a defined trendline between permeability to air and irreducible water saturation for Well B5-NC-74A. The R^2 value when compared to Well B2-NC-74A is less, however, it has a higher saturation exponent value of 2.244. Well B5-NC-74A and Well B2-NC-74A show a nearly similar rate of decrease in permeability with increase in irreducible water saturation as shown by their "a" values of 0.5843 and 0.4268 respectively. This implies that well B2-NC-74A will lose permeability with increasing irreducible water saturation at a slightly faster rate than Well B5-NC-74A would. Permeability can be predicted at any point on the plot by simply inputting the S_{wi} value at such a point.

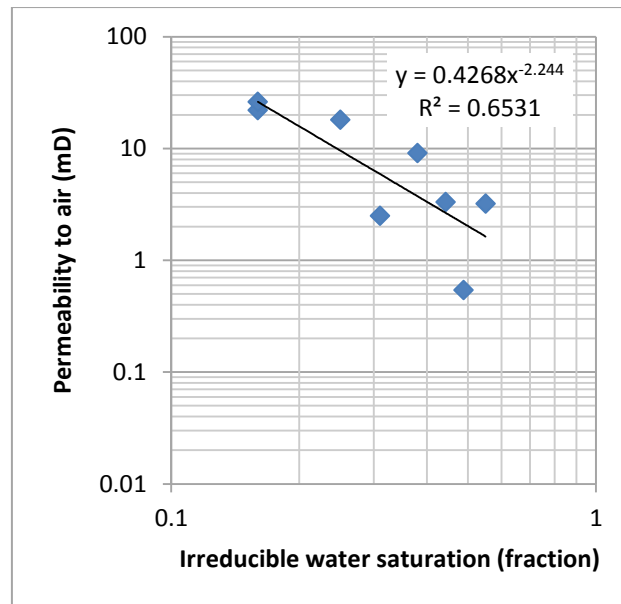


FIGURE 4.19: K_{air} versus S_{wi} for Well B5-NC-74A

Well B6-NC-74A

Comparatively, this is the well (**FIGURE 4.20**) with the best approximation and quality of fit as shown by its R^2 value of 0.8900. The accuracy of regression is highest in this well and the data points are all nearly on the trendline. The permeability to air decreases with increase in irreducible water saturation. This trend is likely to be very reliable given by its R^2 value of 0.8900. Therefore permeability predictions using S_{wi} values will be of high level of certainty.

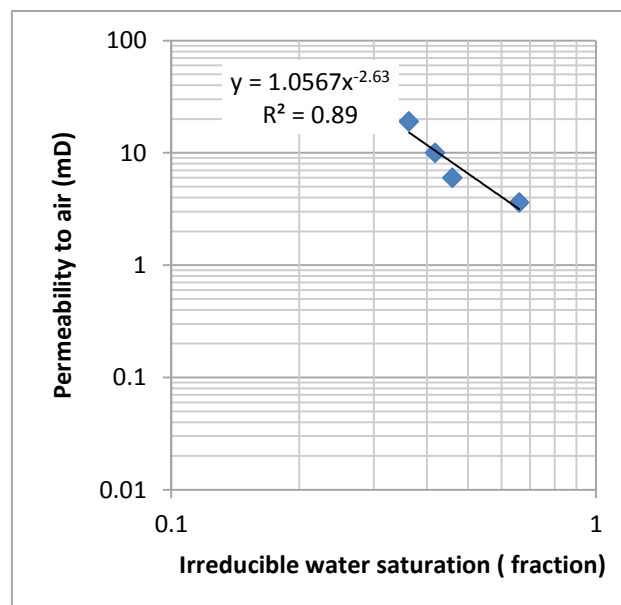


FIGURE 4.20: K_{air} versus S_{wi} for Well B6-NC-74A

The power law equation is $K = 1.0567 * S_{wi}^{2.63}$ and has a grain size coefficient of 1.0567 and saturation exponent of 2.63.

Well B8-NC-74A

This is the well (**FIGURE 4.21**) with the least regression quality among all (R^2 value of 0.3421). Even though the trendline is straight, the data points are largely dispersed from it; however, it exhibits a general decrease in permeability with increase in irreducible water saturation. Its power law equation is described by $K = 1.1944 * S_{wi}^{1.815}$ which is very useful in the prediction of permeability at any S_{wi} value.

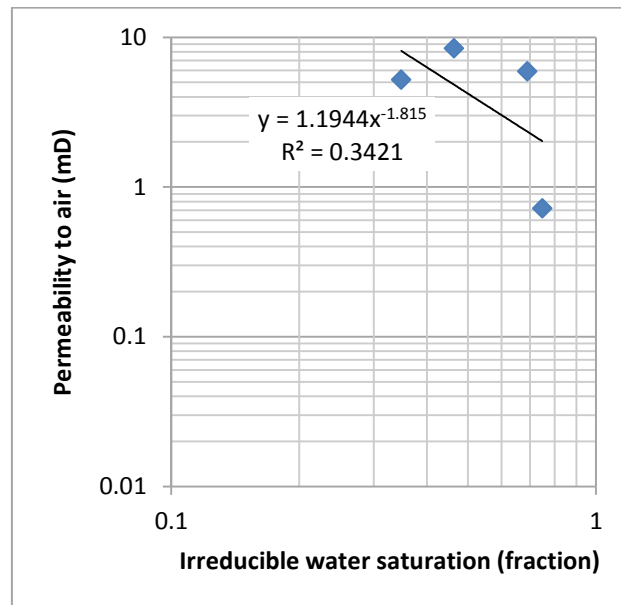


FIGURE 4.21: K_{air} versus S_{wi} for Well B8-NC-74A

Compilation for all wells

In order to have a holistic approach to the petrophysical properties of all the wells under investigation, data from all 4 (four) wells were combined to create as before, plots of (1) permeability to air versus porosity fraction, and (2) permeability to air versus irreducible water saturation.

In the composite wells in **FIGURE 4.22**, we find a defined trendline which implies that the power law is in good approximation. More data points cluster around the trendline than fits directly on it. It has R^2 value of 0.6176 which can be inferred as an average of all R^2 values. It also shows an overall increase in permeability with porosity. Power law results in the equation, $K = 993.15 * \phi^{3.2607}$ with a grain size coefficient of 993.15 and cementation-compaction coefficient of 3.2607. This is useful in the prediction of permeability at any point on the plot. You do so by simply introducing the matrix porosity, fraction value at such a point to derive the permeability value.

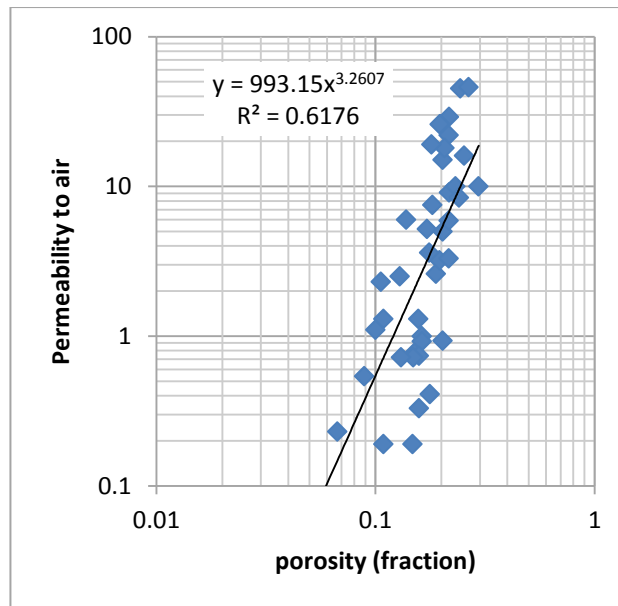


FIGURE 4.22: K_{air} versus ϕ for all wells

FIGURE 4.23 is the permeability relationship with irreducible water saturation for all the wells. Power law equation is given by $K = 0.8153 * S_{wi}^{1.938}$ and shows a straight trendline result describing overall loss in permeability to air as irreducible water saturation for all the wells increases. It is also useful in the prediction of permeability at any given S_{wi} value. The regression accuracy is not a perfect one (i.e. not approximately 1) but fair as shown by the R^2 value of 0.5727.

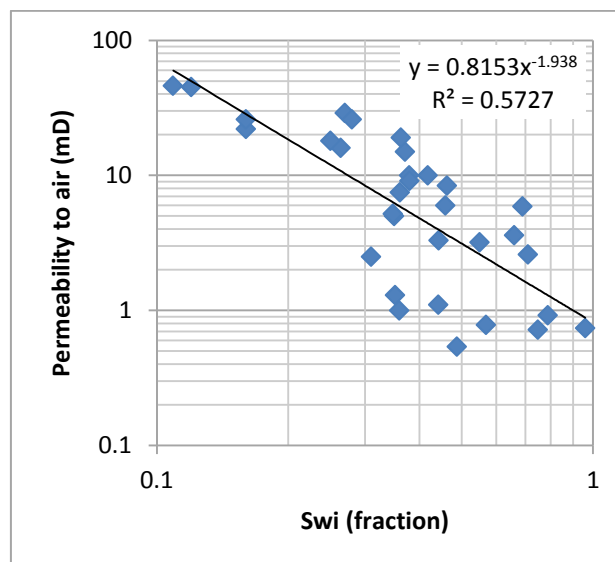


FIGURE 4.23: K_{air} versus S_{wi} for all wells

TABLE 4.4 is a summary of the petrophysical parameters obtained from the analysis of Archie equations of the individual and composite wells of previously discussed plots (FIGURES 4.13 through 4.23).

TABLE 4.4: Petrophysical parameters of the individual and composite wells (**FIGURES 4.13 – 4.23**)

Subject Well	Plot of K_{air} versus ϕ on a logarithmic scale			Plot of K_{air} versus S_{wi} on a logarithmic scale		
	Equation	a	b	Equation	a	b
B2-NC-74A	$R^2 = 0.6303$	10223	4.6132	$R^2 = 0.6592$	0.5843	2.138
B5-NC-74A	$R^2 = 0.8$	713.09	2.9168	$R^2 = 0.6531$	0.4268	2.244
B6-NC-74A	$R^2 = 0.5204$	2219.8	3.7724	$R^2 = 0.89$	1.0567	2.63
B8-NC-74A	$R^2 = 0.275$	65.617	1.8919	$R^2 = 0.3421$	1.1944	1.815
ALL WELLS	$R^2 = 0.6176$	993.15	3.2607	$R^2 = 0.5727$	0.8153	1.938

Results show that:

- Empirically determined porosity (ϕ) values for permeability (K), ranges from 1.8919 4.6132 with an overall mean value of 3.2607.
- Empirically determined irreducible water saturation (S_{wi}) values for permeability (K) ranges from 1.815..... 2.63 with an overall mean value of 1.938.
- There is no correlation between the “grain size coefficients” for correlation with porosity and irreducible water saturation. This indicates a more complex influence of pore size related dimensions.
- When compared with similar empirical equations from literature, there is a strong correlation between the empirically determined exponents from literature and the predicted exponents from our analyses. For example, as proposed by Wyllie and Rose (See page 48 Physical Properties of Rocks, J.H. Schön 1996), we find a generalized expression for K

$$K = a \cdot \frac{\phi^b}{S_{wi}^c} \quad (4.8)$$

where a , b and c are empirically determined.

$$\text{Timur (1968)} \quad K = 10^4 \cdot \frac{\phi^{4.5}}{S_{wi}^2} \quad (4.9)$$

$$\text{Our predicted} \quad K = A \cdot \frac{\phi^{3.2}}{S_{wi}^{1.9}} \quad (4.10)$$

Predicted correlates well with Timur (1968).

4.3 Detailed capillary pressure evaluation combined with permeability

Capillary pressure (P_c) is defined as the pressure difference between the non-wetting phase and the wetting phase as a function of the wetting phase saturation. It describes the height at which a fluid will rise in the reservoir and is an important parameter for the study of vertical saturation distribution. Capillary pressure curve is simulated in the laboratory and the applied fluid pressure is represented by the equivalent height above the free water level. An insight into the homogeneity or heterogeneity of the reservoir is depicted by the shape of the capillary curve in the transition zone (FIGURE 4.24). The steeper the capillary curves, the less uniform the pore throats i.e. the more heterogeneous the reservoir becomes.

Capillary pressure also offers us with a good indication of the permeability of the reservoir. A reservoir with low capillary pressures has large pore throat diameters and is a good indication for high permeability. Such reservoirs are usually coarse grained. Similarly, reservoirs with high capillary pressures exhibit small pore throats diameters, low permeability and are common with fine grained reservoirs.

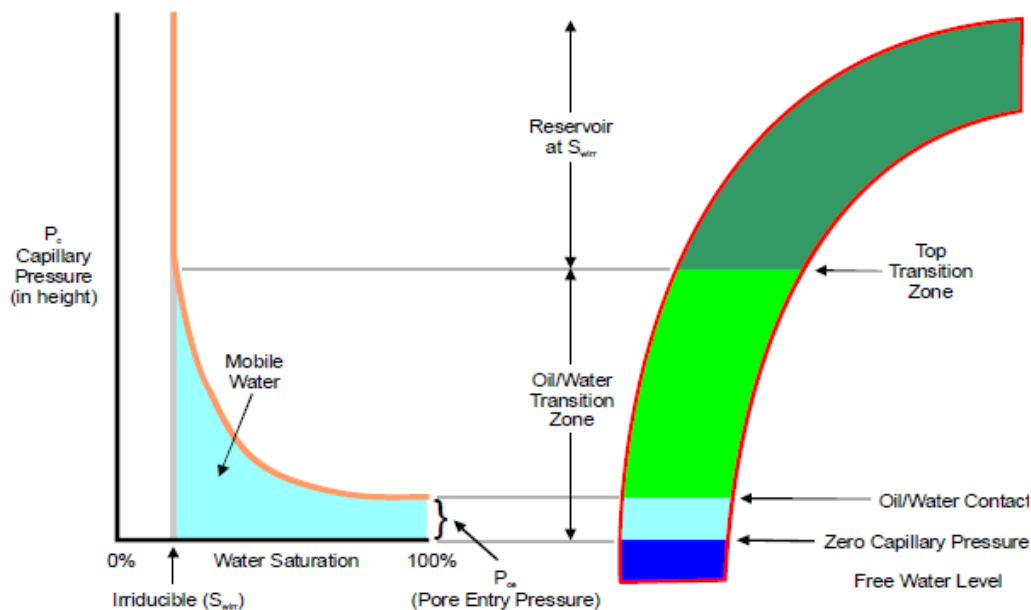


FIGURE 4.24: A schematic representation of the relationship between a capillary pressure curve and oil accumulation [Holmes, 2002]

Terminology:

- Irreducible water saturation (S_{wi}) – water saturation of bound capillary water.
- Pore entry pressure (P_{ce}) – minimum pressure required before oil can begin to invade the pore structure (displacement pressure).
- Transition zone – reservoir interval over which oil and water will flow.

Well B2-NC-74A

Representative curves of the core samples account for the influence of heterogeneity in a reservoir. Well B2-NC-74A (FIGURE 4.25) shows a combination of different capillary pressure curve types generated from representative core samples. Six (Sample Nos. 55, 56, 58, 70, 80, 91 & 106) out of the whole sample capillary pressure curves differ greatly from the general curve trend. A most plausible reason to account for this variation and steepness is a reservoir with less uniform pore throat and a heterogeneous condition. Whereas the greater set of the capillary pressure curves suggest good reservoir conditions, the other five depicts bad reservoir conditions. To highlight this disparity and make further comparisons, the capillary pressure curve plot for Well B2-NC-74A is unbundled into two plots as seen in FIGURE 4.26 and FIGURE 4.27.

From observation of FIGURE 4.26, the capillary pressure curves are not steep and all reduce to almost one pattern of capillary pressure curve. Core samples obtained from this depth section of the well are typical of rock with good reservoir conditions. The reservoir is homogeneous, coarse grained and has far less displacement pressure when compared with FIGURE 4.27. By implication it should demonstrate larger pore throat diameter and higher permeability.

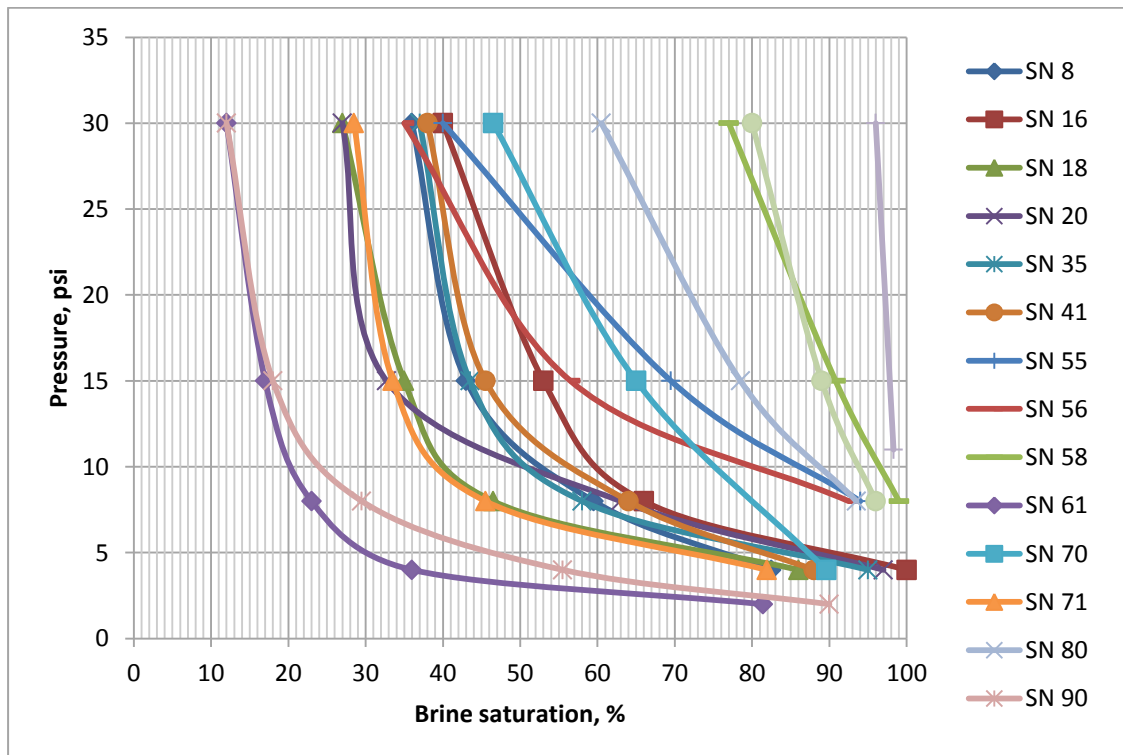


FIGURE 4.25: Capillary pressure curve for Well B2-NC-74A

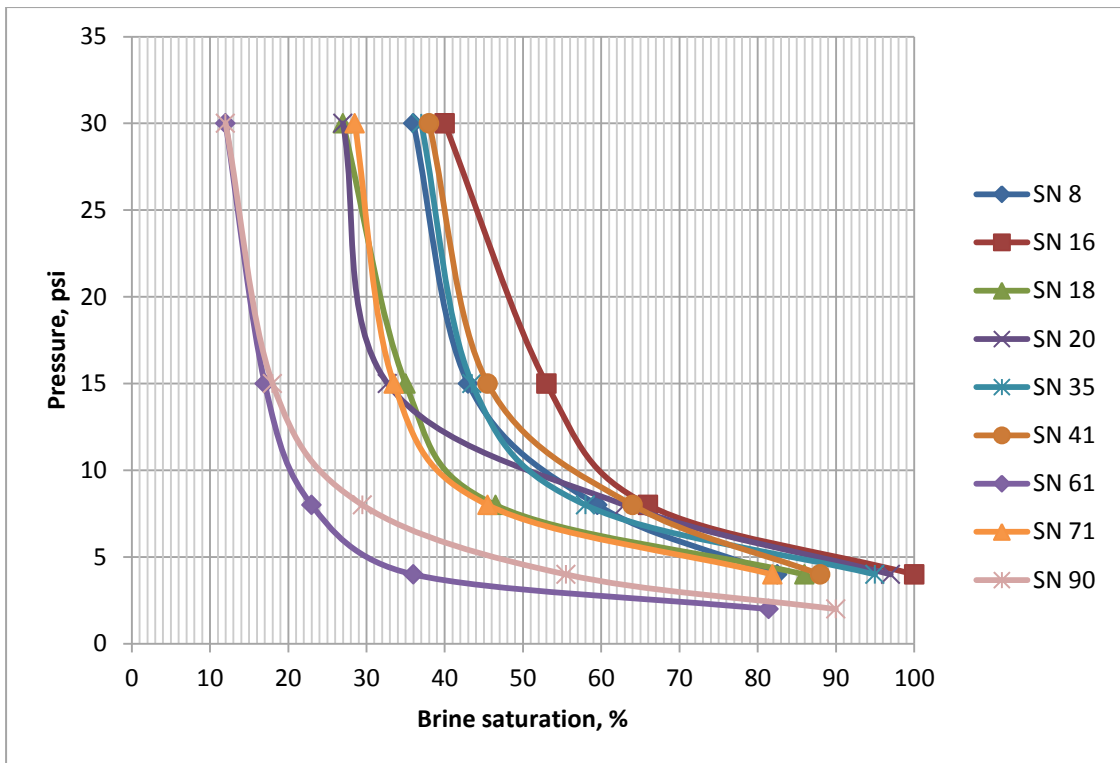


FIGURE 4.26: Capillary pressure curve for Well B2-NC-74A(1) homogeneous

In FIGURE 4.27, we see strong disparity in the P_c curves. The curves are steep with high displacement pressure which is a good indication of fine grained, small pore throat diameter and low permeability heterogeneous reservoir condition.

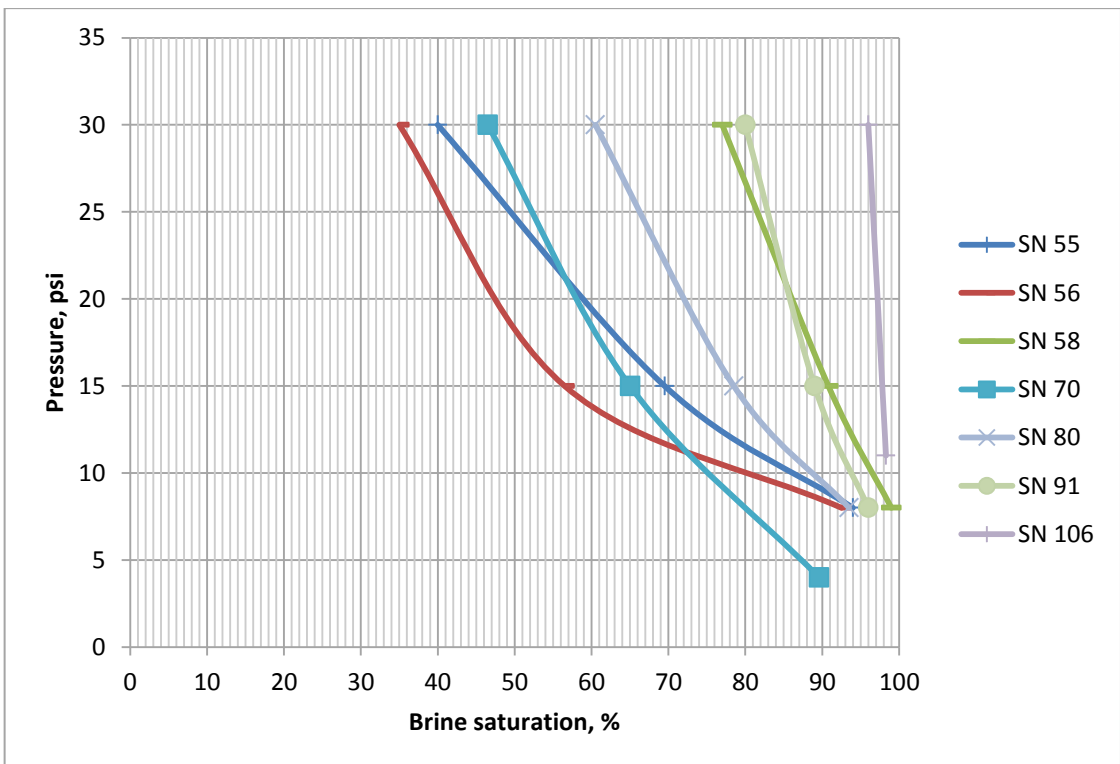


FIGURE 4.27: Capillary pressure curve for Well B2-NC-74A(2) heterogeneous

To further corroborate the findings from our earlier analysis, **TABLE 4.5** shows the Sample Numbers, Permeabilities and Porosities of the split plots.

TABLE 4.5: Comparison of split wells

Well B2-NC-74A (1) homogenous			Well B2-NC-74A (2) heterogeneous		
Sample Number	Permeability, K (mD)	Porosity (%)	Sample Number	Permeability, K (mD)	Porosity (%)
SN 8	1.3	10.9	SN 55	1	16.3
SN 16	10	29.6	SN 56	5	20.3
SN 18	29	21.7	SN 58	2.6	18.9
SN 20	16	25.4	SN 70	1.1	10
SN 35	7.5	18.2	SN 80	0.78	15.2
SN 41	15	20.3	SN 91	0.92	16.3
SN 61	45	24.4	SN 106	0.74	
SN 71	26	19.8			
SN 90	46	26.6			

TABLE 4.5 clearly shows the reason for the difference in reservoir quality between the compared sections of Well B2-NC-74A. The permeability and porosity values of well section B2-NC-74A(1) are way higher relative to well section B2-NC-74A(2). Higher permeabilities will obviously require lower capillary pressures and vice versa. For instance, SN61 and SN90 with permeabilities of 45mD and 46mD respectively exhibit the lowest displacement pressures than their equivalents in well section B2-NC-74A(2). In addition to their larger pore spaces, they demonstrate reservoirs with better conditions than well section B2-NC-74A(2).

Well B5-NC-74A

The capillary pressure curves of **FIGURE 4.28** are not steep and all share almost great similarity in their curve pattern. This is a reflection of homogeneity and a desirable quality of good reservoir conditions. The reservoir conditions of Well B5-NC-74A is therefore comparable to the well section B2-NC-74A(1) (**FIGURE 4.26**). On the overall the displacement pressure is a little relatively higher than that of well section B2-NC-74A(1) but by implication it should also hold large pore throat diameters and high permeability.

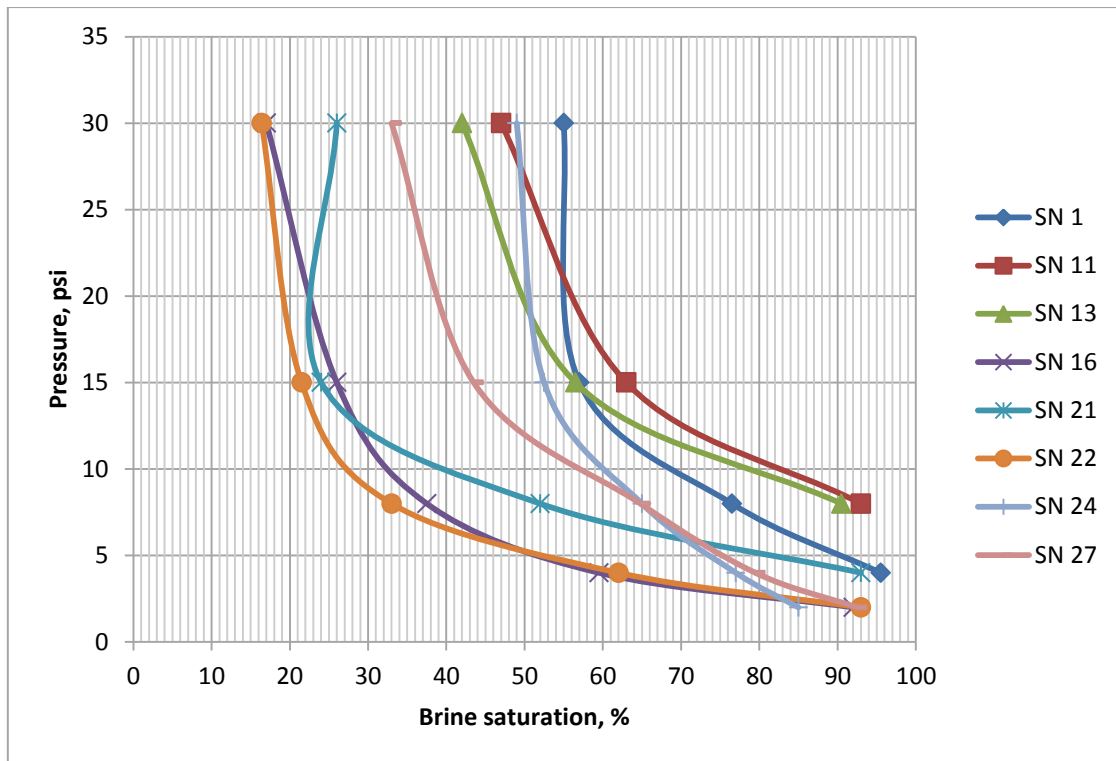


FIGURE 4.28: Capillary pressure curve for Well B5-NC-74A

The permeability and porosity data of the core samples for Well B5-NC-74A are shown in **TABLE 4.6**. The generated capillary curves correlates fairly well with the information in **TABLE 4.6**. For example, SN22 in **FIGURE 4.28** has the lowest displacement pressure which is understandable given its maximum permeability value of 26mD. The pore entry pressures seem to increase as permeability decreases.

TABLE 4.6: Well B5-NC-74A

Sample Number	Permeability, K (mD)	Porosity (%)
SN 1	3.2	19.6
SN 11	3.3	21.6
SN 13	9.1	21.7
SN 16	22	21.6
SN 21	18	20.7
SN 22	26	19.7
SN 24	0.54	8.9
SN 27	2.5	12.9

Well B6-NC-74A

There is homogeneity in the section of the reservoir covered by sample numbers SN68, SN82 and SN90 as shown by the capillary pressure curves (**FIGURE 4.29**). All the sample capillary pressure curves share almost the same displacement pressures as they approximate nearly to the same pattern except for SN128 with a steep pattern which suggests an indication

of heterogeneity. The reservoir condition in the homogenous section is good. However, the displacement pressures of Well B6-NC-74A still seem way higher than the previously

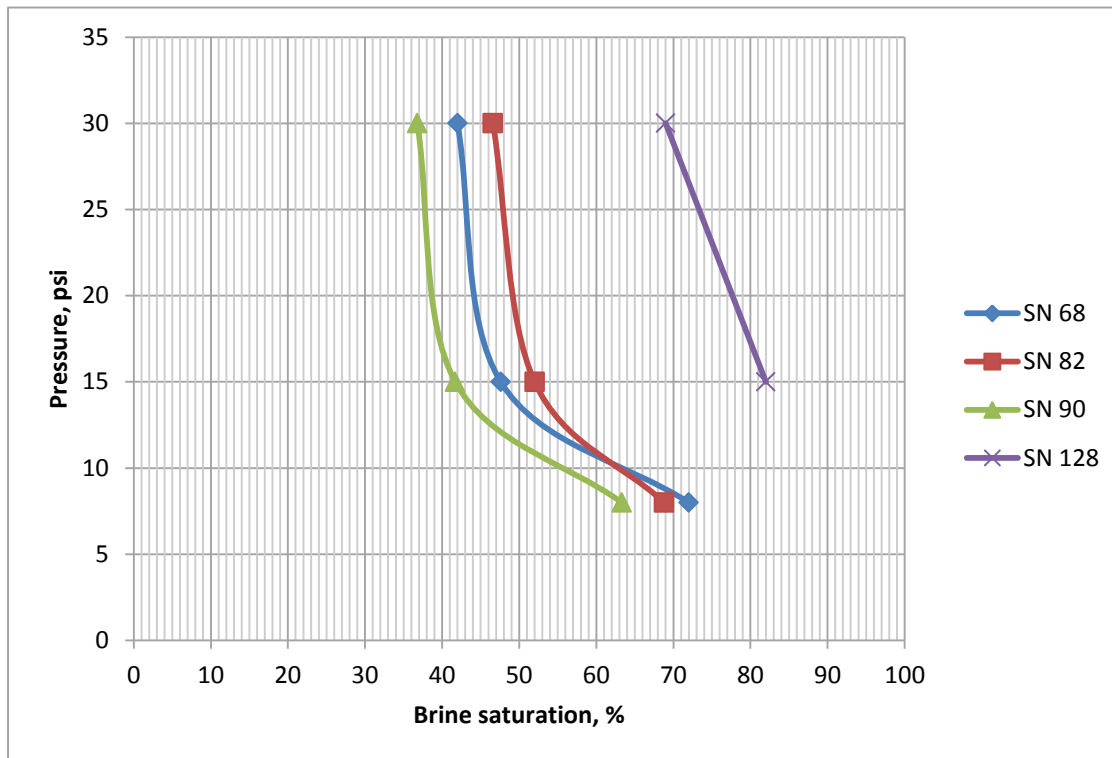


FIGURE 4.29: Capillary pressure curve for Well B6-NC-74A

discussed wells (Well B2-NC-74A(1) & Well B5-NC-74A). Comparatively and according to the number of the sample capillary pressure curves with the least displacement pressures which in turn reflects large permeability and pore throat, the order of reservoirs with decreasing desirable condition is Well B2-NC-74A(1); Well B5-NC-74A; Well B6-NC-74A and Well B8-NC-74A(**FIGURE 4.30**).

The created capillary pressure curves correlates fairly well with the information in **TABLE 4.7**. For example, SN90 in **FIGURE 4.29** has the lowest displacement pressure given its

TABLE 4.7: Well B6-NC-74A

Sample Number	Permeability, K (mD)	Porosity (%)
SN 68	10	23.2
SN 82	6	13.8
SN 90	19	18
SN 128	3.6	17.6

maximum permeability value of 19mD. Pore entry pressures seem to increase as permeability decreases. SN128 with the least permeability of 3.6mD has the highest pore entry pressure.

This is quite understandable given the heterogeneity of that section of the well as confirmed by its incomparable porosity of 17.6%.

Well B8-NC-74A

The reservoir condition in this well is dispersed as only the well section covered by SN163 &

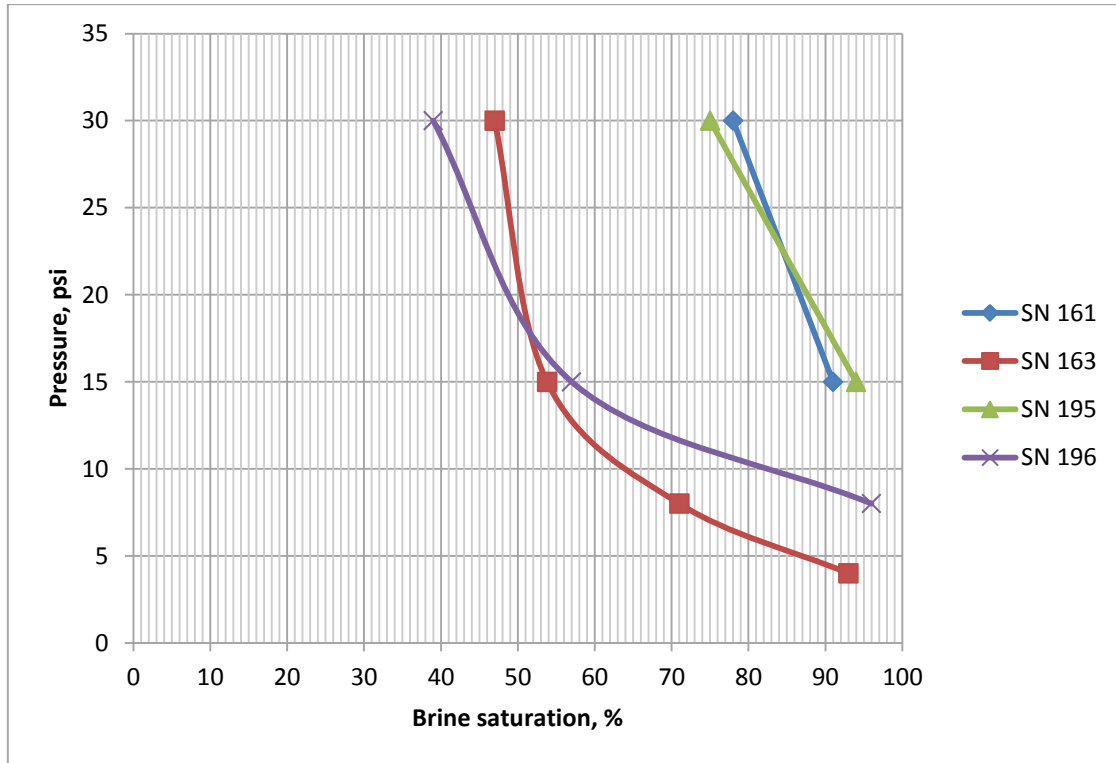


FIGURE 4.30: Capillary pressure curve for Well B8-NC-74A

SN196 seem favourable for homogeneity in reservoir quality. The section of the well covered by SN161 & SN195 is heterogeneous as depicted by the steep pattern of the capillary pressure curves. Comparing the density of favourable capillary pressure curves, Well B8-NC-74A seems to be the least in reservoir quality among all. Only one (SN163) out of the four capillary pressure curves has relatively low pore entry pressure which is not sufficient for the overall productivity of the well.

TABLE 4.8: Well B8-NC-74A

Sample Number	Permeability, K (mD)	Porosity (%)
SN 161	0.72	14.9
SN 163	8.4	24.1
SN 195	5.9	21.6
SN 196	5.2	17.2

In **TABLE 4.8** and as confirmed by **FIGURE 4.30**, we find that SN163 with the highest permeability and porosity has the lowest pore entry pressure. Again, this explains the

relationship among pore throat diameter, permeability and capillary pressure. Pore entry pressures seem to increase as permeability decreases. Even though SN195 has appreciable permeability and porosity, the heterogeneity of that section of the well made it difficult for this sample to plot correctly. Also in porosity versus permeability (**FIGURE 4.17**) you find two groups as separated by two distinct permeability-porosity relationships. This is a strong reflection and reconfirmation of the presence of two lithologies in this well. The first group identified as higher dataset (red coloured) with high permeability values are coarse-grained and correlates very well with SN163 and SN196 given their low pore entry pressures. The second group constituted by the lower dataset (blue coloured) have lower permeability and are fine-grained as exemplified by their high pore entry pressures. SN161 and SN195 belong to this second group.

4.4 Summary

A total of four (4) wells were subjected to core data analysis. Relationship between resistivity and porosity showed that all the investigated wells exhibited a general decrease in formation resistivity factor as porosity increased. I observed a decreasing accuracy of regression quality of the wells in the following order B6-NC-74A; B5-NC-74A; B2-NC-74A and B8-NC-74A. The cementation exponent values ranged from 1.813 to 2.010 and had an overall mean value of 1.90. Results from composite well plot showed that the overall mean value of regression accuracy is 0.87 with a cementation exponent value of 1.90.

The porosity-permeability correlation of all the wells I investigated described a general decrease in permeability as porosity decreased. Empirically determined porosity values for permeability ranged from 1.8919 through 4.6132 with an overall mean value of 3.2607. However, permeability decreased with increasing irreducible water saturation in all the wells. The empirically determined irreducible water saturation values for permeability ranged from 1.815 through 2.63 with an overall mean value of 1.938. From my analysis and comparison with literature, I observed a strong correlation between the empirically determined exponents and predicted exponents.

I found from the capillary pressure curves, two wells (B2-NC-74A & B5-NC-74A) with desirable reservoir conditions (low capillary pore entry pressure, large pore throat size and permeability). However from further analysis, only a section of the B2-NC-74A well [B2-NC-74A(1)] is in good reservoir condition. This I demonstrated clearly by splitting the Well B2-NC-74A into two seemingly distinct sections based on the similarity of shape of the

capillary pressure curves. Well section B2-NC-74A(1) is the good one and likely coarse grained and well section B2-NC-74A(2) is the bad one. The reservoir condition of well B6-NC-74A appears fair if we disregard the only steep capillary pressure curve on that plot. Well B8-NC-74A is situated in a reservoir with two lithologies as uncovered by detailed analyses. Interpretations identify both fine and coarse grained lithologies being present in this well.

5 LOG DATA ANALYSIS

5.1 Principles

This is the principle of formation evaluation. Log analysis involves majorly two basic steps:

1. A qualitative analysis – “Quick-look method”,
2. A quantitative analysis.

The qualitative analysis describes the lithology and zones of interest by taking a snappy look at the logs for possible indications of hydrocarbons that could provide further reasons for a detailed investigation.

The quantitative analysis of our log data involved the following important steps:

1. Volume of shale
2. Porosity
3. Water saturation
4. Permeability

5.1.1 Volume of shale

The shale content of logs is evaluated using any of the following methods:

- Gamma Ray Log Analysis
- Neutron-Density combination

As previously captured in chapter one, the basis in gamma ray analysis is the correlation between shale content and gamma activity. The volume of shale is expressed as a decimal fraction or percentage. The basis of evaluation of volume of shale V_{shale} using Neutron – Density – Combination is the high sensitivity of neutron logs to shale (clay bound water). Neutron logs count the number of hydrogen atoms in a formation.

5.1.2 Porosity

Porosity is necessary for the occupation of fluids in the reservoir. We estimate the porosity from the neutron, density and sonic logs. Porosity determination using logs is often an indirect method because some additional matrix parameters and a rock model are usually required. Therefore the porosity we get in the end is dependent on the rock composition.

5.1.3 Water saturation

The log analysis for water saturation relates to the resistivity of the formation. The Archie's equations are applied where shale content is minimal. Input parameters will include porosity log data, resistivity log data and Archie's parameters "*a*", "*m*", "*n*" from core laboratory measurements and resistivity R_w .

5.1.4 Permeability

There is no standard permeability log. Derivation and analysis of permeability log is done using equations from poro-perm correlation of core measurements. Having derived the constant, *K* from poro-perm correlation, a permeability log can be created by substituting log porosity values into the equation. A good example is using the **Multi Line Formulae** of Interactive Petrophysics (IP) software programme.

5.2 Log analysis using Interactive Petrophysics (IP)

To maximize the potential from the four (4) well data, Interactive Petrophysics (IP) was used in the log analysis for the evaluation of volume of shale, porosity and water saturation. The process began with the creation of new database and wells on the main menu. These wells are later loaded with log and core data (referred to as **ASCII load**) required for the log analysis. Load data options are available under the Input/Output menu. Having imported the log curves and core analysis measurements, the programme software is now able to carry out the following log analysis:

5.2.1 Volume of shale calculation

This is derived from clay volume analysis. It calculates clay volume curves from multiple clay indicators. This procedure required gamma ray, neutron, resistivity, density and sonic curve information inputted into a well. The IP software is run to generate results which include minimum clay volume VCLmin, average clay volume VCLAV and clay volume from gamma ray VCLGR. The minimum clay volume VCLmin gave the lowest value with VCLGR being the highest. The anomalous VCLGR value is explained by potassium feldspar and other radioactive contents that may be present in the carbonate reservoir and not shale and as such is ignored. A more realistic shale volume is the minimum clay volume VCLmin and is displayed on the log plots (see file jacket on inside back cover for attached correct-scaled log plots; **CD-ROM** for soft copies).

5.2.2 Porosity and water saturation calculations

This log analysis begins with the loading of porosity and resistivity logs, and core measurements into a given well. Porosity and water saturation analysis module interactively

calculates porosity(PHI), water saturation S_w etc. The module is accessed under the main menu **Interpretation**. A porosity and water saturation dialogue box opens for the selection of porosity and water saturation model of choice. The **Initial porosity model** used is the Neutron Density model. Archie saturation equation was applied for water saturation because of low shale volume. Result curves for porosity and water saturation are finally created and saved in the **Output Set**. These result curves vary as Archie parameter set " a ", " m ", " n " changes. Result curves are finally displayed on a log plot by clicking on the curve in the Output Set and dragging onto the work area of the log plot format (See file jacket on inside back cover for attached correct-scaled log plots; **CD-ROM** for soft copies).

5.2.3 Resistivity R_w calculations

Since no section on the log plot is saturated by water only, R_w is substituted by apparent water resistivity R_{wa} and processed by Interactive Petrophysics IP on the basis of the expression $R_{wa} = \frac{Phi * R_t}{a}$

where:

R_{wa} : apparent water resistivity,

Phi : porosity from log,

R_t : Resistivity of the formation,

a : Archie parameter.

A second possibility to determining R_w is the availability of neighbouring wells with depth sections completely saturated with water. However, in the absence of such the apparent water resistivity is the closest approximation at our disposal. Lastly, IP also offers a default R_w value of 0.1ohm which is also useful in saturation calculations.

6 CONVENTIONAL ANALYSIS

6.1 Porosity

6.1.1 Calculation with Interactive Petrophysics (IP)

In the conventional porosity analysis, I simply created porosity curves from raw porosity log data files using default Archie parameter set ($a = 1, m = 2, n = 2$) hereafter tagged RB1 (Result-Basil 1). A porosity log is created by clicking on the curve in the Output Set RB1 and dragging onto the work area of the log plot format. Observably, change of parameter sets to a set of different values shows no effect on the conventional porosity curves implemented with IP. The reason is because porosity is not influenced by " a ", " m ", " n " values.

6.1.2 Comparison with core data

The porosity from cores is at sampled depths in the subsurface and not continuous as those from logs. The core porosity compared very closely with log porosity as shown in the log plots of considered wells (See file jacket on inside back cover for attached correct scaled log plots; **CD-ROM** for soft copies). This is a good pointer indicating minimal comparative errors in the log and core data measurements.

6.2 Water saturation

6.2.1 Default parameters

The porosity and water saturation analysis dialogue box uses the loaded resistivity and porosity log raw data files to create a water saturation curve with default parameters as defined by RB1 ($a = 1, m = 2, n = 2$). To display the curve on the log plot format, the considered well and subsequently the Output Set is highlighted. The curve is then clicked and dragged onto a desired track on the log plot format area. This curve is sensitive to Archie parameters (" a ", " m " and " n ") as you shall soon see in the following chapter.

7 REPROCESSING WITH CORE DATA

7.1 Implementing core data for reprocessing water saturation using output parameter set RB2

In this chapter I tried to repeat the analysis as before but this time with a new output parameter set called RB2 ($a = x, m = y, n = z$). These x, y , and z values of RB2 parameter set in each well case are the average " a ", " m " and " n " values from core measurements for each well. Results show that a change in parameter set had no effect on the volume of shale and porosity but on the water saturation (See file jacket on inside back cover for attached correct-scaled log plots; **CD-ROM** for soft copies). This is understandable given the empirical relationships that govern their behaviour.

TABLE 7.1: Averaged Archie parameter set of individual wells

Well	Cored interval (ft)	Logged interval (ft)	Average parameter sets		
			a	m	n
B2-NC-74A	6127.8 – 6267.8	6030 – 6400	1	1.9	2.0262
B5-NC-74A	6112 – 6181	6030 – 6400	1	1.98	1.9875
B6-NC-74A	6156 – 6237	6040 – 6300	1	1.82	2.655
B8-NC-74A	6113 - 6170	6000 - 6400	1	1.89	2.1675

Well B2-NC-74A

The water saturation (S_w2) for average parameter set RB2 in this well is less than the water saturation (S_w1) of default parameter set RB1 as shown on the log plot (**FIGURE 7.1**; see also log plot image [**FIGURE 7.1**] drawn to scale in the file jacket on inside back cover). This is further made visible by a log plot of ($S_w2 - S_w1$). The difference in water saturation is highest in this well as depicted by the coverage area of the blue zone under ($S_w2 - S_w1$); the difference describes the decrease of water saturation (or increase of hydrocarbon) as a result of detailed analyses. The difference in bulk volume oil BVO2-BVO1 is between 0.001 and 0.01 or between 0.1 and 1 percent oil. This demonstrates the strong influence of Archie parameter on the saturation of a reservoir.

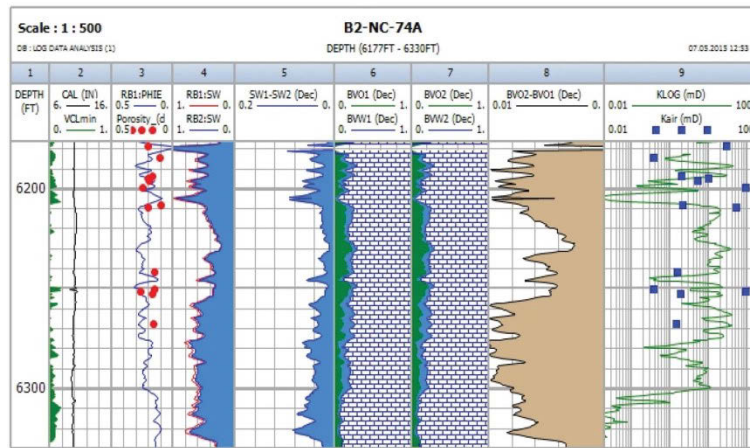


FIGURE 7.1: Log plot for Well B2-NC-74A (image plot not to scale)

Well B5-NC-74A

The water saturation (S_w2) for average parameter set RB2 is less than the default parameter set RB1 (S_w1) (FIGURE 7.2; see also log plot image [FIGURE 7.2] drawn to scale in the file jacket on inside back cover). This difference impacts positively on the bulk volume oil BVO2-BVO1 and is between 0.001 and 0.002 or between 0.1 and 0.2 percent oil increase along the entire well section. This is the well with the least percentage oil increase among studied wells. This is a second proof that saturation is strongly governed by Archie parameter set.

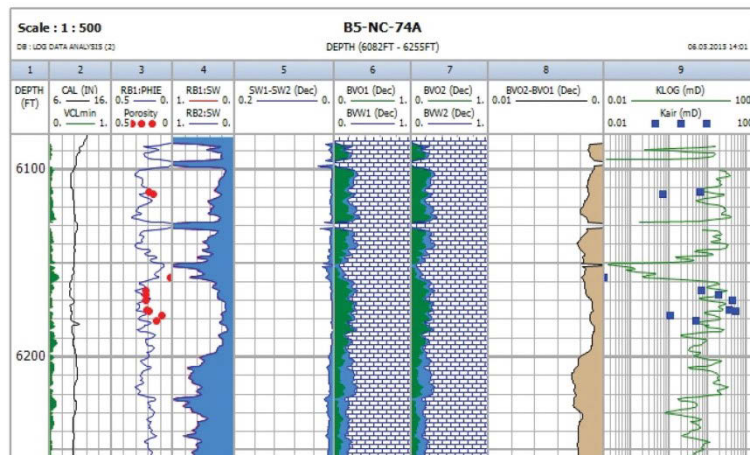


FIGURE 7.2: Log plot for Well B5-NC-74A (image plot not to scale)

Well B6-NC-74A

The water saturation (S_w1) from default parameter set RB1 and water saturation (S_w2) of average parameter set RB2 conspicuously differ from the other than in any other well studied. (FIGURE 7.3; see also log plot image [FIGURE 7.3] drawn to scale in the file jacket on inside back cover). The water saturation (S_w2) is much greater than water saturation (S_w1)

in major sections of the well. Consequently, sections with negative difference in bulk volume oil (increase in water saturation and decrease in hydrocarbon) are numerically higher than sections with positive difference (decrease in water saturation or increase in hydrocarbon). The difference in bulk volume oil BVO2-BVO1 for the negatively impacted long well section is between 0.001 and 0.02 or between 0.1 and 2 percent decrease in hydrocarbon. Similarly, the difference in bulk volume oil BVO2-BVO1 for the positively impacted short well section is between 0.001 and 0.013 or between 0.1 and 1.3 percent increase in hydrocarbon. This is another influence of Archie parameter set on reservoir saturation.

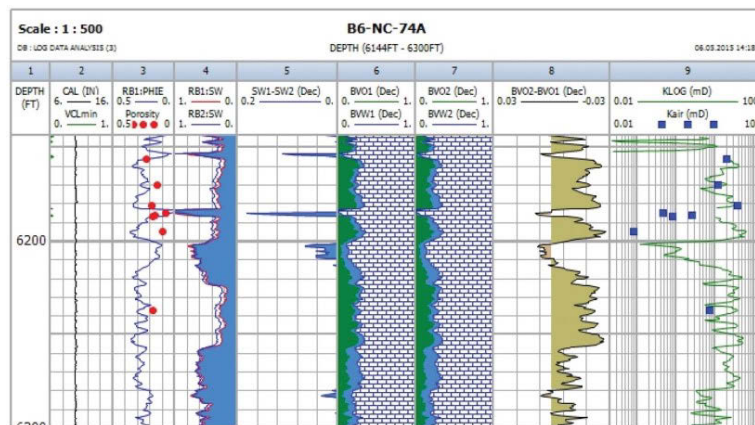


FIGURE 7.3: Log plot for Well B6-NC-74A (image plot not to scale)

Well B8-NC-74A

In Well B8-NC-74A, water saturation (S_w1) leads in major depth sections of the well and only along the middle section do you find (S_w2) higher (**FIGURE 7.4**; see also log plot image [**FIGURE 7.4**] drawn to scale in the file jacket on inside back cover). This means for this well a negative difference in BVO2-BVO1 (increase in water saturation or decrease in hydrocarbon) in the middle section of the well and a positive difference (decrease in water saturation or increase in hydrocarbon) in remaining sections of the well. The situation is similar to the preceding Well B6-NC-74A. The coverage area with increase in hydrocarbon is greater than the area with decrease in hydrocarbon. Increase in bulk volume oil is between 0.001 and 0.010 or 0.1 and 1 percent while decrease in bulk volume oil is between 0.001 and 0.005 or 0.1 and 0.5 percent. Similarly, this difference originates from the influence of Archie parameter set on the reservoir water saturation.

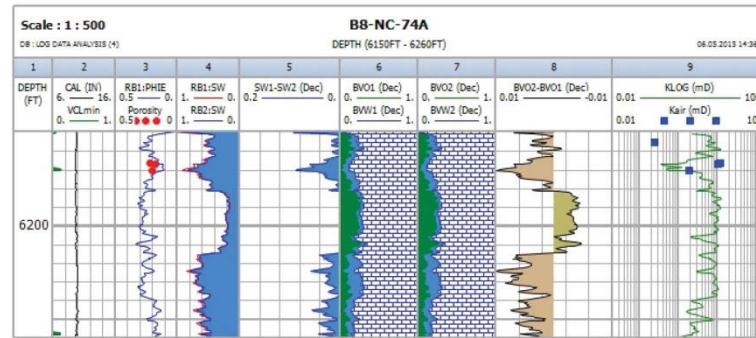


FIGURE 7.4: Log plot for Well B8-NC-74A (image plot not to scale)

7.2 Permeability estimate from poro-perm regression and comparison with core data

No standard wireline log exists for permeability. NMR (Nuclear Magnetic Resonance) logs estimate permeability but are expensive and rarely available. Measurements are usually based on drill core. A plot of porosity against permeability derived from core data generated an equation that correlates in the form $K = a \cdot \phi^b$. Substituting log porosity for core porosity using the Multi-Line Formulae of IP created an output curve for permeability log (KLOG). This estimated permeability log (KLOG) is then compared with core permeability (K_{air}) for each well. In general log permeability is continuous downhole for all the wells but core permeability is only sampled at discrete depths. However, at equally sampled depths, the permeability from cores shows higher readings than their log counterparts. A good explanation for this anomaly is the significant difference in subsurface porosity conditions compared to the surface. Log porosity reflects the porosity of the in-situ reservoir conditions while core porosity is porosity at surface conditions. Core porosity measurements are prone to increased porosity values due to the absence of in-situ reservoir lateral stress conditions and activities resulting from core extraction and preparation methods. This difference is the reason for the higher core permeability readings over log permeability readings at equally sampled depths. It is also a result of the inhomogeneity of the formation.

8 DISCUSSION

The study of the core and wireline log data included 4 (four) wells. These wells are B2-NC-74A; B5-NC-74A; B6-NC-74A and B8-NC-74A. Data from both core and wireline logs were combined, and with the aid of **Interactive Petrophysics (IP)** software programme log plots and crossplots of output curves used for data interpretation were created.

8.1 Log plots

Professional-looking log plots were created using Interactive Petrophysics (IP) software programme. At first the desired well is created and saved on the IP database. Core and log data are then loaded into the newly created wells using the **ASCII load** on the **Input/Output** menu. Care is taken to load and save curve data into the wells in stages to avoid stability issues arising from the system memory. The number of wells and curves that can be loaded simultaneously is limited by the amount of system memory available. However, this is not an issue with IP if the loaded conventional curves are less than 1500. There is considerable flexibility that allows you to build any kind of curve you desire using the **Multi-Line Formulae**. Additional curves absent from the loaded data such as (SW1-SW2), BVO1, BVO2, BVW1, BVW2, (BVO2-BVO1) and KLOG were created using the Multi-Line Formulae. The petrophysical formula describing the intended curve is entered into the Multi-Line Formulae and the resulting curve is automatically calculated and displayed in the chosen **Output Set** of the highlighted well. In order to display a log plot, select the intended well by double-clicking on it (well name is highlighted). Click on the **View menu** and then on the drop down icon **Create a new log plot for the current well**, a **Log plot format** is displayed. The log plot can now be customized by adding, moving or deleting log tracks and log curves to display preferred characteristics. To add a curve to the log plot, simply click on the desired curve under a given well Output Set, drag and drop on the chosen track on the log plot format. You can do some editing such as working on the grid, curves, shading, etc. of the log plot by clicking on the **Edit Format** button on the Log Plot window. All log plot (**FIGURES 7.1, 7.2, 7.3 and 7.4**) images are drawn to scale and have been carefully attached for you in the file jacket on the inside back cover; See also **CD-ROM** for soft copies.

8.2 Crossplots

Crossplots show relationships between petrophysical parameters of interest. In order to launch crossplots on **Interactive Petrophysics (IP)** software programme, first select a well of interest by double-clicking on it (well name is highlighted). From the **View menu**, select

crossplot. A crossplot dialogue is displayed which offers you the flexibility of defining the initial crossplot parameters like crossplot Scales, Discriminators, Z-axis, Options and Histograms. Curve names are then assigned to the desired axes, etc., click **Apply** and then **OK**. The intended crossplot is now displayed on screen.

To create a crossplot of (BVO2-BVO1) against RB1:PHIE, I entered the equation that defined the curve BVO2-BVO1 into the Multi-Line Formulae since such curve did not exist originally. BVO1 is the calculated bulk volume oil resulting from default Archie parameter set while BVO2 is the bulk volume oil from a new averaged Archie parameter set RB2. RB1:PHIE which represents the porosity of the reservoir. At first I created curves BVO1 and BVO2 by using the Multi-Line Formulae. Curve BVO1 = RB1:PHIE $(1 - S_w1)$ and curve BVO2 = RB1:PHIE $(1 - S_w2)$. Finally I created curve (BVO2-BVO1) by simply entering their difference into the Multi-Line Formulae. (BVO2-BVO1) is assigned to the Y-axis while RB1:PHIE is assigned to the X-axis. Click Apply and OK; automatically the desired crossplot is displayed for you on the screen.

The bulk volume oil (BVO) is the percentage of the total rock volume that is occupied by oil. BVO2-BVO1 tries to establish if a difference exists in the calculated bulk volume oil between the different Archie parameter sets. This difference could be positive or negative as determined by the crossplots. In the crossplot of (BVO2-BVO1) versus RB1: PHIE, the horizontal line running across the zero mark on the Y-axis distinguishes the plot area into two major domains. The area above the zero mark is the positive domain while the area below is the negative. The domains imply different things for the reservoir as shown in the following crossplots for the different wells.

Well B2-NC-74A

In Well B2-NC-74A (**FIGURE 8.1**) all the points plotted in the area above the horizontal line at the zero mark. This is an indication of a positive difference between BVO1 and BVO2. The implication for the reservoir is an increase in bulk volume oil due to a decrease in saturation exponent (n) from the default value. It is therefore reasonable to expect oil volumes greater than values from standard parameter sets out of this well section of the reservoir.

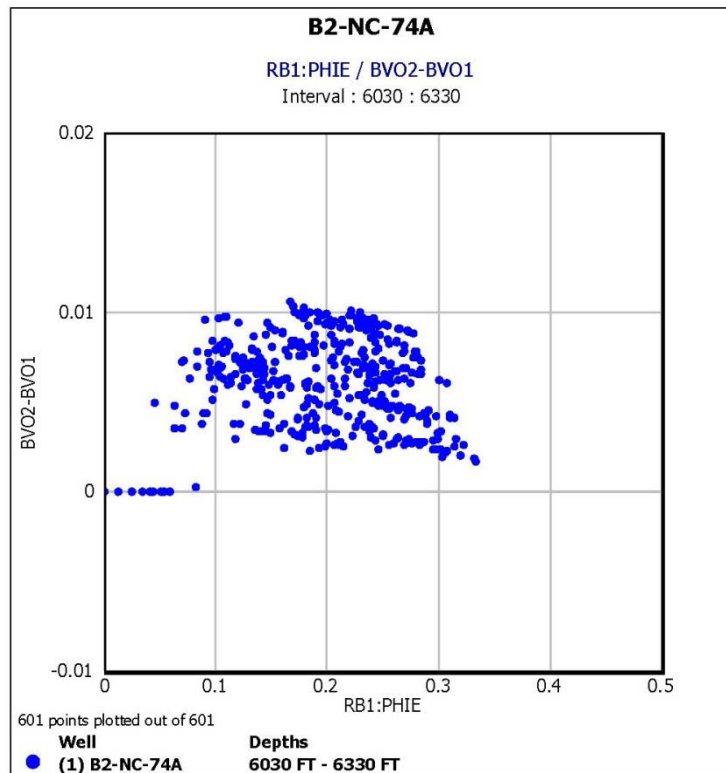


FIGURE 8.1: (BVO2-BVO1) - RB1:PHIE - Crossplot for Well B2-NC-74A

Well B5-NC-74A

The scenario in Well B2-NC-74A (**FIGURE 8.1**) is almost typified in Well B5-NC-74A (**FIGURE 8.2**). The major difference is in the magnitude of the bulk volume oil and density of the sampled points. All the plotted points lie in the positive domain and so Well B5-NC-74A shows an overall increase in the volume of oil due to a saturation exponent (n) lesser than the default value.

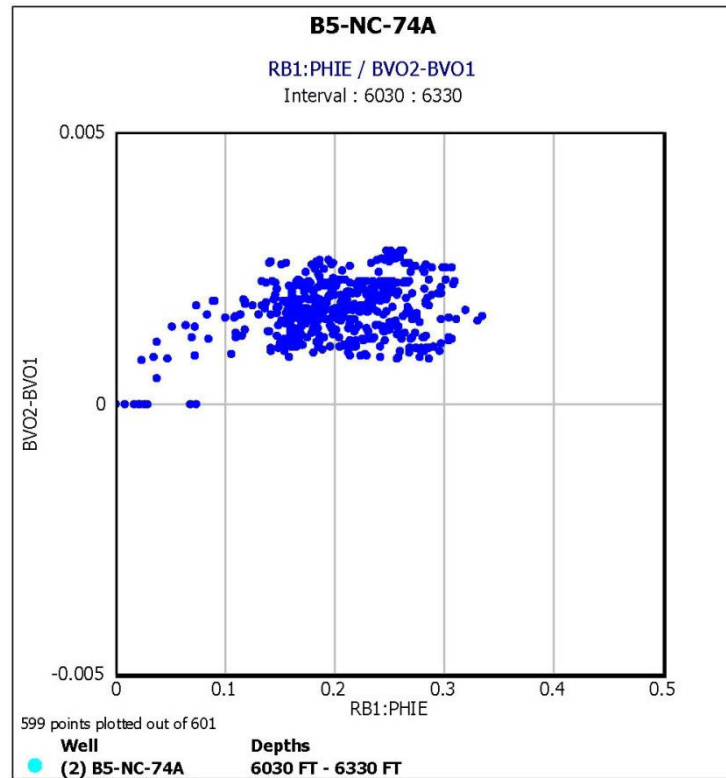


FIGURE 8.2: (BVO2-BVO1) - RB1: PHIE – Crossplot for Well B5-NC-74A

Well B6-NC-74A

This is the well with the highest saturation exponent (n) value. The plotted points are unequally distributed into the two major domains (**FIGURE 8.3**). The negative domain hosts a greater density of the plotted points because of the high water saturation exponent in this section. This high water saturation exponent is accompanied by decreased bulk volume oil. However, the fewer points which plotted in the positive domain demonstrates an increase in oil (corresponding decrease in saturation exponent (n)) in that section of the well. This section of the well is likely to be a good target for production.

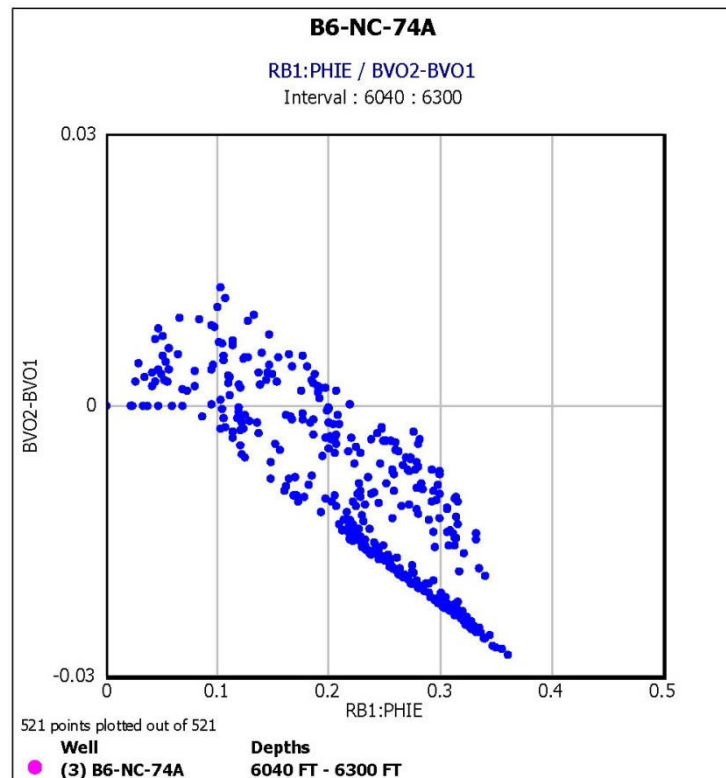


FIGURE 8.3: (BVO2-BVO1) - RB1: PHIE - Crossplot for Well B6-NC-74A

Well B8-NC-74A

Similar to the preceding Well B6-NC-74A (**FIGURE 8.3**) I found again in **FIGURE 8.4** for Well B8-NC-74A a dual distribution of the plotted points into the positive and negative domains of the crossplot. All plotted points in the positive domain (above the zero mark horizontal line across the Y-axis) imply an increase in bulk volume oil. The plotted points in the negative domain (below the zero mark horizontal line across the Y-axis) imply a decrease in bulk volume oil. Well productivity and completion considerations will give greater attention to the section of the well in the positive domain.

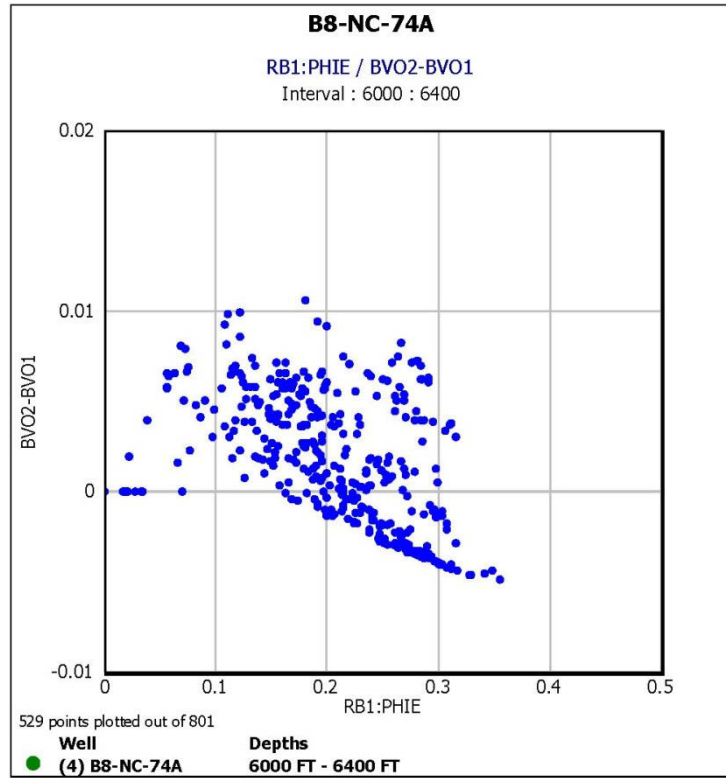


FIGURE 8.4: (BVO2-BVO1) - RB1: PHIE - Crossplot for Well B8-NC-74A

9 CONCLUSION

Initial hydrocarbon reserve estimation is strongly dependent on accurate determination of saturation exponent (n) and cementation exponent (m) values because they are of essential importance in the calculation of initial water saturations from logs. Utmost care should be taken during core measurements and determination of these exponents. Insufficient and inaccurate knowledge of these exponents may lead to gross over or under estimation of initial reserves, bypass of potentially productive pay zones and erroneous completion of ineffective pay resulting in heavy losses in the overall economics of the Oil and Gas business.

10 References

- Amyx, J.W., Bass, D.M, Jr., Whiting, R. L., 1960. Petroleum Reservoir Engineering Physical Properties, McGraw-Hill.
- Anderson, G., 1975. Coring and Core Analysis Handbook, Tulsa.
- Asquith, G., Krygowski, D., 2004. Basic Well Log Analysis (second edition), AAPG Methods in Exploration Series, No. 16, Tulsa.
- Dare, K.K., 1972. Core Analysis Techniques and Applications, American Institute of Mining, Metallurgical, and Petroleum Engineers SPE 4160, Eastern Regional Meeting Columbus Ohio, November 8-9.
- John, H.D., 1999. Basics of Oil and Gas Log Analysis, Doveton.
- Michael, H., 2002. Capillary Pressure and Relative Permeability Petrophysical Reservoir Models, Denver.
- Peters, E.J., 2012. Advanced Petrophysics, Live Oak.
- Serra, O., 2008. The Well Logging Handbook, Editions Technip.
- Schön, J.H., 1996. Physical Properties of Rocks, Volume 18, Elsevier.
- Schön, J.H., 2011. Physical Properties of Rocks, Elsevier.
- Schön, J.H., Borehole Geophysics study material Montanuniversität, Leoben, (unpublished).
- Schön, J.H., Petrophysics of Reservoir Rocks study material Montanuniversität, Leoben, (unpublished).
- Tiab, D., Donaldson, E. C., 2004. Petrophysics, Elsevier.

APPENDIXES

APPENDIX A [See **CD-ROM** for database/Log plots real-scale]

APPENDIX B [See attached file jacket on inside back cover for log plots real- scale (hard copies)]

APPENDIX A

DATABASE

3.1 CORE DATABASE

Definition of terms

FF: Formation resistivity factor

Krel(water): Relative permeability to water

Krel(oil): Relative permeability to oil

Pc: Capillary pressure

Kair: Permeability to air

m: Cementation exponent

n: Saturation exponent

Swirr: Irreducible water saturation

SCAL: Special Core Analysis

RCAL: Routine Core Analysis

3.1.1 Well B2-NC-74A

TABLE 3.1 Core data Well B2-NC-74A

Sample Number	Depth (ft)	Porosity (%)	Porosity (dec)	Log Por	FF	Log FF	m	n	K-air (mD)	Krel,water (mD)	Krel,water (mD)
8	6127.8	10.9	0.109	-0.962573502	76	1.880813592	1.9	2.14	1.3		
16	6136	29.6	0.296	-0.528708289	8	0.903089987	1.9	1.84	10		
18	6137.1	21.7	0.217	-0.663540266	19	1.278753601	1.9	2.04	29		
20	6139	25.4	0.254	-0.595166283	13	1.113943352	1.9	2.01	16		
35	6154.2	18.2	0.182	-0.739928612	27	1.431363764	1.9	1.97	7.5		
41	6179.2	20.3	0.203	-0.692503962	22	1.342422681	1.9	2.18	15		
46	6184.4	10.9	0.109	-0.962573502	45	1.653212514	1.9		0.19		
55	6193.9	16.3	0.163	-0.787812396	36	1.556302501	1.9	2.06	1		
56	6194.9	20.3	0.203	-0.692503962	19	1.278753601	1.9	2	5		
58	6196.2	18.9	0.189	-0.723538196	18	1.255272505	1.9	1.82	2.6		
61	6199.4	24.4	0.244	-0.612610174	19	1.278753601	1.9	1.92	45		
70	6208.2	10	0.1	-1	73	1.86332286	1.9	2	1.1		
71	6209.3	19.8	0.198	-0.70333481	22	1.342422681	1.9	2.43	26		
80	6241.4	15.2	0.152	-0.818156412	38	1.579783597	1.9	1.91	0.78		
90	6251.3	26.6	0.266	-0.575118363	16	1.204119983	1.9	1.99	46		
91	6252.5	16.3	0.163	-0.787812396	32	1.505149978	1.9	2.09	0.92		
97	6250.7	14.8	0.148	-0.829738285	35	1.544068044	1.9		0.19		
106	6267.6	15.8	0.158	-0.801342913	32	1.505149978	1.9	2.02	0.74		

TABLE 3.1 Core data Well B2-NC-74A (Continued)

Pc (Psi)	Sw-irr (%)	Sw-irr	K-Timur forward (mD)	A	K-predicted (our eq)	K-Timur/K-measured	K-predicted (our eq)/K-measured
	35.2	0.352	3.761264836	3456.28	0.901739144	2.893280643	0.693645496
	37.9	0.379	290.7597454	343.927	69.70778593	29.07597454	6.970778593
	27	0.27	141.6906766	2046.71	33.96943183	4.885885398	1.171359718
	26.4	0.264	300.9843198	531.589	72.15906215	18.81151999	4.509941384
	36.1	0.361	35.91756134	2088.12	8.611005193	4.789008179	1.148134026
	37.1	0.371	55.58842271	2698.4	13.32696817	3.705894848	0.888464545
					.	.	.
	36	0.36	21.99070832	454.738	5.272131417	21.99070832	5.272131417
	35	0.35	62.45915176	800.523	14.97418143	12.49183035	2.994836287
	71	0.71	11.00427465	2362.72	2.638204339	4.232413328	1.014693977
	12	0.12	1215.882832	370.101	291.5001184	27.01961849	6.477780408
	44.2	0.442	1.618659354	6795.75	0.388063209	1.471508504	0.352784735
	28	0.28	87.23229399	2980.55	20.91338355	3.35508823	0.804360906
	56.9	0.569	6.42793702	1213.45	1.541056714	8.240944898	1.975713736
	10.9	0.109	2173.273423	211.662	521.028378	47.2450744	11.32670387
	78.8	0.788	4.589779109	2004.45	1.100370133	4.988890335	1.196054492
					.	.	.
	96	0.96	2.687908157	10000	0.644408758	3.63230832	0.870822646
			AVERAGE	2397.4359	66.16726802	12.4268718	2.97926289
			AVEDEV	1742.9754	86.21578405	10.25918691	2.459574328

3.1.2 Well B5-NC-74A

TABLE 3.2 Core data Well B5-NC-74A

Sample Number	Depth (ft)	Porosity (%)	Porosity (dec)	log Por	FF	log FF	m	n	K-air (mD)	Krel,water (mD)	Krel,oil (mD)
1	6112	19.6	0.196	-0.707743929	24	1.380211242	1.98	1.91	3.2		
3	6113	15.8	0.158	-0.801342913	34	1.531478917	1.98	n/a	0.33		
5	6158	2	0.02	-1.698970004			1.98	n/a	0.01		
11	6165	21.6	0.216	-0.665546249	20	1.301029996	1.98	1.9	3.3		
13	6167	21.7	0.217	-0.663540266	17	1.230448921	1.98	1.93	9.1		
16	6170	21.6	0.216	-0.665546249	22	1.342422681	1.98	1.84	22		
21	6175	20.7	0.207	-0.684029655	20	1.301029996	1.98	1.88	18		
22	6176	19.7	0.197	-0.705533774	27	1.431363764	1.98	1.88	26		
24	6178	8.9	0.089	-1.050609993	192	2.283301229	1.98	2.53	0.54		
27	6181	12.9	0.129	-0.88941029	64	1.806179974	1.98	2.03	2.5		

TABLE 3.2 Core data Well B5-NC-74A (Continued)

Pc (Psi)	Swirr (%)	Sw-irr	K Timur forward mD	A	K-predicted (our eq) mD	K -Timur/K-measured	K-predicted(our eqn)/K-measured
	55	0.55	21.59866667	1481.57	4.206029031	6.749583335	1.314384072
	44.3	0.443	51.55068348	640.147	10.0387526	15.62141924	3.042046244
	38	0.38	71.53220444	1272.15	13.92986582	7.860681806	1.530754485
	16	0.16	395.1863314	556.699	76.95684218	17.96301506	3.498038281
	25	0.25	133.6554084	1346.75	26.0274644	7.425300465	1.445970244
	16	0.16	261.1307718	995.67	50.85145412	10.04349122	1.955825158
	48.8	0.488	0.785987041	6870.34	0.153059648	1.455531558	0.283443792
	31	0.31	10.34976071	2415.51	2.015466726	4.139904282	0.80618669
			AVERAGE	1947.36	23.02236682	8.907365871	1.734581121
			AVEDEV	1347.79	21.19216506	4.226456977	0.82304158

3.1.3 Well B6-NC-74A

TABLE 3.3 Core data Well B6-NC-74A

Sample Number	Depth (ft)	Porosity (%)	Porosity (dec)	log por	FF	log FF	m	n	K-air (mD)	Krel,water (mD)	Krel,oil (mD)	Pc (Psi)
68	6156	23.2	0.232	-0.634512015	17	1.230448921	1.82	2.72	10			
82	6170	13.8	0.138	-0.860120914	33	1.51851394	1.82	2.43	6			
90	6181	18	0.18	-0.744727495	24	1.380211242	1.82	2.73	19			
93	6185	6.7	0.067	-1.173925197	118	2.071882007	1.82	n/a	0.23			
94	6186	15.7	0.157	-0.804100348	28	1.447158031	1.82	„	1.3			
95	6187	17.7	0.177	-0.752026734	24	1.380211242	1.82	„	0.41			
103	6195	9.4	0.094	-1.026872146			1.82	„	0.04			
128	6237	17.6	0.176	-0.754487332	25	1.397940009	1.82	2.74	3.6			

TABLE 3.3 Core data Well B6-NC-74A(Continued)

Pc (Psi)	Swirr (%)	Sw-irr	Timur forward K	A	K Predicted (our eqn)	K Timur/K measured	K predicted(our eqn)/K measured
	41.8	0.418	79.86258594	1252.151	40.234227	7.986258594	4.0234227
	45.9	0.459	6.394852294	9382.547	3.221683042	1.065808716	0.536947174
	36.3	0.363	33.7997138	5621.349	17.02806567	1.778932305	0.896213982
	66	0.66	9.241003486	3895.681	4.655554633	2.566945413	1.29320962
			AVERAGE	5037.932	16.28488258	3.349486257	1.687448369
			AVEDEV	2464.016	12.34626375	2.318386168	1.167987165

3.1.4 Well B8-NC-74A

TABLE 3.4 Core data Well B8-NC-74A

Sample Number	Depth (ft)	Porosity (%)	Porosity (dec)	log por	FF	log FF	m	n	K-air (mD)	Krel,water (mD)	Krel,oil (mD)
161	6113	14.9	0.149	-0.826813732	31.8	1.50242712	1.89	2.24	0.72		
163	6115	24.1	0.241	-0.617982957	15.9	1.201397124	1.89	2.13	8.4		
166	6118	13.1	0.131	-0.882728704	34.4	1.536558443	1.89		0.72		
177	6132	10.6	0.106	-0.974694135	147	2.167317335	1.89		2.3		
181	6135	5.5					1.89		0.04		
184	6155	6.3					1.89		0.12		
195	6166	21.6	0.216	-0.665546249	15.2	1.181843588	1.89	2.15	5.9		
196	6167	17.2	0.172	-0.764471553	26.8	1.428134794	1.89	2.15	5.2		
199	6170	20.3	0.203	-0.692503962	20.3	1.307496038	1.89		0.93		

TABLE 3.4 Core data Well B8-NC-74A(Continued)

Pc (Psi)	Swirr (%)	Sw-irr	Timur forward K	A	K predicted (our eqn)	K Timur/K measured	K Predicted(our eqn)/K measured
	74.8	0.748	3.400439185	2117.37355	0.655963168	4.722832201	0.911059955
	46.3	0.463	77.25288544	1087.33803	14.90250073	9.196772076	1.77410723
	69	0.69	21.24925453	2776.56799	4.099096486	3.601568565	0.694762116
	34.8	0.348	29.9722622	1734.93744	5.781811991	5.763896577	1.111886921
			AVERAGE	1929.05425	6.359843094	5.821267355	1.122954056
			AVEDEV	517.916519	4.271328819	1.687752361	0.325576587

3.2 LOG DATABASE

Log data description

Curve Information			
MNEM	UNIT	API CODE	Curve Description
DEPT	FT		Depth
VCL	V/V		Volume of clay
DD	INCH		Caliper-bit size
SPI-CPX	V/V		Secondary Porosity Indicator = PHIT-PHIS ≥ 0 (Complex Litho Model)
SW-CPX	V/V		Formation Water Saturation ≤ 1.0 (Complex Litho Model)
PHIE-CPX	V/V		Effective Porosity (Complex Litho Model)
PHSW-CPX			Product (PHIE * SW) (Complex Litho Model)

3.2.1 Well B2-NC-74A

TABLE 3.5 Log data Well B2-NC-74A

DEPT (FT)	VCL (V/V)	DD (INCH)	SPI-CPX (V/V)	SW-CPX (V/V)	PHIE-CPX (V/V)	PHSW- CPX
6120	0	0.28018	-999.25	-999.25	-999.25	-999.25
6120.5	0	0.2857828	-999.25	-999.25	-999.25	-999.25
6121	0	0.2913857	-999.25	-999.25	-999.25	-999.25
6121.5	0	0.2969894	-999.25	-999.25	-999.25	-999.25
6122	0	0.3030443	-999.25	-999.25	-999.25	-999.25
6122.5	0	0.31147	-999.25	-999.25	-999.25	-999.25
6123	0	0.3198957	-999.25	-999.25	-999.25	-999.25
6123.5	0	0.3283215	-999.25	-999.25	-999.25	-999.25
6124	0	0.3367472	-999.25	-999.25	-999.25	-999.25
6124.5	0.0579949	0.3380632	0	0.9481059	0.0447834	0.0424594
6125	0.0671502	0.2822304	0	0.5526064	0.0867922	0.047962
6125.5	0.0678487	0.2519493	0	0.4116089	0.1208885	0.0497588
6126	0.0675513	0.2057562	0	0.3929605	0.1248162	0.0490478
6126.5	0.0593498	0.1338043	0	0.3904127	0.1202318	0.04694
6127	0.057325	0.0987425	0	0.454755	0.0927711	0.0421881
6127.5	0.0454702	0.2288418	0	0.5299711	0.0716226	0.0379579
6128	0.0299289	0.314847	0	0.8312879	0.0375703	0.0312317
6128.5	0	0.336154	-999.25	-999.25	-999.25	-999.25
6129	0	0.3478861	-999.25	-999.25	-999.25	-999.25
6129.5	0	0.3596182	-999.25	-999.25	-999.25	-999.25
6130	0	0.3609819	-999.25	-999.25	-999.25	-999.25
6130.5	0	0.3427591	-999.25	-999.25	-999.25	-999.25
6131	0	0.3418055	-999.25	-999.25	-999.25	-999.25
6131.5	0	0.3408518	-999.25	-999.25	-999.25	-999.25
6132	0	0.3408165	-999.25	-999.25	-999.25	-999.25
6132.5	0	0.4130306	-999.25	-999.25	-999.25	-999.25
6133	0	0.4273653	-999.25	-999.25	-999.25	-999.25
6133.5	0	0.3774452	-999.25	-999.25	-999.25	-999.25
6134	0	0.3227158	-999.25	-999.25	-999.25	-999.25
6134.5	0	0.2422256	-999.25	-999.25	-999.25	-999.25
6135	0	0.2074366	-999.25	-999.25	-999.25	-999.25
6135.5	0	0.2019424	-999.25	-999.25	-999.25	-999.25
6136	0	0.1964483	-999.25	-999.25	-999.25	-999.25
6136.5	0.0285089	0.1715565	-999.25	-999.25	-999.25	-999.25
6137	0.0508633	0.1286545	-999.25	-999.25	-999.25	-999.25
6137.5	0.0675004	0.0857525	0	0.4985884	0.0719902	0.0358935
6138	0.0669967	0.024539	0	0.3271158	0.1260587	0.0412358

Appendix A – log database

6138.5	0.0763678	-0.045037	0	0.2763388	0.1549848	0.0428283
6139	0.0362204	-0.073981	0	0.3118195	0.14896	0.0464486
6139.5	0.0671716	0.0467405	0	0.3958828	0.1075818	0.0425898
6140	0.0715038	0.1047935	0	0.4317783	0.0947387	0.0409061
6140.5	0.0679293	0.0593243	0	0.3567519	0.1159152	0.041353
6141	0.0176063	0.0226049	0	0.2860764	0.1575235	0.0450638
6141.5	0.0191882	-0.015483	0	0.2828804	0.1597102	0.0451789
6142	0	-0.055091	0	0.2758318	0.1682035	0.0463959
6142.5	0	-0.094699	0	0.287837	0.158342	0.0455767
6143	0.0241882	-0.11017	0	0.2892551	0.1423109	0.0411642
6143.5	0.0693001	-0.036776	0	0.2836472	0.1274126	0.0361402
6144	0.0600182	-0.024083	0	0.2655895	0.1279803	0.0339902
6144.5	0.0599636	-0.042638	0	0.2834429	0.1137442	0.03224
6145	0.0547053	-0.053414	0	0.4531542	0.0624461	0.0282977
6145.5	0	-0.053456	-999.25	-999.25	-999.25	-999.25
6146	0	0.0202618	-999.25	-999.25	-999.25	-999.25
6146.5	0	0.0475225	-999.25	-999.25	-999.25	-999.25
6147	0	0.0734138	-999.25	-999.25	-999.25	-999.25
6147.5	0	0.0832243	-999.25	-999.25	-999.25	-999.25
6148	0	0.0280018	-999.25	-999.25	-999.25	-999.25
6148.5	0	-0.006063	-999.25	-999.25	-999.25	-999.25
6149	0.0586228	-0.006395	-999.25	-999.25	-999.25	-999.25
6149.5	0.0963149	0.0514584	-999.25	-999.25	-999.25	-999.25
6150	0.0726496	-0.126033	-999.25	-999.25	-999.25	-999.25
6150.5	0.0546845	-0.266056	0	0.2040814	0.2492763	0.0508727
6151	0.0106868	-0.314873	0.0130891	0.1842112	0.2971284	0.0547344
6151.5	0	-0.298268	0.0203661	0.1972729	0.2929108	0.0577834
6152	0	-0.288214	0.0149059	0.2116949	0.2769089	0.0586202
6152.5	0.0000919	-0.272446	0	0.2297099	0.2600789	0.0597427
6153	0	-0.256981	0	0.2364004	0.253965	0.0600374
6153.5	0.0028904	-0.242073	0.0044569	0.2320898	0.2591842	0.060154
6154	0.0099877	-0.227164	0	0.2328281	0.2591568	0.060339
6154.5	0.0077045	-0.212256	0	0.2329618	0.2607165	0.060737
6155	0.0434854	-0.197348	0	0.2520418	0.2359861	0.0594783
6155.5	0.0477189	-0.18244	0	0.2752552	0.2164536	0.05958
6156	0.0365693	-0.180867	0	0.3023192	0.2008695	0.0607267
6156.5	0	-0.183492	0.0108778	0.2746119	0.2323188	0.0637975
6157	0	-0.182002	0.0180164	0.263567	0.2441732	0.064356
6157.5	0	-0.181009	0.0082105	0.2665768	0.2425466	0.0646573
6158	0	-0.180016	0.0037893	0.2659439	0.2431182	0.0646558
6158.5	0.0176168	-0.179195	0	0.2725048	0.2344454	0.0638875
6159	0.0379502	-0.178817	0	0.2792019	0.2229205	0.0622398

Appendix A – log database

6159.5	0.0527112	-0.17844	0	0.3152269	0.1920602	0.0605425
6160	0.0425172	-0.178062	0	0.3195409	0.1918235	0.0612955
6160.5	0.033951	-0.177685	0	0.346747	0.1799137	0.0623846
6161	0	-0.177308	0	0.3663772	0.1785826	0.0654286
6161.5	0	-0.17693	0.0279205	0.3440973	0.1952974	0.0672013
6162	0	-0.160207	0.0547622	0.333191	0.2034722	0.0677951
6162.5	0	-0.138614	0.0536859	0.3388303	0.2028746	0.0687401
6163	0	-0.117022	0.0231749	0.356093	0.1966894	0.0700397
6163.5	0	-0.095429	0.0010952	0.366246	0.1921641	0.0703794
6164	0.0361114	-0.079672	0	0.3826159	0.1782196	0.0681897
6164.5	0.0499634	-0.078001	0	0.3941357	0.1719404	0.0677679
6165	0.043042	-0.076329	0	0.4300998	0.1607364	0.0691327
6165.5	0.0400899	-0.074657	0	0.4396212	0.1600925	0.0703801
6166	0.0707489	-0.072986	0	0.4621597	0.146517	0.0677143
6166.5	0.1138629	-0.071314	0	0.5262029	0.1176006	0.0618818
6167	0.1257855	-0.069296	0	0.560645	0.1080824	0.0605958
6167.5	0.1371747	-0.066714	0	0.5558809	0.10948	0.0608578
6168	0.1371903	-0.064133	0	0.5681933	0.110295	0.0626689
6168.5	0.1309489	-0.06155	0	0.5354083	0.1242927	0.0665474
6169	0.0864551	-0.058969	0	0.5188035	0.1446783	0.0750596
6169.5	0.0350778	-0.057244	0	0.4569078	0.1848587	0.0844634
6170	0.016474	-0.066963	0	0.3830167	0.2335181	0.0894413
6170.5	0.0164047	-0.074261	0	0.3745539	0.2455677	0.0919783
6171	0.0153442	-0.081557	0	0.3839915	0.243095	0.0933464
6171.5	0.044576	-0.088854	0	0.4205986	0.2159398	0.090824
6172	0.0492404	-0.08901	0	0.4378605	0.2039843	0.0893167
6172.5	0.0482261	0.0004387	0	0.4384209	0.2020053	0.0885633
6173	0.0443825	0.0253067	0	0.4011083	0.217335	0.0871749
6173.5	0.017686	0.0477276	0	0.372907	0.2362967	0.0881167
6174	0.021647	0.0665951	0	0.3492324	0.2400727	0.0838412
6174.5	0.0266583	0.0759754	0	0.3204553	0.2464712	0.078983
6175	0.0029423	0.0853558	0	0.289685	0.2635758	0.076354
6175.5	0.017111	0.0864639	0	0.2667719	0.2663451	0.0710534
6176	0.0202092	0.0840473	0	0.26191	0.255943	0.067034
6176.5	0.0259906	0.0827637	0	0.288479	0.2141638	0.0617817
6177	0.0668166	0.0819426	0	0.3250017	0.1650845	0.0536527
6177.5	0.0423787	0.0878572	-999.25	-999.25	-999.25	-999.25
6178	0.0548748	0.092206	-999.25	-999.25	-999.25	-999.25
6178.5	0	0.0923376	-999.25	-999.25	-999.25	-999.25
6179	0	0.0859737	-999.25	-999.25	-999.25	-999.25
6179.5	0	0.0827427	-999.25	-999.25	-999.25	-999.25
6180	0	0.0795116	-999.25	-999.25	-999.25	-999.25

Appendix A – log database

6180.5	0	0.0762806	-999.25	-999.25	-999.25	-999.25
6181	0.0392342	0.0730495	-999.25	-999.25	-999.25	-999.25
6181.5	0.0467972	0.0698185	-999.25	-999.25	-999.25	-999.25
6182	0.0628985	0.0665884	-999.25	-999.25	-999.25	-999.25
6182.5	0.0843413	0.0633574	0	0.5447468	0.1379765	0.0751622
6183	0.0663427	0.0601263	0	0.5436659	0.1510351	0.0821127
6183.5	0.0855184	0.0568953	0	0.6067628	0.135226	0.0820501
6184	0.0894612	0.0536642	0	0.640348	0.1309001	0.0838216
6184.5	0.0903795	0.0504332	0	0.7624936	0.1099643	0.0838471
6185	0.0678423	0.0493984	0	0.8256034	0.1102654	0.0910355
6185.5	0.0616313	0.0683584	0	0.8065832	0.1208313	0.0974605
6186	0.0551854	0.0796461	0	0.7806526	0.1341035	0.1046882
6186.5	0.0446869	0.0909338	0	0.7924039	0.1412962	0.1119637
6187	0.0327845	0.1022215	0	0.7119582	0.1666234	0.1186289
6187.5	0.030094	0.1135092	0	0.5888542	0.2091213	0.123142
6188	0.036668	0.1247969	0	0.5102371	0.2473984	0.1262318
6188.5	0	0.1329432	0.0061875	0.4954323	0.2646044	0.1310936
6189	0	0.0573845	0.006348	0.5390668	0.2467436	0.1330113
6189.5	0	-0.001722	0.0053679	0.6395614	0.208325	0.1332366
6190	0	-0.012979	0.0027931	0.7896805	0.167539	0.1323023
6190.5	0.0142654	0.0059652	0	0.9348335	0.1341055	0.1253664
6191	0.0355099	0.0164337	0	0.9566334	0.1235727	0.1182138
6191.5	0.030659	0.0228872	0	0.7565488	0.1539943	0.1165042
6192	0.0414707	0.02388	0	0.5854736	0.1951208	0.1142381
6192.5	0.0462671	0.0248737	0	0.5069321	0.2242791	0.1136943
6193	0.0015824	0.0258675	0.0082074	0.4831358	0.2428102	0.1173103
6193.5	0.0005271	0.0268602	0.0091605	0.4941018	0.2344671	0.1158506
6194	0.0359137	0.027854	0	0.5391179	0.2030195	0.1094514
6194.5	0.0639233	0.0288477	0	0.6180301	0.1652324	0.1021186
6195	0.0561809	0.0316906	0	0.7114815	0.1408297	0.1001977
6195.5	0.0779146	0.0350523	0	0.8489571	0.1099425	0.0933365
6196	0.0917834	0.038413	0	0.9892713	0.0877441	0.0868027
6196.5	0.0718788	0.0417747	0	0.9298012	0.099309	0.0923377
6197	0.0834626	0.0451355	0	0.785391	0.1169555	0.0918558
6197.5	0.0834821	0.0502672	0	0.7272559	0.127143	0.0924655
6198	0.0908358	0.0561571	0	0.8493517	0.104231	0.0885288
6198.5	0.0991198	0.0608559	0	1	0.0751693	0.0751693
6199	0.1004824	0.0618496	0	1	0.0761559	0.0761559
6199.5	0.0345744	0.0627594	0	0.9815434	0.1019664	0.1000845
6200	0	0.039607	0	0.7735718	0.1392002	0.1076813
6200.5	0	0.0182486	0	0.643191	0.1671117	0.1074847
6201	0.0072921	-0.00311	0	0.6358685	0.1666364	0.1059588

Appendix A – log database

6201.5	0.0339638	-0.024468	0	0.7189138	0.1391422	0.1000313
6202	0.073084	-0.044534	0	0.8682534	0.1010817	0.0877645
6202.5	0.0928488	-0.031158	0	1	0.0740556	0.0740556
6203	0.1122228	-0.018544	0	1	0.0552663	0.0552663
6203.5	0.0876353	-0.005931	0	1	0.049907	0.049907
6204	0.0642139	0.0030785	0	1	0.0430439	0.0430439
6204.5	0.0496456	0.0097771	0	1	0.038571	0.038571
6205	0.0751061	0.0164766	0	1	0.0428747	0.0428747
6205.5	0.1182181	0.0231762	0	1	0.0506739	0.0506739
6206	0.1412389	0.0272455	0	1	0.054383	0.054383
6206.5	0.1728079	0.0210476	0	0.9044162	0.068412	0.0618729
6207	0.0834204	0.0165977	0	0.8576754	0.1032251	0.0885336
6207.5	0	0.0121469	0	0.7142836	0.1540165	0.1100115
6208	0	0.0076971	0.002607	0.6758476	0.1710548	0.1156069
6208.5	0	0.007575	0	0.6785402	0.1751081	0.1188179
6209	0	0.1207085	0	0.6251732	0.1960595	0.1225711
6209.5	0	0.1780586	0.0047412	0.5937178	0.2130344	0.1264823
6210	0	0.2354097	0.0076882	0.5806192	0.2207901	0.128195
6210.5	0	0.2927599	0.0054652	0.5773515	0.2230426	0.1287739
6211	0	0.3213348	0.0019285	0.5802478	0.2219402	0.1287803
6211.5	0.0086641	0.3417139	0	0.5819752	0.2163662	0.1259197
6212	0.0226884	0.362093	0	0.6311755	0.1944659	0.1227421
6212.5	0	0.3779802	0.0044554	0.5728863	0.2187003	0.1252904
6213	0	0.381196	0.0123317	0.5483024	0.2212309	0.1213014
6213.5	0	0.3844118	0.0133438	0.5381618	0.2202785	0.1185455
6214	0	0.3876276	0.0091276	0.5319608	0.215821	0.1148083
6214.5	0	0.3908434	0.0044666	0.5310579	0.2103499	0.111708
6215	0	0.3940601	0.0066605	0.5221183	0.2090947	0.1091722
6215.5	0	0.413949	0.0107877	0.5309812	0.2010026	0.1067286
6216	0	0.4368124	0.0149556	0.5330389	0.1930622	0.1029097
6216.5	0	0.4596758	0.0150855	0.4955513	0.1929187	0.0956011
6217	0	0.4658155	0.0161676	0.4651558	0.1962414	0.0912828
6217.5	0.0024632	0.4354219	0.0097785	0.4356816	0.1958945	0.0853477
6218	0.0252738	0.4272003	0.0023934	0.4147528	0.1833872	0.0760603
6218.5	0.0200279	0.4260378	0.021601	0.4067574	0.1805405	0.0734362
6219	0.0044286	0.4248762	0.0276793	0.4040469	0.1730007	0.0699004
6219.5	0.0016967	0.4237137	0.0266578	0.4063714	0.1671844	0.067939
6220	0	0.4225512	0.0339454	0.3669689	0.1779063	0.0652861
6220.5	0.0183318	0.4213896	0.0187829	0.3423337	0.1796259	0.061492
6221	0.0552158	0.4202271	0	0.3499006	0.1603879	0.0561198
6221.5	0.0623206	0.4147701	0	0.3462053	0.1557218	0.0539117
6222	0.0302488	0.3800383	0.0255234	0.3216266	0.1731401	0.0556865

Appendix A – log database

6222.5	0	0.3453064	0.0439969	0.3054851	0.1886174	0.0576198
6223	0	0.3105755	0.0330162	0.3004414	0.1891473	0.0568277
6223.5	0	0.2787228	0.0185617	0.2605343	0.1821569	0.0474581
6224	0	0.2584457	0.0163648	0.2649712	0.1743412	0.0461954
6224.5	0	0.2381687	0.0304918	0.272259	0.1658294	0.0451486
6225	0	0.2178917	0.0466128	0.2829444	0.1605776	0.0454345
6225.5	0	0.2085581	0.0582569	0.2887096	0.1610815	0.0465058
6226	0	0.2018652	0.0567782	0.2821106	0.1677544	0.0473253
6226.5	0	0.1951714	0.0442805	0.2572403	0.18566	0.0477592
6227	0	0.1884785	0.0373805	0.2368048	0.2033397	0.0481518
6227.5	0	0.1817856	0.0227248	0.2271636	0.2107002	0.0478634
6228	0	0.1776304	0	0.2353216	0.2089354	0.049167
6228.5	0	0.1752472	0.0029587	0.2242372	0.225957	0.050668
6229	0	0.1728649	0.0042997	0.2324862	0.2284332	0.0531076
6229.5	0	0.1704817	0.0236143	0.2293033	0.2489461	0.0570842
6230	0	0.1680994	0.0401719	0.2349336	0.2562729	0.0602071
6230.5	0	0.1677132	0.0438193	0.2576611	0.2447976	0.0630748
6231	0	0.178278	0.0503134	0.2965192	0.2263261	0.06711
6231.5	0	0.1840267	0.064147	0.3428535	0.2211978	0.0758385
6232	0	0.1897745	0.0428735	0.3787484	0.2128295	0.0806088
6232.5	0	0.1969185	0.0056319	0.4207293	0.2087459	0.0878255
6233	0.0194022	0.2049131	0	0.4360047	0.2135009	0.0930874
6233.5	0.0391877	0.2129078	0	0.4244691	0.2212701	0.0939223
6234	0	0.2209024	0.0184795	0.43396	0.2301375	0.0998705
6234.5	0	0.2285852	0.0139022	0.4660598	0.2149423	0.100176
6235	0.0067139	0.1938524	0.0063418	0.4789878	0.2050767	0.0982293
6235.5	0.011335	0.1604252	0	0.4921555	0.1930342	0.0950029
6236	0.005283	0.1297684	0	0.4828981	0.1914898	0.0924701
6236.5	0	0.1002493	0.0003021	0.4429303	0.1952928	0.0865011
6237	0	0.074316	0.0114376	0.427346	0.1931079	0.0825239
6237.5	0	0.061718	0.0211663	0.4185013	0.1897588	0.0794143
6238	0	0.0491199	0.0312054	0.4133645	0.1884959	0.0779175
6238.5	0	0.0472498	0.0301986	0.3932715	0.1961067	0.0771232
6239	0	0.0490904	0.0421328	0.3537306	0.2181056	0.0771506
6239.5	0	0.0500832	0.0308556	0.3444104	0.2234672	0.0769644
6240	0	0.0510769	0.0059766	0.3720476	0.2063348	0.0767664
6240.5	0	0.0516052	0	0.3763454	0.20478	0.077068
6241	0.0030706	-0.063492	0	0.3567961	0.2143195	0.0764684
6241.5	0	-0.062237	0	0.3369508	0.2187171	0.0736969
6242	0	-0.061243	0	0.3381323	0.2113617	0.0714682
6242.5	0	-0.048791	0	0.3369618	0.2027223	0.0683097
6243	0	0.0331268	0.0032802	0.3526274	0.182406	0.0643214

Appendix A – log database

6243.5	0	0.1150436	0.0031383	0.3922209	0.1550509	0.0608142
6244	0.0317276	0.1969614	0	0.5042421	0.10535	0.0531219
6244.5	0.0178649	0.2500362	0	0.5878571	0.089065	0.0523575
6245	0	0.271184	0.0292316	0.5796078	0.0964537	0.0559053
6245.5	0.0123606	0.290494	0.02386	0.6132798	0.0943822	0.0578827
6246	0	0.2629728	0.0179363	0.6220946	0.1033452	0.0642905
6246.5	0	0.2376518	0.0140708	0.5355203	0.1321212	0.0707536
6247	0	0.2137947	0.0065003	0.437227	0.1701915	0.0744123
6247.5	0	0.1961241	0	0.386163	0.2021126	0.0780484
6248	0	0.1784525	0.0027289	0.372126	0.2192011	0.0815704
6248.5	0	0.1678219	0.0064749	0.3766842	0.2218311	0.0835603
6249	0	0.281374	0.0209448	0.3752809	0.2284493	0.0857327
6249.5	0.1647642	0.3625736	0	0.4305297	0.1597303	0.0687687
6250	0.1656578	0.4437723	0	0.4371118	0.1524585	0.0666414
6250.5	0.1587442	-0.575	0	0.4296052	0.1511184	0.0649212
6251	0.1651181	0.4201641	0	0.4076878	0.1517732	0.0618761
6251.5	0	0.5299854	0.0227103	0.3530806	0.2163454	0.0763874
6252	0	0.2605524	0.0067897	0.3416798	0.2231601	0.0762493
6252.5	0.0276124	0.2814054	0	0.3449117	0.2148809	0.0741149
6253	0	0.3014936	0.0195799	0.3339133	0.2288704	0.0764229
6253.5	0	0.3233814	0.0201074	0.348157	0.2186019	0.0761078
6254	0	0.3452702	0.0298786	0.3616726	0.215012	0.077764
6254.5	0.0613624	0.3455906	0	0.428477	0.1713726	0.0734292
6255	0.0219431	0.2889109	0.0027085	0.4308002	0.1916421	0.0825595
6255.5	0	0.2755842	0.045351	0.4655536	0.1944844	0.0905429
6256	0	0.3440628	0.0418559	0.511391	0.1882949	0.0962923
6256.5	0	0.3781271	0.0152331	0.6873632	0.1781464	0.1224513
6257	0.0268692	0.3230839	0	0.7630353	0.158986	0.121312
6257.5	0.1192186	0.2785978	0	0.7979136	0.1344574	0.1072854
6258	0.1133089	0.2550154	0	0.7545457	0.1501556	0.1132993
6258.5	0.0767916	0.2350216	0	0.7593579	0.1625431	0.1234284
6259	0.0309465	0.2150269	0.0046672	0.7034735	0.1925617	0.135462
6259.5	0.0121709	0.2137575	0.0114492	0.6733076	0.2086502	0.1404858
6260	0.0176644	0.2191887	0.0012697	0.6666072	0.2114554	0.1409577
6260.5	0	0.2219934	0.0164143	0.6465809	0.2230327	0.1442087
6261	0	0.2232533	0.0258914	0.6436314	0.2250684	0.1448611
6261.5	0	0.1539984	0.0243517	0.6375483	0.2282323	0.1455091
6262	0	0.1093397	0.0363653	0.6080075	0.240301	0.1461048
6262.5	0	0.0723763	0.0454682	0.5752873	0.2538294	0.1460248
6263	0	0.0362453	0.0570332	0.563345	0.2603391	0.1466607
6263.5	0	-0.026532	0.047357	0.6068764	0.2429514	0.1474415
6264	0	-0.098237	0.019015	0.7121841	0.2092535	0.149027

Appendix A – log database

6264.5	0.0176247	-0.098447	0	0.8339409	0.1765906	0.1472661
6265	0	-0.087912	0	0.8390222	0.181935	0.1526475
6265.5	0	-0.08866	0	0.8556603	0.1817166	0.1554877
6266	0	-0.09155	0	0.8392518	0.1852339	0.1554579
6266.5	0	-0.096774	0.0296342	0.6896253	0.22808	0.1572898
6267	0	-0.098412	0.028538	0.6604719	0.2424297	0.160118
6267.5	0	-0.095677	0.0243077	0.6488667	0.2478503	0.1608218
6268	0	-0.094057	0.0193207	0.6486068	0.2479486	0.1608212
6268.5	0	-0.091801	0.0314262	0.6109635	0.2606777	0.1592645
6269	0.0023427	-0.088075	0.023604	0.6319475	0.2481726	0.1568321
6269.5	0.0115884	-0.084349	0.0070828	0.6822141	0.2238021	0.152681
6270	0.0333503	-0.080841	0	0.7394073	0.1985558	0.1468136
6270.5	0.0476763	-0.077471	0	0.7725138	0.1810127	0.1398348
6271	0.02573	-0.074101	0	0.7907459	0.177653	0.1404784
6271.5	0	-0.073064	0	0.7695944	0.1850766	0.1424339
6272	0	-0.095212	0.024959	0.7178037	0.1964926	0.1410431
6272.5	0	-0.108299	0.0542275	0.6569514	0.2154857	0.1415637
6273	0	-0.146323	0.0595992	0.6141679	0.230343	0.1414693
6273.5	0	-0.18451	0.0311237	0.608041	0.2315823	0.1408115
6274	0	-0.160184	0.013781	0.6098835	0.2308896	0.1408157
6274.5	0	-0.132027	0.0004486	0.6249932	0.2233164	0.1395712
6275	0.0466057	-0.099852	0	0.6927102	0.1899465	0.1315779
6275.5	0.0432961	-0.092169	0	0.6968374	0.185965	0.1295874
6276	0.0719361	-0.032178	0	0.7728022	0.1565731	0.1210001
6276.5	0.0128149	0.0315933	0.0290764	0.7536346	0.1719321	0.129574
6277	0.0107076	0.0867071	0.0303548	0.8168841	0.1560881	0.1275059
6277.5	0.0082099	-0.034561	0.0017466	0.9662159	0.1311594	0.1267283
6278	0.0312903	-0.110353	0	1	0.1190106	0.1190106
6278.5	0.0578289	-0.1204	0	1	0.1103786	0.1103786
6279	0.0934398	-0.130447	0	1	0.0827858	0.0827858
6279.5	0.0802108	-0.137464	0	1	0.0981935	0.0981935
6280	0.0478198	-0.016714	0	0.956359	0.1244025	0.1189734
6280.5	0.0246534	0.006258	0	0.893158	0.1421334	0.1269476
6281	0.0286753	0.0118694	0	0.9050822	0.141942	0.1284692
6281.5	0.0653974	0.0123787	0	0.9335402	0.129811	0.1211838
6282	0.0925745	0.0080214	0	0.9073792	0.127048	0.1152807
6282.5	0.1240224	-0.000377	0	0.9063902	0.1183163	0.1072408
6283	0.1311861	-0.008775	0	0.9098859	0.1124991	0.1023613
6283.5	0.1282484	-0.010776	0	0.9580266	0.1023116	0.0980173
6284	0.1211847	0.0644684	0	0.9449934	0.104165	0.0984352
6284.5	0.032896	0.0107307	0	0.9179111	0.1255067	0.115204
6285	0	-0.011113	0	0.9067247	0.1322515	0.1199157

Appendix A – log database

6285.5	0	-0.015315	0.0227364	0.6485037	0.1483724	0.09622
6286	0	-0.019557	0.0191084	0.6269456	0.1516669	0.0950869
6286.5	0	-0.024081	0.0347126	0.5496231	0.1752707	0.0963328
6287	0	-0.028606	0.0187044	0.5657969	0.1758948	0.0995207
6287.5	0	-0.033131	0.0070352	0.5871641	0.1740797	0.1022133
6288	0	-0.033423	0	0.6562899	0.1612163	0.1058046
6288.5	0.0365119	0.2219687	0	0.7388151	0.1419495	0.1048745
6289	0.0557335	0.0780611	0	0.6899781	0.1542103	0.1064017
6289.5	0.0221705	-0.023541	0	0.6176836	0.1898731	0.1172815
6290	0.0351199	-0.102298	0	0.6475388	0.1828819	0.1184231
6290.5	0.044329	-0.166313	0	0.6637039	0.1804665	0.1197763
6291	0.037937	-0.215084	0	0.6723971	0.182075	0.1224267
6291.5	0.0371673	-0.218643	0	0.6604515	0.1870013	0.1235053
6292	0.0393037	-0.222202	0	0.6591628	0.1869375	0.1232222
6292.5	0.047775	-0.232546	0	0.6672989	0.1814379	0.1210733
6293	0.0627529	-0.279526	0	0.6742342	0.1748841	0.1179128
6293.5	0.0839229	-0.326507	0	0.6823776	0.1665342	0.1136392
6294	0.071486	-0.373487	0	0.696772	0.1643846	0.1145386
6294.5	0.0479952	-0.420466	0	0.7172744	0.1632946	0.1171271
6295	0.0402632	-0.428954	0	0.68487	0.1731278	0.11857
6295.5	0.0372034	-0.379034	0	0.717861	0.1638204	0.1176003
6296	0.0449369	-0.351595	0	0.7295374	0.1582424	0.1154438
6296.5	0.0262194	-0.331336	0	0.7150897	0.1661007	0.1187769
6297	0.0098682	-0.331227	0	0.6912961	0.1751962	0.1211124
6297.5	0.0471374	-0.33112	0	0.682401	0.1686571	0.1150917
6298	0.0612509	-0.331011	0	0.6465223	0.1734525	0.1121409
6298.5	0.0613299	-0.330902	0	0.6092041	0.1810179	0.1102769
6299	0.0352481	-0.322481	0	0.5799788	0.1936404	0.1123073
6299.5	0.015588	-0.308138	0	0.5569105	0.1957658	0.109024
6300	0.0161935	-0.293795	0	0.5702732	0.184733	0.1053483
6300.5	0.0550983	-0.287046	0	0.6090036	0.1544459	0.0940581
6301	0.0617364	-0.284187	0	0.6298734	0.1383177	0.0871226
6301.5	0.0724914	-0.267078	0	0.6400303	0.124556	0.0797196
6302	0.062098	-0.231648	0	0.6153037	0.1204278	0.0740997
6302.5	0.0564176	-0.196218	0	0.6217532	0.1137214	0.0707066
6303	0.0783005	-0.188329	0	0.6566432	0.0919822	0.0603995
6303.5	0.0713947	-0.26232	0	0.8351825	0.0815048	0.0680714
6304	0.0852886	-0.298583	0	0.9234319	0.0661887	0.0611208
6304.5	0.0770353	-0.163849	0	1	0.0581134	0.0581134
6305	0.0517755	-0.044499	0	1	0.0643169	0.0643169
6305.5	0.0326892	0.072814	0	0.922812	0.0770161	0.0710714
6306	0.0322175	0.2037954	0	0.8257604	0.0887088	0.0732522

Appendix A – log database

6306.5	0.0289902	0.3314524	0.001362	0.7064082	0.1086666	0.076763
6307	0.0695441	-0.123096	0	0.635649	0.1162014	0.0738633
6307.5	0.0898163	-0.215159	0	0.8856168	0.0755681	0.0669243
6308	0.1164539	-0.108871	0	0.9939809	0.0600678	0.0597063
6308.5	0.1310692	-0.096562	0	1	0.0551974	0.0551974
6309	0.1484959	-0.084254	0	0.9422824	0.0572323	0.053929
6309.5	0.1638979	-0.081755	0	0.8435327	0.0612271	0.051647
6310	0.1678248	-0.113236	0	0.8222427	0.0604259	0.0496847
6310.5	0.1615199	-0.130755	0	0.8318934	0.0577294	0.0480247
6311	0.1525883	-0.148274	0	0.8090479	0.0597083	0.0483069
6311.5	0.1394632	-0.162567	0	0.8736296	0.0543641	0.0474941
6312	0.1127241	-0.167379	0	0.9943026	0.0499786	0.0496938
6312.5	0.0978982	-0.172192	0	1	0.0479786	0.0479786
6313	0.084932	-0.177004	0	1	0.0465388	0.0465388
6313.5	0.0835812	-0.180341	0	1	0.0473728	0.0473728
6314	0.0907096	-0.160286	0	1	0.0494532	0.0494532
6314.5	0.1097293	-0.144938	0	0.9884235	0.0530408	0.0524268
6315	0.1233485	-0.121323	0	0.9069313	0.0561923	0.0509625
6315.5	0.1187873	-0.095837	0	0.9010066	0.0567773	0.0511567
6316	0.1097744	-0.07035	0	0.9194811	0.0559023	0.0514011
6316.5	0.0607894	-0.044864	0	0.9015115	0.0667438	0.0601703
6317	0.0467677	-0.044714	0	0.933489	0.0619403	0.0578206
6317.5	0.0755179	-0.142215	0	0.9824041	0.0486301	0.0477744
6318	0.0793679	-0.185064	0	0.983305	0.0460727	0.0453035
6318.5	0.0979114	-0.219291	0	0.8901031	0.0480549	0.0427738
6319	0.1062635	-0.253518	0	0.807508	0.0535506	0.0432426
6319.5	0.0882588	-0.277551	0	0.8856032	0.0536272	0.0474924
6320	0.0848771	-0.210097	0	0.9895992	0.0488477	0.0483397
6320.5	0.087819	-0.158123	0	1	0.0470112	0.0470112
6321	0.0857532	-0.139192	0	1	0.0456349	0.0456349
6321.5	0.0792673	-0.234653	0	1	0.044966	0.044966
6322	0.0806635	-0.256993	0	1	0.0456441	0.0456441
6322.5	0.0807354	-0.117742	0	1	0.0461528	0.0461528
6323	0.0863657	-0.068796	0	1	0.0488625	0.0488625
6323.5	0.0863747	-0.054622	0	1	0.0503121	0.0503121
6324	0.0880326	-0.040448	0	1	0.0511708	0.0511708
6324.5	0.0782572	-0.031457	0	1	0.0491335	0.0491335
6325	0.074112	-0.024749	0	1	0.0486707	0.0486707
6325.5	0.0699618	-0.018079	0	0.9777568	0.0488164	0.0477305
6326	0.0446696	-0.018831	0	1	0.0444486	0.0444486
6326.5	0.0121601	-0.01958	0	1	0.0366041	0.0366041
6327	0	-0.019693	0	1	0.0235202	0.0235202

6327.5	0	-0.016518	0	1	0.0202729	0.0202729
6328	0	-0.0148	0	1	0.0185743	0.0185743
6328.5	0	-0.013902	0	1	0.0163868	0.0163868
6329	0	-0.013557	0	1	0.0170733	0.0170733
6329.5	0	-0.013212	0	1	0.0179962	0.0179962
6330	0	-0.012867	0	1	0.0214986	0.0214986

3.2.2 Well B5-NC-74A

TABLE 3.6 Log data Well B5-NC-74A

DEPT (FT)	VCL (V/V)	DD (INCH)	SPI-CPX (V/V)	SW-CPX (V/V)	PHIE-CPX (V/V)	PHSW-CPX
6070	0	2.7964	-999.25	-999.25	-999.25	-999.25
6070.5	0	2.7955	-999.25	-999.25	-999.25	-999.25
6071	0	2.7946	-999.25	-999.25	-999.25	-999.25
6071.5	0	2.7937	-999.25	-999.25	-999.25	-999.25
6072	0	2.7928	-999.25	-999.25	-999.25	-999.25
6072.5	0	2.7919	-999.25	-999.25	-999.25	-999.25
6073	0	2.7712	-999.25	-999.25	-999.25	-999.25
6073.5	0	2.7703	-999.25	-999.25	-999.25	-999.25
6074	0	2.7694	-999.25	-999.25	-999.25	-999.25
6074.5	0.0178017	2.7685	0	0.711167	0.0528171	0.0375618
6075	0.0200062	2.7875	0	0.5031424	0.0823412	0.0414293
6075.5	0.0194695	2.7866	0	0.432232	0.103945	0.0449284
6076	0.0202962	2.7664	0	0.3067999	0.1494225	0.0458428
6076.5	0.0224233	2.5967	0	0.369692	0.1227302	0.0453724
6077	0.0159888	2.5054	0	1	0.0327787	0.0327787
6077.5	0	2.4745	-999.25	-999.25	-999.25	-999.25
6078	0	2.4641	-999.25	-999.25	-999.25	-999.25
6078.5	0	2.4788	-999.25	-999.25	-999.25	-999.25
6079	0	2.4814	-999.25	-999.25	-999.25	-999.25
6079.5	0	2.4614	-999.25	-999.25	-999.25	-999.25
6080	0	2.4058	-999.25	-999.25	-999.25	-999.25
6080.5	0	2.3472	-999.25	-999.25	-999.25	-999.25
6081	0	2.3008	-999.25	-999.25	-999.25	-999.25
6081.5	0	2.262	-999.25	-999.25	-999.25	-999.25
6082	0	2.2191	-999.25	-999.25	-999.25	-999.25
6082.5	0	2.1503	-999.25	-999.25	-999.25	-999.25
6083	0	2.0769	-999.25	-999.25	-999.25	-999.25
6083.5	0	2.0135	-999.25	-999.25	-999.25	-999.25
6084	0	1.9084	-999.25	-999.25	-999.25	-999.25
6084.5	0	1.8353	-999.25	-999.25	-999.25	-999.25

Appendix A – log database

6085	0	1.7678	-999.25	-999.25	-999.25	-999.25
6085.5	0	1.6981	-999.25	-999.25	-999.25	-999.25
6086	0	1.6745	-999.25	-999.25	-999.25	-999.25
6086.5	0.0168491	1.5747	-999.25	-999.25	-999.25	-999.25
6087	0.0200175	1.4835	-999.25	-999.25	-999.25	-999.25
6087.5	0.0228957	1.3645	0	0.2302051	0.2032322	0.0467851
6088	0.0263574	1.1752	0	0.2255965	0.2137409	0.0482192
6088.5	0.0087602	1.0234	0.0007567	0.3231473	0.153469	0.0495931
6089	0.0330896	0.9932003	0	0.5573925	0.0834236	0.0464997
6089.5	0.0294527	1.0301	0	0.9102598	0.0497657	0.0452997
6090	0.0231123	1.071	0	0.5232864	0.0925812	0.0484465
6090.5	0.0194293	1.0222	0	0.4019513	0.1192653	0.0479388
6091	0.0215129	0.8838997	0	0.253967	0.184094	0.0467538
6091.5	0.0247338	0.7588997	0	0.2245057	0.2069656	0.046465
6092	0.0279484	0.6612997	0	0.2186764	0.2119206	0.046342
6092.5	0.0294977	0.5725002	0	0.2253263	0.2052825	0.0462555
6093	0.0258058	0.4914999	0	0.2248638	0.201982	0.0454184
6093.5	0.0212893	0.4483995	0	0.2434519	0.1804122	0.0439217
6094	0.0182166	0.4475002	0	0.2692993	0.1412004	0.0380252
6094.5	0.017516	0.4466	0	0.4242281	0.0749807	0.0318089
6095	0	0.4259005	0	1	0.0225602	0.0225602
6095.5	0	0.4097996	-999.25	-999.25	-999.25	-999.25
6096	0	0.4436998	-999.25	-999.25	-999.25	-999.25
6096.5	0	0.4392004	-999.25	-999.25	-999.25	-999.25
6097	0	0.4062004	-999.25	-999.25	-999.25	-999.25
6097.5	0	0.3694	-999.25	-999.25	-999.25	-999.25
6098	0	0.3403997	-999.25	-999.25	-999.25	-999.25
6098.5	0	0.3058996	-999.25	-999.25	-999.25	-999.25
6099	0.0282677	0.2503004	-999.25	-999.25	-999.25	-999.25
6099.5	0.0351459	0.1641998	-999.25	-999.25	-999.25	-999.25
6100	0.0409127	0.1056004	-999.25	-999.25	-999.25	-999.25
6100.5	0.0612116	- 0.0455999	0	0.1447237	0.2338932	0.0338499
6101	0.0544373	- 0.1677999	0	0.1441901	0.262087	0.0377903
6101.5	0.0451852	- 0.2783003	0	0.153613	0.2660734	0.0408723
6102	0.0371579	- 0.3619003	0	0.1632837	0.2699248	0.0440743
6102.5	0.0285116	-0.3827	0	0.1687493	0.2772045	0.0467781
6103	0.0273203	- 0.3836002	0.0049431	0.1712227	0.2838916	0.0486087
6103.5	0.0262598	- 0.3796997	0.0136068	0.1747573	0.2864484	0.0500589
6104	0.0249194	- 0.3655005	0.0104016	0.1904944	0.2695982	0.051357

Appendix A – log database

6104.5	0.02622	- 0.3648996	0	0.2237112	0.2340941	0.0523695
6105	0.0296267	- 0.3613005	0	0.2503271	0.2144882	0.0536922
6105.5	0.0323661	- 0.3842001	0	0.2449612	0.2238173	0.0548266
6106	0.0294883	- 0.3888998	0	0.2457716	0.2313218	0.0568523
6106.5	0.0247534	- 0.3898001	0	0.2464525	0.2358831	0.058134
6107	0.0225089	- 0.3952999	0	0.256614	0.2304723	0.0591424
6107.5	0.0214188	-0.4115	0	0.2589496	0.2332554	0.0604014
6108	0.0220575	- 0.3924999	0	0.2531406	0.2409242	0.0609877
6108.5	0.0219907	- 0.3882999	0	0.2591202	0.2386932	0.0618502
6109	0.0252706	- 0.3744001	0	0.2813188	0.2179376	0.0613099
6109.5	0.0358196	- 0.3446999	0	0.3104508	0.1903274	0.0590873
6110	0.0236584	-0.2556	0.0028535	0.3231151	0.1784947	0.0576743
6110.5	0.0347699	- 0.2334003	0.0011039	0.3295777	0.1668406	0.0549869
6111	0.0416899	- 0.1188002	0	0.350413	0.1512194	0.0529892
6111.5	0.0437505	- 0.0601997	0	0.3384883	0.1543027	0.0522297
6112	0.047956	- 0.0228004	0.0029131	0.2855242	0.1824308	0.0520884
6112.5	0.0475392	- 0.0768003	0	0.2588169	0.2033764	0.0526372
6113	0.036429	- 0.1449003	0.0031162	0.2285764	0.2331329	0.0532887
6113.5	0.0286665	- 0.1637001	0.0179437	0.2115298	0.2534783	0.0536182
6114	0.0216101	- 0.1627998	0.0208899	0.2172307	0.2511378	0.0545548
6114.5	0.0213742	- 0.1456003	0.0133655	0.245801	0.2260966	0.0555748
6115	0.0272745	- 0.1300001	0.0049929	0.2754075	0.2043248	0.0562726
6115.5	0.0318678	- 0.0943003	0	0.344622	0.1686281	0.058113
6116	0.040302	- 0.0453997	0	0.3870454	0.1547731	0.0599042
6116.5	0.0459156	0.0212002	0	0.4271525	0.1465183	0.0625857
6117	0.046136	0.1191998	0	0.4526219	0.1436335	0.0650117
6117.5	0.043489	0.1630001	0	0.4446039	0.1532096	0.0681176

Appendix A – log database

6118	0.0434224	0.1543999	0	0.4291343	0.1648909	0.0707603
6118.5	0.046292	0.1455002	0	0.4016848	0.1835596	0.0737331
6119	0.0491924	0.1318998	0	0.3505196	0.2212923	0.0775673
6119.5	0.0517844	0.1238003	0	0.3399791	0.2435265	0.0827939
6120	0.0475015	0.1230001	0	0.350451	0.252735	0.0885712
6120.5	0.0389443	0.1220999	0	0.3675319	0.2551866	0.0937892
6121	0.0364077	0.1211996	0	0.3812664	0.2574592	0.0981605
6121.5	0.0371022	0.1381998	0	0.3965371	0.2606377	0.1033525
6122	0.0428761	0.1393003	0	0.3945752	0.2640777	0.1041985
6122.5	0.050621	0.1490002	0	0.3935604	0.2610582	0.1027422
6123	0.0553903	0.1574001	0	0.4084581	0.2478279	0.1012273
6123.5	0.0627619	0.1764002	0	0.4048957	0.2403372	0.0973115
6124	0.0738107	0.2188997	0	0.3782765	0.2413825	0.0913093
6124.5	0.0668487	0.2888002	0	0.3332847	0.2567982	0.0855869
6125	0.0642664	0.2930002	0	0.2876495	0.2829072	0.0813781
6125.5	0.0714664	0.2868004	0.0060518	0.2545173	0.2937174	0.0747562
6126	0.0861948	0.2522001	0	0.2400337	0.2809407	0.0674352
6126.5	0.1112358	0.2505999	0	0.2709436	0.2211374	0.0599158
6127	0.042317	0.2496996	0	0.317527	0.1859989	0.0590597
6127.5	0	0.2884998	0	0.3807627	0.1529849	0.058251
6128	0.0450176	0.3853998	0	1	0.044335	0.044335
6128.5	0	0.4579	-999.25	-999.25	-999.25	-999.25
6129	0	0.5367002	-999.25	-999.25	-999.25	-999.25
6129.5	0	0.6091995	-999.25	-999.25	-999.25	-999.25
6130	0	0.6548004	-999.25	-999.25	-999.25	-999.25
6130.5	0	0.6808004	-999.25	-999.25	-999.25	-999.25
6131	0	0.6799002	-999.25	-999.25	-999.25	-999.25
6131.5	0.0040138	0.6724005	-999.25	-999.25	-999.25	-999.25
6132	0.0110674	0.6309004	-999.25	-999.25	-999.25	-999.25
6132.5	0.0116404	0.5411997	0	0.3415777	0.1642388	0.0561003
6133	0.017673	0.4466	0	0.2756948	0.2193346	0.0604694
6133.5	0.0287578	0.3760004	0	0.2763762	0.2325622	0.0642747
6134	0.0388314	0.3413	0	0.30224	0.2374458	0.0717656
6134.5	0.0392498	0.3003998	0	0.3169257	0.2407394	0.0762965
6135	0.0385865	0.2951002	0	0.3376443	0.2373388	0.0801361
6135.5	0.0409643	0.2941999	0	0.3814291	0.2165025	0.0825804
6136	0.0425848	0.2932997	0	0.4195379	0.2022616	0.0848564
6136.5	0.0442689	0.3100996	0	0.4142081	0.2179053	0.0902582
6137	0.042485	0.3114004	0.0011546	0.4202061	0.2331367	0.0979655
6137.5	0.0457115	0.3105001	0.0043741	0.4276121	0.2368672	0.1012873
6138	0.0538332	0.3095999	0	0.4928776	0.2156595	0.1062938
6138.5	0.0623004	0.3257999	0	0.5847145	0.1923694	0.1124812
6139	0.0392577	0.3476	0	0.5685043	0.2099459	0.1193551
6139.5	0.0264835	0.3404999	0	0.5413474	0.2324937	0.1258598

Appendix A – log database

6140	0.018844	0.2663002	0.0185929	0.4904367	0.2620626	0.1285251
6140.5	0.0194432	0.2184	0.0242808	0.4632353	0.274489	0.127153
6141	0.0372689	0.1761999	0.0128373	0.4466691	0.2692627	0.1202713
6141.5	0.0306691	0.1641998	0.0091517	0.4326293	0.267453	0.115708
6142	0.0316869	0.1632996	0.0008901	0.4288186	0.2593053	0.1111949
6142.5	0.0375723	0.1779003	0	0.438215	0.2328766	0.10205
6143	0.0454636	0.1815004	0	0.4956497	0.1837533	0.0910773
6143.5	0.0465632	0.1806002	0	0.5733653	0.1457659	0.0835771
6144	0.0417103	0.1796999	0	0.55826	0.1408296	0.0786195
6144.5	0.0172069	0.1655998	0.002101	0.4595511	0.1726069	0.0793217
6145	0.0244298	0.0773001	0.0114291	0.3807566	0.2007366	0.0764318
6145.5	0.0260051	0.0377998	0.0103657	0.3702795	0.2012471	0.0745177
6146	0.027629	0.0368996	0	0.4325497	0.167806	0.0725844
6146.5	0.0284284	0.0558996	0.0008064	0.5182552	0.1386691	0.071866
6147	0.0290844	0.0709	0	0.7580928	0.0945774	0.0716985
6147.5	0.0293897	0.1349001	0	0.7505962	0.0962038	0.0722102
6148	0.0332538	0.1527004	0	0.5918318	0.1226618	0.0725952
6148.5	0.041397	0.1302996	0	0.5237023	0.1378986	0.0722178
6149	0.0599573	0.0913	0	0.5496276	0.125394	0.06892
6149.5	0.0941313	0.0903997	0	0.727183	0.0821768	0.0597576
6150	0.0639361	0.1028996	0	1	0.0415286	0.0415286
6150.5	0	0.1282997	0	1	0.0264556	0.0264556
6151	0	0.1274996	0	1	0.0236114	0.0236114
6151.5	0.018696	0.1143999	0	1	0.028112	0.028112
6152	0.0494613	0.0711002	0	1	0.0341092	0.0341092
6152.5	0.0780976	- 0.0199003	0	1	0.0393182	0.0393182
6153	0.0761027	- 0.0390997	0	1	0.0410205	0.0410205
6153.5	0.0375778	- 0.0558996	0	1	0.0363114	0.0363114
6154	0.0277648	- 0.0436001	0	1	0.034651	0.034651
6154.5	0.0394274	0.0184002	0	1	0.0372294	0.0372294
6155	0.0624609	0.0650997	0	1	0.0428995	0.0428995
6155.5	0.0640781	0.0528002	0	0.8903622	0.0617046	0.0549394
6156	0.0997336	- 0.0838003	0	0.8074751	0.0623809	0.050371
6156.5	0.1356596	- 0.2283001	0	0.8528072	0.0518699	0.0442351
6157	0.1296631	- 0.2807999	0	0.9243351	0.0498125	0.0460434
6157.5	0.11869	- 0.2817001	0	1	0.0479999	0.0479999
6158	0.1501963	- 0.2826004	0	0.9279571	0.0502362	0.0466171

Appendix A – log database

6158.5	0.1348723	- 0.2834997	0	0.7437299	0.0762734	0.0567268
6159	0.1127327	- 0.3147001	0	0.5647522	0.1160107	0.0655173
6159.5	0.0783663	- 0.3690996	0	0.4659318	0.1538936	0.0717039
6160	0.0471068	-0.474	0	0.3728218	0.2026597	0.075556
6160.5	0.0417704	- 0.5354004	0	0.3432329	0.2198955	0.0754754
6161	0.0185702	- 0.5775995	0.00673	0.3298772	0.2329282	0.0768377
6161.5	0.0158943	- 0.6069002	0.0119026	0.3301723	0.23236	0.0767188
6162	0.055176	- 0.6061001	0	0.3539771	0.2067298	0.0731776
6162.5	0.0555185	- 0.5888004	0	0.3868763	0.1872249	0.0724329
6163	0.070585	- 0.5227003	0	0.3989308	0.1761841	0.0702853
6163.5	0.0605342	- 0.4912004	0	0.36691	0.1926222	0.070675
6164	0.048574	- 0.5005999	0	0.3078657	0.2327752	0.0716635
6164.5	0.0149076	-0.5604	0.018256	0.276628	0.2649494	0.0732924
6165	0.0169703	-0.5913	0.0176185	0.2682189	0.2703357	0.0725091
6165.5	0.0354227	- 0.6140003	0.0054587	0.2736392	0.2551202	0.0698109
6166	0.0309777	-0.6348	0.0025754	0.289876	0.2372598	0.0687759
6166.5	0.0217855	- 0.6357002	0.0046205	0.3003646	0.224795	0.0675205
6167	0.0199592	- 0.6167002	0.0119981	0.292803	0.2215499	0.0648705
6167.5	0.0130267	- 0.5866003	0.0185654	0.2894838	0.2148351	0.0621913
6168	0.0042643	- 0.5057001	0.0133992	0.2981159	0.1954991	0.0582814
6168.5	0.0034151	-0.4052	0.008842	0.2992188	0.1802637	0.0539383
6169	0.0296115	-0.2893	0	0.3067963	0.1537922	0.0471829
6169.5	0.0348331	- 0.1059999	0	0.2574709	0.1609785	0.0414473
6170	0.0430803	0.0457001	0	0.221865	0.1763892	0.0391346
6170.5	0.0427246	0.1533003	0	0.1626447	0.2018145	0.0328241
6171	0.0350525	0.1541004	0.0151028	0.1349187	0.2486249	0.0335441
6171.5	0.0349668	0.0037003	0.0084368	0.1290042	0.2617328	0.0337646
6172	0.0300345	- 0.2017002	0.0025254	0.1308923	0.2607556	0.0341309
6172.5	0.0297445	- 0.3919001	0	0.1355648	0.2509895	0.0340253

Appendix A – log database

6173	0.0372918	- 0.5178003	0	0.1408154	0.2386284	0.0336025
6173.5	0.0460212	- 0.5089998	0	0.1468957	0.2246405	0.0329987
6174	0.0242415	- 0.4764996	0.0070136	0.1436982	0.2325419	0.0334158
6174.5	0	- 0.4350996	0.0246413	0.1358267	0.2455407	0.033351
6175	0	- 0.3921003	0.0315622	0.130713	0.2497919	0.0326511
6175.5	0	- 0.3528004	0.0195595	0.1341515	0.2378571	0.0319089
6176	0	- 0.2932997	0.0045355	0.1597744	0.1963523	0.0313721
6176.5	0.0269526	- 0.2152004	0	0.1953623	0.1698939	0.0331909
6177	0.0488829	- 0.1781998	0	0.2079099	0.1692402	0.0351867
6177.5	0.0436268	-0.25	0	0.1937817	0.1917831	0.0371641
6178	0.0412157	- 0.3705997	0	0.183804	0.2094435	0.0384966
6178.5	0.0427625	- 0.4780998	0	0.1853794	0.2192552	0.0406454
6179	0.0306636	- 0.4790001	0.0053678	0.1822793	0.2336521	0.0425899
6179.5	0.0322969	- 0.4506998	0.0014269	0.1803902	0.2391864	0.0431469
6180	0.0346819	- 0.4243002	0	0.1789626	0.2354834	0.0421427
6180.5	0.0180333	- 0.3731003	0.0051086	0.1807348	0.2275952	0.0411344
6181	0.0319531	- 0.2763996	0	0.2048361	0.1830882	0.0375031
6181.5	0.0601064	0.0115004	0	0.2216361	0.1504253	0.0333397
6182	0.0700043	0.5419998	0	0.212936	0.141459	0.0301217
6182.5	0.0434024	0.8858004	0.001652	0.1795213	0.1623494	0.0291452
6183	0.0546597	0.4916	0	0.155557	0.1755587	0.0273094
6183.5	0.0440739	- 0.0471001	0	0.1417674	0.1858287	0.0263444
6184	0.0809642	- 0.2945995	0	0.1379272	0.1736892	0.0239565
6184.5	0.0706247	- 0.3297005	0	0.1310059	0.1813123	0.023753
6185	0.0320104	-0.2802	0.0070523	0.112697	0.2263412	0.025508
6185.5	0	- 0.2320995	0.0412769	0.1049487	0.2539549	0.0266522
6186	0	- 0.2067003	0.0440573	0.1082818	0.2498638	0.0270557

Appendix A – log database

6186.5	0	- 0.1743002	0.0431127	0.1162927	0.2345695	0.0272787
6187	0.0428787	- 0.1885996	0	0.1356993	0.1909111	0.0259065
6187.5	0.063901	- 0.1911001	0	0.1624588	0.1543252	0.0250715
6188	0.0687594	- 0.1396999	0	0.1937192	0.1282568	0.0248458
6188.5	0.0765467	- 0.0635004	0	0.2340769	0.1056105	0.024721
6189	0.0795881	0.0174999	0	0.2415541	0.1053743	0.0254536
6189.5	0.0695198	0.1134005	0	0.2280845	0.1192415	0.0271971
6190	0.0574141	0.1575003	0	0.199339	0.1482744	0.0295569
6190.5	0.0565486	0.1007996	0	0.1887732	0.1619895	0.0305793
6191	0.0629604	- 0.0019999	0	0.1786104	0.1735687	0.0310012
6191.5	0.0965927	- 0.0823002	0	0.1683728	0.1785144	0.030057
6192	0.1108065	- 0.0846004	0	0.1674408	0.1741924	0.0291669
6192.5	0.1206614	- 0.0854998	0	0.171219	0.166585	0.0285225
6193	0.1182784	-0.0864	0	0.1753055	0.1614607	0.028305
6193.5	0.1042619	-0.0674	0	0.1828858	0.157959	0.0288885
6194	0.0869839	- 0.0149002	0	0.1989773	0.1453632	0.028924
6194.5	0.0709202	0.0157003	0	0.2122919	0.1362285	0.0289202
6195	0.0608404	0.0600996	0	0.2208398	0.1318891	0.0291263
6195.5	0.0593608	0.1189003	0	0.2332869	0.1266301	0.0295411
6196	0.0603052	0.1872997	0	0.2495787	0.1242654	0.031014
6196.5	0.0590342	0.2265997	0	0.2796117	0.1236203	0.0345657
6197	0.052312	0.2444	0	0.3062545	0.1272025	0.0389564
6197.5	0	0.2593002	0.0057649	0.3204892	0.149472	0.0479042
6198	0	0.2916002	0.0189543	0.3281986	0.1573131	0.0516299
6198.5	0	0.3359003	0.0254123	0.3783054	0.1544109	0.0584145
6199	0	0.3682003	0.0124213	0.4421515	0.1479759	0.0654278
6199.5	0.0468101	0.3781996	0	0.5950615	0.137553	0.0818525
6200	0.055087	0.3584003	0	0.6244845	0.1475159	0.0921214
6200.5	0.0615074	0.3575001	0	0.6340696	0.1564358	0.0991912
6201	0.0575955	0.3698997	0	0.6187959	0.1702303	0.1053378
6201.5	0.0418678	0.3755999	0	0.582622	0.1932696	0.1126031
6202	0.0202024	0.3945999	0.0107078	0.5539343	0.2146152	0.1188827
6202.5	0	0.4136	0.0367763	0.5058009	0.243159	0.12299
6203	0.0288861	0.4273996	0.0191464	0.5188748	0.2292081	0.1189303
6203.5	0.0546089	0.4316998	0.0024355	0.5367807	0.2126386	0.1141403
6204	0.0682049	0.4506998	0	0.5444499	0.2032495	0.1106592

Appendix A – log database

6204.5	0.0676167	0.4722004	0	0.5626323	0.1940684	0.1091891
6205	0.0635102	0.4886999	0	0.6330341	0.1715821	0.1086173
6205.5	0.0614023	0.5105	0	0.7499894	0.144763	0.1085707
6206	0.0635926	0.5394001	0	0.901563	0.1237339	0.111554
6206.5	0.0668505	0.5549002	0	0.9146647	0.1279663	0.1170463
6207	0.0707428	0.5446997	0	0.7692789	0.1681873	0.1293829
6207.5	0.0694852	0.5438995	0	0.7349723	0.1884205	0.1384839
6208	0.0574997	0.5663004	0	0.7252718	0.2022315	0.1466728
6208.5	0.0555277	0.5952997	0	0.7327984	0.2119274	0.1553
6209	0.0445078	0.6435003	0.0030037	0.7497943	0.2176113	0.1631637
6209.5	0.0393658	0.6794996	0.0080291	0.7517068	0.2236492	0.1681186
6210	0.03869	0.6934004	0.0114452	0.7498153	0.2287334	0.1715078
6210.5	0.0320913	0.6538	0.0143066	0.750279	0.2311607	0.173435
6211	0.0394374	0.6370001	0.0128178	0.761932	0.2231595	0.1700323
6211.5	0.0424406	0.5964003	0.0126087	0.7588012	0.2207147	0.1674785
6212	0.0371854	0.5263996	0.0162065	0.7270896	0.2274071	0.1653453
6212.5	0.0309141	0.4853001	0.0184964	0.6952063	0.233181	0.1621089
6213	0.0404088	0.4337997	0.0089994	0.7029254	0.223913	0.1573941
6213.5	0.0545331	0.3594999	0.0001838	0.7143006	0.2102709	0.1501967
6214	0.0592708	0.3126001	0	0.729818	0.2010491	0.1467292
6214.5	0.0481264	0.2848997	0	0.6993824	0.2096525	0.1466272
6215	0.0271063	0.2294998	0.0111954	0.6300891	0.2365959	0.1490765
6215.5	0.0168346	0.1674995	0.0195497	0.5947528	0.2532294	0.1506089
6216	0.0061318	0.1332998	0.0316623	0.5625262	0.2703247	0.1520647
6216.5	0	0.0767002	0.0373832	0.5584319	0.2749881	0.1535621
6217	0	0.0497999	0.0326529	0.5819424	0.2647295	0.1540573
6217.5	0.0160351	0.0488997	0.0177309	0.6224762	0.2458915	0.1530616
6218	0.0518773	0.0455999	0	0.6633244	0.2217606	0.1470992
6218.5	0.0439106	0.0272999	0	0.6698138	0.2210079	0.1480342
6219	0.0348164	0.0390997	0	0.6347808	0.2315276	0.1469692
6219.5	0.0297084	0.0255003	0.0035346	0.6074421	0.2375336	0.1442879
6220	0.0063056	0.0368996	0.0160969	0.5937315	0.2401702	0.1425966
6220.5	0.0057206	0.0436001	0.0135275	0.6083952	0.2281323	0.1387946
6221	0.0358864	0.0426998	0	0.7210224	0.1792734	0.1292601
6221.5	0.0354835	0.0417995	0	0.8358703	0.1510775	0.1262812
6222	0.0431636	0.0656004	0	1	0.1146958	0.1146958
6222.5	0.06318	0.0946999	0	1	0.0977863	0.0977863
6223	0.0890863	0.2012997	0	1	0.0998225	0.0998225
6223.5	0.0976384	0.3038998	0	1	0.1073729	0.1073729
6224	0.1014213	0.3536997	0	0.9490367	0.1199305	0.1138185
6224.5	0.1028452	0.4018002	0	0.8694814	0.1366254	0.1187932
6225	0.1027877	0.4132996	0	0.8532092	0.1431215	0.1221126
6225.5	0.1057052	0.4124002	0	0.8535645	0.1454983	0.1241921
6226	0.1059929	0.4115	0	0.8578173	0.144644	0.1240782

Appendix A – log database

6226.5	0.1006069	0.4106998	0	0.8572662	0.1426529	0.1222915
6227	0.0924919	0.3942003	0	0.8507901	0.1411983	0.1201301
6227.5	0.0879654	0.3889999	0	0.8417522	0.134271	0.1130229
6228	0.0482136	0.3843002	0	0.9077672	0.1255693	0.1139877
6228.5	0.0462032	0.3673	0	0.9986079	0.1012211	0.1010802
6229	0.0047261	0.3463001	0	1	0.0917026	0.0917026
6229.5	0.0239025	0.3257999	0	1	0.0791862	0.0791862
6230	0.0487063	0.2938004	0	0.9981954	0.0764563	0.0763184
6230.5	0.0320235	0.1808996	0	0.8593565	0.0908207	0.0780473
6231	0.0217013	0.1077003	0	0.7769746	0.1018252	0.0791156
6231.5	0.0254189	0.0438995	0	0.7458351	0.1044375	0.0778932
6232	0.0532922	0.0142002	0	0.627847	0.1185263	0.0744164
6232.5	0.0514312	- 0.0067997	0	0.4710928	0.1355097	0.0638377
6233	0.0551584	- 0.0278997	0	0.4463908	0.1498908	0.0669099
6233.5	0.058963	- 0.0663996	0	0.4488476	0.1591344	0.0714271
6234	0.0444385	- 0.0797997	0	0.4931234	0.1524375	0.0751705
6234.5	0.0556886	- 0.0806999	0	0.5606788	0.1331324	0.0746445
6235	0.0657263	- 0.0390997	0	0.583768	0.1290158	0.0753153
6235.5	0.0659288	- 0.0228996	0	0.5788978	0.1340936	0.0776265
6236	0.0665276	-0.0267	0	0.556991	0.1438258	0.0801097
6236.5	0.0642375	-0.0576	0	0.5495241	0.1494769	0.0821412
6237	0.0560661	- 0.0686998	0	0.5517853	0.1533852	0.0846357
6237.5	0.0491877	- 0.0860996	0	0.558535	0.1545133	0.0863011
6238	0.0449378	-0.0899	0	0.559223	0.1558534	0.0871568
6238.5	0.0403557	- 0.1006002	0	0.5659025	0.1542502	0.0872906
6239	0.0309882	- 0.0887003	0	0.5911071	0.1487279	0.0879141
6239.5	0.0241877	- 0.0754995	0	0.6542135	0.1324967	0.0866811
6240	0.0221507	- 0.0422001	0	0.6772523	0.1246514	0.0844204
6240.5	0.0196953	- 0.0003996	0	0.6724014	0.1247991	0.0839151
6241	0.0196526	0.0264997	0	0.6827019	0.1217923	0.0831478
6241.5	0.0190303	0.0852003	0	0.7303613	0.112087	0.081864
6242	0.0178726	0.1124001	0	0.7622227	0.1067295	0.0813517
6242.5	0.018193	0.1237001	0	0.9571469	0.1069423	0.1023595

Appendix A – log database

6243	0.0214378	0.1163998	0	0.890439	0.1155435	0.1028844
6243.5	0.0223677	0.1020002	0	0.7914099	0.1327433	0.1050544
6244	0.0222293	0.0476999	0	0.7336898	0.1467989	0.1077048
6244.5	0.0241104	- 0.0198002	0	0.6722275	0.1645195	0.1105946
6245	0.0263062	- 0.0607004	0	0.6286099	0.1794359	0.1127952
6245.5	0.0271741	- 0.0804005	0	0.6076424	0.1885497	0.1145708
6246	0.0270977	- 0.0812998	0	0.6230264	0.1847032	0.115075
6246.5	0.026425	- 0.0622997	0	0.6689343	0.171966	0.115034
6247	0.0257628	-0.0632	0	0.6857097	0.1678841	0.1151197
6247.5	0.0270907	-0.0653	0	0.6863981	0.1666926	0.1144175
6248	0.0291154	- 0.0847998	0	0.6938143	0.1633938	0.1133649
6248.5	0.0290381	-0.0857	0	0.6969458	0.1599168	0.1114534
6249	0.0301738	- 0.0866003	0	0.6718843	0.1628732	0.109432
6249.5	0.0318109	- 0.0874996	0	0.6481304	0.1664151	0.1078587
6250	0.0313633	- 0.0883999	0	0.6456793	0.1651802	0.1066534
6250.5	0.0243345	- 0.0873003	0	0.6957184	0.1519612	0.1057222
6251	0.0177415	- 0.0627003	0	0.7335516	0.1450517	0.1064029
6251.5	0.0166856	-0.0337	0	0.782757	0.1374561	0.1075947
6252	0.0173783	-0.0323	0	0.7821596	0.1384399	0.1082821
6252.5	0.019783	-0.0302	0	0.7888121	0.1362045	0.1074398
6253	0.039217	0.0335999	0	0.7806595	0.1315749	0.1027152
6253.5	0.0486737	0.1183004	0	0.7396557	0.1335797	0.098803
6254	0.0684512	0.2147999	0	0.723409	0.1281855	0.0927306
6254.5	0.070504	0.2416	0	0.8162992	0.1060925	0.0866033
6255	0.0695683	0.2406998	0	0.953824	0.0840394	0.0801588
6255.5	0.0719475	0.2264004	0	1	0.0694307	0.0694307
6256	0.0821016	0.2002001	0	1	0.0624882	0.0624882
6256.5	0.0970563	0.1784	0	1	0.0538956	0.0538956
6257	0.0915783	0.1681995	0	1	0.0503725	0.0503725
6257.5	0.0759624	0.1485996	0	1	0.048529	0.048529
6258	0.0619029	0.1306	0	1	0.0470297	0.0470297
6258.5	0.0482611	0.1126003	0	1	0.0451773	0.0451773
6259	0.0332756	0.0944996	0	1	0.0429688	0.0429688
6259.5	0.0311949	0.0935001	0	1	0.0452812	0.0452812
6260	0.0607016	0.0976	0	1	0.0590584	0.0590584
6260.5	0.0661564	0.1115999	0	0.867035	0.0798304	0.0692157

6261	0.066324	0.1106997	0	0.8050444	0.0898654	0.0723456
6261.5	0.0676942	0.0899	0	0.8022386	0.093097	0.074686
6262	0.0640881	0.0691996	0	0.8371565	0.0920606	0.0770691
6262.5	0.0619543	0.0683002	0	0.8608392	0.0897615	0.0772702
6263	0.0627939	0.0674	0	0.8534484	0.0887619	0.0757537
6263.5	0.0580672	0.0677004	0	0.8326427	0.0875051	0.0728605
6264	0.0544974	0.0854998	0	0.8559575	0.081855	0.0700644
6264.5	0.0583667	0.0977001	0	0.9420707	0.070077	0.0660175
6265	0.0639506	0.1035995	0	1	0.0565582	0.0565582
6265.5	0.0524874	0.0973997	0	1	0.0488315	0.0488315
6266	0.0397977	0.0818996	0	1	0.0438536	0.0438536
6266.5	0.0341333	0.0811005	0	1	0.042315	0.042315
6267	0.0770362	0.0802002	0	1	0.0491266	0.0491266
6267.5	0.1084627	0.0792999	0	1	0.0532628	0.0532628
6268	0.1274366	0.0783997	0	0.8933167	0.0551622	0.0492773
6268.5	0.1260373	0.0775003	0	0.8784942	0.0549041	0.048233
6269	0.0413397	0.0766001	0	1	0.0438528	0.0438528
6269.5	0.0131395	0.0756998	0	1	0.0382339	0.0382339
6270	0	0.0747995	0	1	0.0333644	0.0333644

3.2.3 Well B6-NC-74A

TABLE 3.7 Log data Well B6-NC-74A

DEPTH (FT)	VCL (V/V)	DD (INCH)	SPI-CPX (V/V)	SW-CPX (V/V)	PHIE-CPX (V/V)	PHSW-CPX
6040	0.0254141	0.7103996	-999.25	-999.25	-999.25	-999.25
6040.5	0.0547343	0.6616001	-999.25	-999.25	-999.25	-999.25
6041	0.0398548	0.6616001	-999.25	-999.25	-999.25	-999.25
6041.5	0.0181343	0.6616001	-999.25	-999.25	-999.25	-999.25
6042	0.027287	0.6127996	-999.25	-999.25	-999.25	-999.25
6042.5	0.0401912	0.6127996	-999.25	-999.25	-999.25	-999.25
6043	0.0568455	0.6127996	-999.25	-999.25	-999.25	-999.25
6043.5	0.0678532	0.6127996	-999.25	-999.25	-999.25	-999.25
6044	0.0611434	0.6127996	-999.25	-999.25	-999.25	-999.25
6044.5	0.0396016	0.6127996	-999.25	-999.25	-999.25	-999.25
6045	0.0271776	0.6127996	-999.25	-999.25	-999.25	-999.25
6045.5	0	0.6127996	-999.25	-999.25	-999.25	-999.25
6046	0	0.6127996	-999.25	-999.25	-999.25	-999.25
6046.5	0	0.6127996	-999.25	-999.25	-999.25	-999.25
6047	0	0.6127996	-999.25	-999.25	-999.25	-999.25
6047.5	0	0.6127996	-999.25	-999.25	-999.25	-999.25
6048	0	0.6127996	-999.25	-999.25	-999.25	-999.25
6048.5	0	0.6127996	-999.25	-999.25	-999.25	-999.25

Appendix A – log database

6049	0	0.6127996	-999.25	-999.25	-999.25	-999.25
6049.5	0	0.6127996	-999.25	-999.25	-999.25	-999.25
6050	0	0.6127996	-999.25	-999.25	-999.25	-999.25
6050.5	0	0.6127996	-999.25	-999.25	-999.25	-999.25
6051	0	0.6127996	-999.25	-999.25	-999.25	-999.25
6051.5	0.0158801	0.6127996	-999.25	-999.25	-999.25	-999.25
6052	0.0586466	0.6127996	-999.25	-999.25	-999.25	-999.25
6052.5	0.0258052	0.6127996	-999.25	-999.25	-999.25	-999.25
6053	0	0.6127996	-999.25	-999.25	-999.25	-999.25
6053.5	0	0.6127996	-999.25	-999.25	-999.25	-999.25
6054	0	0.6127996	-999.25	-999.25	-999.25	-999.25
6054.5	0.0118107	0.6127996	-999.25	-999.25	-999.25	-999.25
6055	0.0219946	0.6616001	-999.25	-999.25	-999.25	-999.25
6055.5	0	0.6127996	-999.25	-999.25	-999.25	-999.25
6056	0	0.6127996	-999.25	-999.25	-999.25	-999.25
6056.5	0	0.6127996	-999.25	-999.25	-999.25	-999.25
6057	0	0.6127996	-999.25	-999.25	-999.25	-999.25
6057.5	0	0.6616001	-999.25	-999.25	-999.25	-999.25
6058	0	0.6616001	-999.25	-999.25	-999.25	-999.25
6058.5	0	0.6127996	-999.25	-999.25	-999.25	-999.25
6059	0	0.6616001	-999.25	-999.25	-999.25	-999.25
6059.5	0	0.6127996	-999.25	-999.25	-999.25	-999.25
6060	0	0.6127996	-999.25	-999.25	-999.25	-999.25
6060.5	0	0.6127996	-999.25	-999.25	-999.25	-999.25
6061	0.0437098	0.6616001	-999.25	-999.25	-999.25	-999.25
6061.5	0.0546092	0.6616001	-999.25	-999.25	-999.25	-999.25
6062	0.0144501	0.6127996	-999.25	-999.25	-999.25	-999.25
6062.5	0.0129459	0.6127996	-999.25	-999.25	-999.25	-999.25
6063	0	0.6616001	-999.25	-999.25	-999.25	-999.25
6063.5	0	0.6616001	-999.25	-999.25	-999.25	-999.25
6064	0	0.6616001	-999.25	-999.25	-999.25	-999.25
6064.5	0	0.6616001	-999.25	-999.25	-999.25	-999.25
6065	0	0.6616001	-999.25	-999.25	-999.25	-999.25
6065.5	0	0.6616001	-999.25	-999.25	-999.25	-999.25
6066	0	0.6616001	-999.25	-999.25	-999.25	-999.25
6066.5	0	0.6616001	-999.25	-999.25	-999.25	-999.25
6067	0	0.7103996	-999.25	-999.25	-999.25	-999.25
6067.5	0	0.7103996	-999.25	-999.25	-999.25	-999.25
6068	0	0.7103996	-999.25	-999.25	-999.25	-999.25
6068.5	0	0.7103996	-999.25	-999.25	-999.25	-999.25
6069	0	0.7103996	-999.25	-999.25	-999.25	-999.25
6069.5	0.047781	0.7103996	-999.25	-999.25	-999.25	-999.25
6070	0.0438453	0.7591	-999.25	-999.25	-999.25	-999.25
6070.5	0	0.7103996	-999.25	-999.25	-999.25	-999.25

Appendix A – log database

6071	0	0.7103996	-999.25	-999.25	-999.25	-999.25
6071.5	0	0.7103996	-999.25	-999.25	-999.25	-999.25
6072	0	0.7103996	-999.25	-999.25	-999.25	-999.25
6072.5	0.0369567	0.7103996	-999.25	-999.25	-999.25	-999.25
6073	0.0709951	0.7103996	-999.25	-999.25	-999.25	-999.25
6073.5	0.0669078	0.7103996	-999.25	-999.25	-999.25	-999.25
6074	0.0390869	0.7103996	-999.25	-999.25	-999.25	-999.25
6074.5	0.0164971	0.7103996	-999.25	-999.25	-999.25	-999.25
6075	0	0.7103996	-999.25	-999.25	-999.25	-999.25
6075.5	0	0.7103996	-999.25	-999.25	-999.25	-999.25
6076	0	0.7103996	-999.25	-999.25	-999.25	-999.25
6076.5	0	0.7103996	-999.25	-999.25	-999.25	-999.25
6077	0	0.7591	-999.25	-999.25	-999.25	-999.25
6077.5	0	0.7591	-999.25	-999.25	-999.25	-999.25
6078	0	0.7591	-999.25	-999.25	-999.25	-999.25
6078.5	0	0.7591	-999.25	-999.25	-999.25	-999.25
6079	0	0.8079004	-999.25	-999.25	-999.25	-999.25
6079.5	0	0.8079004	-999.25	-999.25	-999.25	-999.25
6080	0	0.8079004	-999.25	-999.25	-999.25	-999.25
6080.5	0	0.8079004	-999.25	-999.25	-999.25	-999.25
6081	0	0.8079004	-999.25	-999.25	-999.25	-999.25
6081.5	0	0.8079004	-999.25	-999.25	-999.25	-999.25
6082	0	0.8566999	-999.25	-999.25	-999.25	-999.25
6082.5	0	0.8566999	-999.25	-999.25	-999.25	-999.25
6083	0	0.8566999	-999.25	-999.25	-999.25	-999.25
6083.5	0	0.8566999	-999.25	-999.25	-999.25	-999.25
6084	0	0.8566999	-999.25	-999.25	-999.25	-999.25
6084.5	0	0.8566999	-999.25	-999.25	-999.25	-999.25
6085	0	0.8566999	-999.25	-999.25	-999.25	-999.25
6085.5	0	0.8566999	-999.25	-999.25	-999.25	-999.25
6086	0	0.8566999	-999.25	-999.25	-999.25	-999.25
6086.5	0.0133102	0.8566999	-999.25	-999.25	-999.25	-999.25
6087	0.0741532	0.8566999	-999.25	-999.25	-999.25	-999.25
6087.5	0.0791586	0.8566999	-999.25	-999.25	-999.25	-999.25
6088	0.0163221	0.8079004	-999.25	-999.25	-999.25	-999.25
6088.5	0.0317094	0.8079004	-999.25	-999.25	-999.25	-999.25
6089	0.0371629	0.8079004	-999.25	-999.25	-999.25	-999.25
6089.5	0.015236	0.8079004	-999.25	-999.25	-999.25	-999.25
6090	0.0524572	0.8079004	-999.25	-999.25	-999.25	-999.25
6090.5	0.0630608	0.8079004	-999.25	-999.25	-999.25	-999.25
6091	0.0000028	0.8079004	-999.25	-999.25	-999.25	-999.25
6091.5	0	0.8079004	-999.25	-999.25	-999.25	-999.25
6092	0	0.8079004	-999.25	-999.25	-999.25	-999.25
6092.5	0	0.8079004	-999.25	-999.25	-999.25	-999.25

Appendix A – log database

6093	0	0.8079004	-999.25	-999.25	-999.25	-999.25
6093.5	0	0.8079004	-999.25	-999.25	-999.25	-999.25
6094	0	0.8079004	-999.25	-999.25	-999.25	-999.25
6094.5	0	0.7591	-999.25	-999.25	-999.25	-999.25
6095	0	0.8079004	-999.25	-999.25	-999.25	-999.25
6095.5	0	0.8079004	-999.25	-999.25	-999.25	-999.25
6096	0	0.8079004	-999.25	-999.25	-999.25	-999.25
6096.5	0	0.8079004	-999.25	-999.25	-999.25	-999.25
6097	0	0.8079004	-999.25	-999.25	-999.25	-999.25
6097.5	0	0.8079004	-999.25	-999.25	-999.25	-999.25
6098	0	0.8079004	-999.25	-999.25	-999.25	-999.25
6098.5	0	0.8079004	-999.25	-999.25	-999.25	-999.25
6099	0	0.8079004	-999.25	-999.25	-999.25	-999.25
6099.5	0	0.8079004	-999.25	-999.25	-999.25	-999.25
6100	0	0.8079004	-999.25	-999.25	-999.25	-999.25
6100.5	0	0.8079004	-999.25	-999.25	-999.25	-999.25
6101	0	0.8079004	-999.25	-999.25	-999.25	-999.25
6101.5	0	0.8079004	-999.25	-999.25	-999.25	-999.25
6102	0	0.8079004	-999.25	-999.25	-999.25	-999.25
6102.5	0	0.8079004	-999.25	-999.25	-999.25	-999.25
6103	0	0.8079004	-999.25	-999.25	-999.25	-999.25
6103.5	0	0.8079004	-999.25	-999.25	-999.25	-999.25
6104	0	0.8079004	-999.25	-999.25	-999.25	-999.25
6104.5	0	0.8079004	-999.25	-999.25	-999.25	-999.25
6105	0	0.8566999	-999.25	-999.25	-999.25	-999.25
6105.5	0	0.8566999	-999.25	-999.25	-999.25	-999.25
6106	0	0.8566999	-999.25	-999.25	-999.25	-999.25
6106.5	0	0.8566999	-999.25	-999.25	-999.25	-999.25
6107	0	0.8566999	-999.25	-999.25	-999.25	-999.25
6107.5	0	0.9055004	-999.25	-999.25	-999.25	-999.25
6108	0	0.9055004	-999.25	-999.25	-999.25	-999.25
6108.5	0	0.9542999	-999.25	-999.25	-999.25	-999.25
6109	0	1.003	-999.25	-999.25	-999.25	-999.25
6109.5	0	1.0518	-999.25	-999.25	-999.25	-999.25
6110	0	1.003	-999.25	-999.25	-999.25	-999.25
6110.5	0	1.003	-999.25	-999.25	-999.25	-999.25
6111	0	1.003	-999.25	-999.25	-999.25	-999.25
6111.5	0	1.0518	-999.25	-999.25	-999.25	-999.25
6112	0	1.0518	-999.25	-999.25	-999.25	-999.25
6112.5	0	1.0518	-999.25	-999.25	-999.25	-999.25
6113	0	1.0518	-999.25	-999.25	-999.25	-999.25
6113.5	0	1.0518	-999.25	-999.25	-999.25	-999.25
6114	0	1.0518	-999.25	-999.25	-999.25	-999.25
6114.5	0	1.0518	-999.25	-999.25	-999.25	-999.25

Appendix A – log database

6115	0	1.1006	-999.25	-999.25	-999.25	-999.25
6115.5	0	1.1006	-999.25	-999.25	-999.25	-999.25
6116	0	1.1006	-999.25	-999.25	-999.25	-999.25
6116.5	0	1.1006	-999.25	-999.25	-999.25	-999.25
6117	0	1.1006	-999.25	-999.25	-999.25	-999.25
6117.5	0	1.1006	-999.25	-999.25	-999.25	-999.25
6118	0	1.1494	-999.25	-999.25	-999.25	-999.25
6118.5	0	1.1494	-999.25	-999.25	-999.25	-999.25
6119	0	1.1494	-999.25	-999.25	-999.25	-999.25
6119.5	0	1.1494	-999.25	-999.25	-999.25	-999.25
6120	0	1.1982	-999.25	-999.25	-999.25	-999.25
6120.5	0	1.1982	-999.25	-999.25	-999.25	-999.25
6121	0	1.1982	-999.25	-999.25	-999.25	-999.25
6121.5	0	1.1982	-999.25	-999.25	-999.25	-999.25
6122	0	1.247	-999.25	-999.25	-999.25	-999.25
6122.5	0	1.247	-999.25	-999.25	-999.25	-999.25
6123	0	1.1982	-999.25	-999.25	-999.25	-999.25
6123.5	0	1.247	-999.25	-999.25	-999.25	-999.25
6124	0	1.1982	-999.25	-999.25	-999.25	-999.25
6124.5	0	1.1982	-999.25	-999.25	-999.25	-999.25
6125	0	1.1982	-999.25	-999.25	-999.25	-999.25
6125.5	0	1.1982	-999.25	-999.25	-999.25	-999.25
6126	0	1.1982	-999.25	-999.25	-999.25	-999.25
6126.5	0	1.1494	-999.25	-999.25	-999.25	-999.25
6127	0	1.1494	-999.25	-999.25	-999.25	-999.25
6127.5	0	1.1494	-999.25	-999.25	-999.25	-999.25
6128	0	1.1006	-999.25	-999.25	-999.25	-999.25
6128.5	0	1.1006	-999.25	-999.25	-999.25	-999.25
6129	0	1.0518	-999.25	-999.25	-999.25	-999.25
6129.5	0	1.003	-999.25	-999.25	-999.25	-999.25
6130	0.0366624	1.003	-999.25	-999.25	-999.25	-999.25
6130.5	0	0.9542999	0	0.4453293	0.0845774	0.0376648
6131	0	0.9055004	0.0023882	0.3367677	0.1167364	0.0393131
6131.5	0	0.8566999	0	0.331046	0.1237077	0.040953
6132	0	0.8079004	0	0.4007275	0.1038001	0.0415956
6132.5	0	0.8079004	0	0.6138763	0.0677361	0.0415816
6133	0	0.8079004	0	1	0.0160456	0.0160456
6133.5	0	0.7591	-999.25	-999.25	-999.25	-999.25
6134	0	0.7591	-999.25	-999.25	-999.25	-999.25
6134.5	0	0.7103996	-999.25	-999.25	-999.25	-999.25
6135	0	0.6616001	-999.25	-999.25	-999.25	-999.25
6135.5	0	0.6616001	-999.25	-999.25	-999.25	-999.25
6136	0	0.7103996	-999.25	-999.25	-999.25	-999.25
6136.5	0	0.7103996	-999.25	-999.25	-999.25	-999.25

Appendix A – log database

6137	0	0.7103996	-999.25	-999.25	-999.25	-999.25
6137.5	0	0.6127996	-999.25	-999.25	-999.25	-999.25
6138	0	0.6616001	-999.25	-999.25	-999.25	-999.25
6138.5	0	0.7103996	-999.25	-999.25	-999.25	-999.25
6139	0	0.3689003	-999.25	-999.25	-999.25	-999.25
6139.5	0	0.3689003	-999.25	-999.25	-999.25	-999.25
6140	0	0.2713003	-999.25	-999.25	-999.25	-999.25
6140.5	0	0.2713003	-999.25	-999.25	-999.25	-999.25
6141	0	0.2713003	-999.25	-999.25	-999.25	-999.25
6141.5	0	0.2226	-999.25	-999.25	-999.25	-999.25
6142	0	0.2226	-999.25	-999.25	-999.25	-999.25
6142.5	0	0.1738005	-999.25	-999.25	-999.25	-999.25
6143	0	0.1738005	-999.25	-999.25	-999.25	-999.25
6143.5	0.0464788	0.1738005	-999.25	-999.25	-999.25	-999.25
6144	0.0462729	0.1738005	-999.25	-999.25	-999.25	-999.25
6144.5	0	0.1738005	0.0204788	0.3109442	0.155705	0.0484156
6145	0	0.1738005	0	0.2783951	0.1801729	0.0501593
6145.5	0	0.1738005	0	0.3315408	0.1564685	0.0518757
6146	0	0.1738005	0	0.5774296	0.0924169	0.0533642
6146.5	0.0238597	0.2226	0	1	0.0397944	0.0397944
6147	0.0342188	0.2226	0	1	0.0461343	0.0461343
6147.5	0	0.2226	0	0.5595897	0.1016173	0.056864
6148	0	0.2226	0.0425236	0.3494678	0.1568718	0.0548216
6148.5	0	0.2226	0.0420543	0.2733658	0.1946575	0.0532127
6149	0	0.2226	0.0202081	0.2620743	0.2038871	0.0534336
6149.5	0	0.2226	0	0.2851646	0.1901175	0.0542148
6150	0	0.1738005	0	0.3141558	0.1751176	0.0550142
6150.5	0	0.1738005	0	0.3340389	0.1678273	0.0560609
6151	0	0.1738005	0	0.3659827	0.1498615	0.0548467
6151.5	0	0.1738005	0	0.5009811	0.1054042	0.0528055
6152	0	0.2226	0	1	0.0402297	0.0402297
6152.5	0	0.2226	-999.25	-999.25	-999.25	-999.25
6153	0	0.2226	-999.25	-999.25	-999.25	-999.25
6153.5	0	0.2226	-999.25	-999.25	-999.25	-999.25
6154	0	0.2226	-999.25	-999.25	-999.25	-999.25
6154.5	0.0398533	0.2226	-999.25	-999.25	-999.25	-999.25
6155	0.05898	0.125	-999.25	-999.25	-999.25	-999.25
6155.5	0	0.2226	-999.25	-999.25	-999.25	-999.25
6156	0	0.125	-999.25	-999.25	-999.25	-999.25
6156.5	0	0.125	0.0384446	0.2065618	0.2555955	0.0527963
6157	0	0.1738005	0.012941	0.2081067	0.2595675	0.0540177
6157.5	0	0.125	0.001348	0.2208072	0.2573709	0.0568293
6158	0	0.1738005	0.0080199	0.2295585	0.2627782	0.060323
6158.5	0	0.1738005	0.011339	0.2347081	0.2666189	0.0625776

Appendix A – log database

6159	0	0.1738005	0.025512	0.226035	0.2857219	0.0645832
6159.5	0	0.1738005	0.022211	0.226045	0.2896448	0.0654728
6160	0	0.1738005	0.0154016	0.2279785	0.2885242	0.0657773
6160.5	0	0.2226	0.0049792	0.2367036	0.2767285	0.0655026
6161	0	0.2226	0	0.2688266	0.242858	0.0652867
6161.5	0	0.125	0	0.2986333	0.2168596	0.0647615
6162	0	0.2226	0	0.2968781	0.218129	0.0647577
6162.5	0	0.1738005	0.0078185	0.2905312	0.2228466	0.0647439
6163	0	0.1738005	0.0098798	0.2905647	0.2238393	0.0650398
6163.5	0	0.1738005	0.007302	0.2873805	0.2262948	0.0650327
6164	0	0.1738005	0.0030638	0.2870808	0.2286043	0.0656279
6164.5	0	0.2226	0	0.2884802	0.2244151	0.0647393
6165	0	0.2713003	0	0.3055134	0.2110593	0.0644815
6165.5	0	0.1738005	0	0.349688	0.185414	0.0648371
6166	0	0.1738005	0	0.3545531	0.185414	0.0657391
6166.5	0	0.1738005	0	0.3861627	0.171159	0.0660952
6167	0	0.1738005	0	0.3816609	0.1731578	0.0660876
6167.5	0	0.1738005	0.0081565	0.3705066	0.1799524	0.0666736
6168	0	0.1738005	0.0171653	0.3639921	0.1882199	0.0685105
6168.5	0	0.1738005	0.0274254	0.3357034	0.2067255	0.0693985
6169	0	0.1738005	0.0313309	0.309636	0.2270347	0.0702981
6169.5	0	0.1738005	0.0274413	0.2994807	0.2368053	0.0709186
6170	0	0.1738005	0.0190759	0.3092079	0.2325887	0.0719183
6170.5	0	0.2226	0.007812	0.3461189	0.213786	0.0739954
6171	0	0.1738005	0	0.401185	0.1855565	0.0744425
6171.5	0	0.1738005	0	0.4430519	0.1674217	0.0741765
6172	0	0.2226	0	0.4655105	0.1594224	0.0742128
6172.5	0	0.2226	0	0.4503076	0.1655039	0.0745277
6173	0	0.2226	0	0.4226794	0.1770159	0.074821
6173.5	0	0.2226	0	0.4114688	0.1834565	0.0754866
6174	0	0.2226	0	0.4023671	0.1910167	0.0768588
6174.5	0	0.2713003	0	0.3849042	0.2051309	0.0789557
6175	0	0.2713003	0.0090673	0.3581717	0.2263942	0.081088
6175.5	0	0.3200998	0.0196779	0.33905	0.2500941	0.0847944
6176	0	0.2713003	0.0199295	0.3372664	0.259557	0.0875398
6176.5	0	0.3200998	0.0146868	0.3517873	0.2581948	0.0908296
6177	0	0.2226	0.0006857	0.382592	0.2441937	0.0934266
6177.5	0	0.2713003	0	0.3995079	0.2371773	0.0947542
6178	0	0.3200998	0	0.4042362	0.2376599	0.0960707
6178.5	0	0.3689003	0	0.3944401	0.2446157	0.0964862
6179	0	0.3689003	0.0010422	0.3811288	0.2542282	0.0968937
6179.5	0	0.2713003	0.0058104	0.3619987	0.2663111	0.0964043
6180	0	0.125	0.0096157	0.3429696	0.2771198	0.0950437
6180.5	0	0.1738005	0.0031573	0.3321602	0.2758003	0.0916099

Appendix A – log database

6181	0	0.1738005	0	0.3318014	0.2662058	0.0883275
6181.5	0	0.1738005	0	0.3431265	0.2460283	0.0844188
6182	0	0.1738005	0	0.3833432	0.2049482	0.0785655
6182.5	0.0360318	0.1738005	-999.25	-999.25	-999.25	-999.25
6183	0	0.1738005	-999.25	-999.25	-999.25	-999.25
6183.5	0	0.1738005	-999.25	-999.25	-999.25	-999.25
6184	0	0.1738005	-999.25	-999.25	-999.25	-999.25
6184.5	0	0.125	-999.25	-999.25	-999.25	-999.25
6185	0	0.1738005	-999.25	-999.25	-999.25	-999.25
6185.5	0	0.1738005	-999.25	-999.25	-999.25	-999.25
6186	0.0371039	0.1738005	-999.25	-999.25	-999.25	-999.25
6186.5	0.04134	0.1738005	-999.25	-999.25	-999.25	-999.25
6187	0	0.1738005	-999.25	-999.25	-999.25	-999.25
6187.5	0	0.2226	0.0564848	0.2918252	0.2004203	0.0584877
6188	0	0.2226	0.0391742	0.2925466	0.215062	0.0629157
6188.5	0	0.1738005	0.0277988	0.3135584	0.2169704	0.0680329
6189	0	0.1738005	0.0213112	0.3370974	0.2123526	0.0715835
6189.5	0	0.1738005	0.0371411	0.356454	0.2211228	0.0788201
6190	0	0.1738005	0.0510304	0.36162	0.2281643	0.0825088
6190.5	0	0.2226	0.0644226	0.3473307	0.2462777	0.0855398
6191	0	0.2226	0.0717823	0.3309281	0.2631177	0.087073
6191.5	0	0.2226	0.0656078	0.3241922	0.2722269	0.0882538
6192	0	0.2713003	0.0522786	0.332468	0.277904	0.0923942
6192.5	0	0.2713003	0.0382877	0.3516446	0.2726624	0.0958803
6193	0	0.2713003	0.0257008	0.3893221	0.2580224	0.1004538
6193.5	0	0.1738005	0.0389736	0.3822391	0.2663757	0.1018192
6194	0	0.2226	0.0582116	0.3532074	0.2880449	0.1017396
6194.5	0	0.2713003	0.0656635	0.3191539	0.3112813	0.0993466
6195	0	0.2713003	0.0613953	0.3026045	0.3266378	0.0988421
6195.5	0	0.2226	0.0418	0.3160998	0.318586	0.100705
6196	0	0.2226	0.0314034	0.3337507	0.3088607	0.1030825
6196.5	0	0.1738005	0.0204822	0.3553212	0.2942881	0.1045668
6197	0	0.1738005	0.0243165	0.3414839	0.2964787	0.1012427
6197.5	0	0.125	0.0426141	0.3042952	0.3146388	0.0957431
6198	0	0.1738005	0.0246524	0.309869	0.2925779	0.0906608
6198.5	0	0.1738005	0.0068041	0.3314869	0.2626786	0.0870745
6199	0	0.2226	0.0013032	0.3586175	0.2386022	0.0855669
6199.5	0	0.2226	0.0061629	0.3696965	0.2211021	0.0817407
6200	0	0.2713003	0	0.4338723	0.1770274	0.0768073
6200.5	0	0.2713003	0	0.6607572	0.1065531	0.0704057
6201	0	0.1738005	0	0.8874564	0.0723009	0.0641639
6201.5	0	0.1738005	0	1	0.0611388	0.0611388
6202	0	0.1738005	0	1	0.0686064	0.0686064
6202.5	0	0.1738005	0	0.9448601	0.0841903	0.0795481

Appendix A – log database

6203	0	0.1738005	0	0.868467	0.1007157	0.0874683
6203.5	0	0.1738005	0	0.8094658	0.113536	0.0919035
6204	0	0.1738005	0	0.8257403	0.1181177	0.0975346
6204.5	0	0.1738005	0	0.8816383	0.1132532	0.0998484
6205	0	0.1738005	0	0.9348342	0.1083427	0.1012824
6205.5	0	0.2226	0	0.9287731	0.1090427	0.1012759
6206	0	0.1738005	0	0.9301971	0.1078895	0.1003585
6206.5	0	0.2226	0	0.9644902	0.100821	0.0972408
6207	0	0.2226	0	1	0.0915104	0.0915104
6207.5	0	0.2713003	0	1	0.0889726	0.0889726
6208	0	0.1738005	0	0.8648197	0.1020629	0.088266
6208.5	0	0.1738005	0	0.7387145	0.1171435	0.0865356
6209	0	0.1738005	0	0.6698878	0.1308323	0.087643
6209.5	0	0.1738005	0	0.6940461	0.1309469	0.0908832
6210	0	0.2713003	0	0.7612826	0.1233661	0.0939164
6210.5	0	0.1738005	0.0007779	0.7268287	0.1382975	0.1005186
6211	0	0.1738005	0.0087354	0.6855828	0.1526708	0.1046685
6211.5	0	0.1738005	0.0071332	0.7131375	0.1572225	0.1121213
6212	0	0.2226	0.0016762	0.7680426	0.1564317	0.1201462
6212.5	0	0.2226	0	0.8183542	0.1558781	0.1275635
6213	0	0.1738005	0.0014307	0.8438835	0.1626511	0.1372586
6213.5	0	0.1738005	0.015369	0.7783113	0.1819306	0.1415986
6214	0	0.1738005	0.0327858	0.7216137	0.2061632	0.1487702
6214.5	0	0.1738005	0.0369194	0.6915569	0.2199919	0.1521369
6215	0	0.1738005	0.0247829	0.6905106	0.2233565	0.15423
6215.5	0	0.1738005	0.0270246	0.6454189	0.2409841	0.1555357
6216	0	0.1738005	0.027895	0.6106911	0.252243	0.1540426
6216.5	0	0.2226	0.0262243	0.6032922	0.2553058	0.154024
6217	0	0.2226	0.0271814	0.5962916	0.255928	0.1526077
6217.5	0	0.2713003	0.0243719	0.6039475	0.2504216	0.1512415
6218	0	0.2226	0.024595	0.6120751	0.2482589	0.1519531
6218.5	0	0.1738005	0.0470047	0.5645232	0.2739006	0.1546232
6219	0	0.1738005	0.0631991	0.5150573	0.3013037	0.1551887
6219.5	0	0.1738005	0.0512266	0.5142595	0.3017665	0.1551863
6220	0	0.1738005	0.0275565	0.5391343	0.2814927	0.1517623
6220.5	0	0.1738005	0.0166962	0.5422407	0.2637868	0.1430359
6221	0	0.1738005	0.0177719	0.539862	0.2531255	0.1366528
6221.5	0	0.2226	0.0059953	0.5652926	0.2258601	0.127677
6222	0	0.2226	0	0.5862222	0.1900215	0.1113948
6222.5	0	0.3200998	0	0.6153822	0.1645681	0.1012723
6223	0	0.2226	0	0.5042743	0.1693176	0.0853825
6223.5	0	0.2226	0.011849	0.3797466	0.1982393	0.0752807
6224	0	0.2226	0.0179321	0.2839329	0.2348186	0.0666727
6224.5	0	0.3200998	0.0233195	0.1964504	0.2678458	0.0526184

Appendix A – log database

6225	0	0.1738005	0.0406306	0.1768796	0.2857033	0.0505351
6225.5	0	0.125	0.0496611	0.1692192	0.2766414	0.046813
6226	0	0.1738005	0.0728608	0.1668051	0.2658555	0.044346
6226.5	0	0.1738005	0.115711	0.1631612	0.2629149	0.0428975
6227	0	0.0761995	0.1281258	0.1575075	0.2705304	0.0426106
6227.5	0	0.125	0.0985105	0.1621886	0.2673283	0.0433576
6228	0	0.2226	0.0719627	0.1760437	0.2544272	0.0447903
6228.5	0	0.2226	0.0601372	0.1857477	0.2460276	0.045699
6229	0	0.1738005	0.0515384	0.1932539	0.2440462	0.0471629
6229.5	0	0.125	0.0480479	0.1892828	0.2560433	0.0484646
6230	0	0.125	0.0537965	0.1751954	0.277289	0.0485798
6230.5	0	0.1738005	0.0595322	0.1678077	0.2906959	0.048781
6231	0	0.1738005	0.0444624	0.1708525	0.2793271	0.0477237
6231.5	0	0.2713003	0.026676	0.1750116	0.2666228	0.0466621
6232	0	0.3689003	0.0202719	0.1744131	0.2662782	0.0464424
6232.5	0	0.1738005	0.012161	0.1829097	0.2566091	0.0469363
6233	0	0.1738005	0	0.2045853	0.2246899	0.0459683
6233.5	0	0.2713003	0	0.2405258	0.1834817	0.0441321
6234	0	0.3200998	0.004017	0.2620047	0.1713328	0.04489
6234.5	0	0.2713003	0.0396086	0.2436628	0.1941383	0.0473043
6235	0	0.2226	0.0706796	0.231011	0.2276821	0.0525971
6235.5	0	0.2226	0.0827145	0.221478	0.2584982	0.0572517
6236	0	0.2226	0.0572759	0.2395131	0.2584982	0.0619137
6236.5	0	0.2226	0.0612391	0.2321187	0.2799696	0.0649862
6237	0	0.2713003	0.0609825	0.2350414	0.2846465	0.0669037
6237.5	0	0.3689003	0.0576248	0.2510536	0.2743349	0.0688728
6238	0	0.0761995	0.0578635	0.2619029	0.2605866	0.0682484
6238.5	0	0.0761995	0.0649545	0.2657142	0.2526399	0.06713
6239	0	0.125	0.0632664	0.262244	0.2424638	0.0635847
6239.5	0	0.125	0.0450472	0.2644509	0.2284231	0.0604067
6240	0	0.2226	0.0210332	0.2597393	0.2105996	0.054701
6240.5	0	0.1738005	0.0127206	0.2516996	0.2020897	0.0508659
6241	0	0.125	0.0241273	0.2236488	0.2111162	0.0472159
6241.5	0	0.1738005	0.0382372	0.2063186	0.2138125	0.0441135
6242	0	0.2226	0.0343216	0.2253128	0.1893027	0.0426523
6242.5	0	0.1738005	0.0264528	0.2418771	0.1699181	0.0410993
6243	0	0.3200998	0.0511397	0.2281194	0.187696	0.0428171
6243.5	0	0.2713003	0.0993737	0.1965039	0.2313077	0.0454529
6244	0	0.0274	0.1282014	0.1831662	0.2708421	0.0496091
6244.5	0	0.0274	0.1295218	0.180819	0.2802991	0.0506834
6245	0	0.125	0.1347189	0.1835079	0.2828496	0.0519051
6245.5	0	0.125	0.127563	0.1852084	0.2771927	0.0513384
6246	0	0.125	0.1239294	0.185876	0.273329	0.0508053
6246.5	0	0.2226	0.1214664	0.1935338	0.2614989	0.0506089

Appendix A – log database

6247	0	0.2713003	0.0912051	0.2306353	0.2190621	0.0505235
6247.5	0	0.1738005	0.0729008	0.2667061	0.1906223	0.0508401
6248	0	0.2713003	0.0750249	0.2679344	0.1974791	0.0529114
6248.5	0	0.2226	0.0772168	0.2540878	0.2190303	0.0556529
6249	0	0.2226	0.0831506	0.2468048	0.239032	0.0589942
6249.5	0	0.1738005	0.0951074	0.2365874	0.2567678	0.060748
6250	0	0.125	0.1025882	0.2382381	0.2693654	0.0641731
6250.5	0	0.1738005	0.0940031	0.2539878	0.2736111	0.0694939
6251	0	0.1738005	0.075671	0.2531457	0.2888259	0.073115
6251.5	0	0.1738005	0.0591671	0.2450474	0.3054062	0.074839
6252	0	0.125	0.0549023	0.2394926	0.3100333	0.0742507
6252.5	0	0.2226	0.0418689	0.2478153	0.2941513	0.0728952
6253	0	0.2226	0.0303398	0.2526494	0.2850981	0.0720299
6253.5	0	0.2226	0.0294011	0.2402245	0.2937893	0.0705754
6254	0	0.2226	0.0393669	0.2323273	0.3047515	0.0708021
6254.5	0	0.2226	0.0598901	0.2329022	0.3101256	0.072229
6255	0	0.2713003	0.0715037	0.2430531	0.3050593	0.0741456
6255.5	0	0.2713003	0.0632375	0.2696311	0.2820555	0.0760509
6256	0	0.3689003	0.0311416	0.3422278	0.2366539	0.0809895
6256.5	0	0.3689003	0.000159	0.507146	0.1971105	0.0999638
6257	0	0.125	0.0048835	0.560924	0.1927676	0.108128
6257.5	0	0.1738005	0.0166254	0.5904689	0.2007079	0.1185118
6258	0	0.2226	0.0176442	0.6062878	0.2065193	0.1252101
6258.5	0	0.2226	0.0169579	0.6595023	0.2119871	0.139806
6259	0	0.2226	0.0140533	0.6836824	0.2170568	0.1483979
6259.5	0	0.1738005	0.0147749	0.6759785	0.227661	0.1538939
6260	0	0.1738005	0.0212843	0.6595102	0.2430564	0.1602981
6260.5	0	0.2226	0.0271682	0.6400869	0.2538106	0.1624608
6261	0	0.1738005	0.0343313	0.6328729	0.2613961	0.1654305
6261.5	0	0.1738005	0.038871	0.6182479	0.2650902	0.1638914
6262	0	0.1738005	0.0416509	0.6162955	0.2647145	0.1631424
6262.5	0	0.1738005	0.03753	0.6299946	0.2543283	0.1602255
6263	0	0.1738005	0.0458378	0.6213015	0.2531919	0.1573085
6263.5	0	0.1738005	0.0571474	0.6164591	0.2516938	0.1551589
6264	0	0.2226	0.0553486	0.6413774	0.2387245	0.1531125
6264.5	0	0.2713003	0.0566699	0.6510561	0.2330776	0.1517466
6265	0	0.2713003	0.0525147	0.6806855	0.2261022	0.1539045
6265.5	0	0.2713003	0.0473612	0.6849375	0.2257351	0.1546144
6266	0	0.1738005	0.0363165	0.686303	0.2252904	0.1546175
6266.5	0	0.2226	0.0394204	0.6651549	0.2366588	0.1574148
6267	0	0.1738005	0.0447677	0.6558475	0.2455191	0.1610231
6267.5	0	0.1738005	0.0386044	0.677908	0.2419812	0.164041
6268	0	0.2226	0.0307154	0.7103519	0.2385277	0.1694386
6268.5	0	0.2226	0.0199277	0.7389117	0.2336193	0.172624

Appendix A – log database

6269	0	0.1738005	0.0123963	0.7521901	0.232696	0.1750316
6269.5	0	0.1738005	0.0126569	0.7398467	0.2387066	0.1766063
6270	0	0.1738005	0.0155106	0.7245629	0.2459269	0.1781895
6270.5	0	0.1738005	0.0197748	0.7020318	0.2537403	0.1781338
6271	0	0.1738005	0.0274049	0.6760617	0.262188	0.1772553
6271.5	0	0.1738005	0.0302287	0.6646804	0.2654194	0.1764191
6272	0	0.1738005	0.0242631	0.6726975	0.2622873	0.17644
6272.5	0	0.125	0.0370438	0.6294064	0.2787387	0.1754399
6273	0	0.125	0.0466391	0.593864	0.2925678	0.1737455
6273.5	0	0.1738005	0.0437318	0.5856322	0.2912854	0.1705861
6274	0	0.125	0.040233	0.5895547	0.2841333	0.1675121
6274.5	0	0.1738005	0.0357479	0.5941221	0.2756149	0.1637489
6275	0	0.1738005	0.0257103	0.6204625	0.261633	0.1623335
6275.5	0	0.1738005	0.0184674	0.6404385	0.2489668	0.1594479
6276	0	0.1738005	0.0096555	0.6648749	0.2377308	0.1580612
6276.5	0	0.1738005	0.0145017	0.636226	0.2438341	0.1551336
6277	0	0.2226	0.0241139	0.5832839	0.2585703	0.1508199
6277.5	0	0.2226	0.0305344	0.5493068	0.2694419	0.1480063
6278	0	0.2226	0.0276754	0.5492924	0.2609848	0.143357
6278.5	0	0.1738005	0.0143193	0.5891889	0.2358322	0.1389497
6279	0	0.2226	0	0.7046976	0.1921934	0.1354382
6279.5	0	0.2713003	0	0.825971	0.1583058	0.130756
6280	0	0.2226	0	0.8582548	0.148295	0.1272749
6280.5	0	0.1738005	0	0.8346482	0.1476578	0.1232423
6281	0	0.1738005	0	0.8104679	0.1513269	0.1226456
6281.5	0	0.1738005	0	0.7884728	0.1562171	0.1231729
6282	0	0.1738005	0	0.8038623	0.1575069	0.1266138
6282.5	0	0.2226	0	0.796236	0.1604558	0.1277607
6283	0	0.1738005	0	0.7487559	0.1720912	0.1288543
6283.5	0	0.1738005	0.0042173	0.6888745	0.1835174	0.1264204
6284	0	0.1738005	0.0054513	0.6614017	0.1876113	0.1240864
6284.5	0	0.2226	0	0.6520681	0.180962	0.1179996
6285	0	0.1738005	0	0.6882127	0.1661608	0.114354
6285.5	0	0.2226	0	0.7114025	0.1522341	0.1082998
6286	0	0.2713003	0.0091396	0.6817409	0.1476192	0.100638
6286.5	0	0.2713003	0.0281661	0.5015106	0.1585011	0.07949
6287	0	0.2226	0.0404722	0.4427631	0.1719153	0.0761177
6287.5	0	0.3200998	0.0340702	0.4403073	0.1712289	0.0753933
6288	0	0.3200998	0.0248721	0.4574868	0.1700963	0.0778168
6288.5	0	0.2713003	0.0216459	0.4643233	0.1805436	0.0838306
6289	0	0.2226	0.0224634	0.4476003	0.1977259	0.0885022
6289.5	0	0.1738005	0.0194945	0.445075	0.2124892	0.0945736
6290	0	0.2713003	0.0117058	0.4433295	0.2188764	0.0970344
6290.5	0	0.2226	0	0.4925645	0.1979403	0.0974984

6291	0	0.1738005	0	0.5581583	0.1742867	0.0972796
6291.5	0	0.125	0	0.6560861	0.148154	0.0972018
6292	0	0.0761995	0	0.7280715	0.136904	0.0996759
6292.5	0	0.125	0	0.692807	0.1475352	0.1022134
6293	0	0.0761995	0	0.6178401	0.1716097	0.1060273
6293.5	0	0.0761995	0.1155573	0.515521	0.2136692	0.110151
6294	0	0.0761995	0.2390452	0.4559498	0.2495362	0.113776
6294.5	0	0.1738005	0.2091886	0.4594821	0.2576524	0.1183867
6295	0	0.2713003	0.0573474	0.5319253	0.2249857	0.1196756
6295.5	0	0.125	0.0054334	0.696999	0.2013295	0.1403265
6296	0	0.125	0.0054334	0.7034586	0.2013295	0.141627
6296.5	0	0.1738005	0.0147262	0.6662537	0.2105261	0.1402638
6297	0	0.2226	0.0246213	0.6130472	0.2204212	0.1351286
6297.5	0	0.1738005	0	0.6780981	0.1923321	0.13042
6298	0	0.1738005	0	0.8075206	0.1559894	0.1259646
6298.5	0	0.2713003	0	0.8490362	0.138624	0.1176968
6299	0	0.2226	0	0.8325563	0.1356573	0.1129423
6299.5	0	0.1738005	0	0.7773421	0.1380918	0.1073445
6300	0	0.1738005	0	0.7569589	0.1379469	0.1044201

3.2.4 Well B8-NC-74A

TABLE 3.8 Log data Well B8-NC-74A

DEPT (FT)	VCL (V/V)	DD (INCH)	SPI-CPX (V/V)	SW-CPX (V/V)	PHIE-CPX (V/V)	PHSW-CPX
6080	0	0.7968998	-999.25	-999.25	-999.25	-999.25
6080.5	0	0.8046999	-999.25	-999.25	-999.25	-999.25
6081	0	0.7968998	-999.25	-999.25	-999.25	-999.25
6081.5	0	0.7890997	-999.25	-999.25	-999.25	-999.25
6082	0	0.7734003	-999.25	-999.25	-999.25	-999.25
6082.5	0	0.7656002	-999.25	-999.25	-999.25	-999.25
6083	0	0.7421999	-999.25	-999.25	-999.25	-999.25
6083.5	0	0.7343998	-999.25	-999.25	-999.25	-999.25
6084	0	0.7421999	-999.25	-999.25	-999.25	-999.25
6084.5	0	0.7343998	-999.25	-999.25	-999.25	-999.25
6085	0	0.7265997	-999.25	-999.25	-999.25	-999.25
6085.5	0	0.7031002	-999.25	-999.25	-999.25	-999.25
6086	0	0.6953001	-999.25	-999.25	-999.25	-999.25
6086.5	0	0.6640997	-999.25	-999.25	-999.25	-999.25
6087	0	0.6328001	-999.25	-999.25	-999.25	-999.25
6087.5	0	0.6171999	-999.25	-999.25	-999.25	-999.25
6088	0	0.5859003	-999.25	-999.25	-999.25	-999.25

Appendix A – log database

6088.5	0	0.5781002	-999.25	-999.25	-999.25	-999.25
6089	0	0.5468998	-999.25	-999.25	-999.25	-999.25
6089.5	0	0.5234003	-999.25	-999.25	-999.25	-999.25
6090	0	0.5078001	-999.25	-999.25	-999.25	-999.25
6090.5	0	0.4921999	-999.25	-999.25	-999.25	-999.25
6091	0.0227016	0.4609003	-999.25	-999.25	-999.25	-999.25
6091.5	0	0.4296999	0	0.4982765	0.1113538	0.055485
6092	0	0.3984003	0.0059358	0.3426323	0.1633291	0.0559618
6092.5	0	0.3828001	0.0043194	0.3147938	0.175586	0.0552734
6093	0	0.3359003	0	0.3444075	0.1545984	0.0532449
6093.5	0	0.3203001	0	0.4822451	0.1034667	0.0498963
6094	0.004886	0.3203001	0	1	0.03537	0.03537
6094.5	0	0.2734003	-999.25	-999.25	-999.25	-999.25
6095	0	0.2656002	-999.25	-999.25	-999.25	-999.25
6095.5	0	0.2343998	-999.25	-999.25	-999.25	-999.25
6096	0	0.2031002	-999.25	-999.25	-999.25	-999.25
6096.5	0	0.1796999	-999.25	-999.25	-999.25	-999.25
6097	0	0.1484003	-999.25	-999.25	-999.25	-999.25
6097.5	0	0.1406002	-999.25	-999.25	-999.25	-999.25
6098	0	0.1328001	-999.25	-999.25	-999.25	-999.25
6098.5	0	0.1093998	-999.25	-999.25	-999.25	-999.25
6099	0	0.0781002	-999.25	-999.25	-999.25	-999.25
6099.5	0	0.0468998	-999.25	-999.25	-999.25	-999.25
6100	0	0.0390997	-999.25	-999.25	-999.25	-999.25
6100.5	0	0.0156002	-999.25	-999.25	-999.25	-999.25
6101	0	- 0.0156002	-999.25	-999.25	-999.25	-999.25
6101.5	0	- 0.0078001	-999.25	-999.25	-999.25	-999.25
6102	0	- 0.0234003	-999.25	-999.25	-999.25	-999.25
6102.5	0	- 0.0468998	-999.25	-999.25	-999.25	-999.25
6103	0	- 0.0468998	-999.25	-999.25	-999.25	-999.25
6103.5	0	- 0.0703001	-999.25	-999.25	-999.25	-999.25
6104	0.0466413	- 0.1640997	-999.25	-999.25	-999.25	-999.25
6104.5	0	- 0.1796999	0	0.3583324	0.1528738	0.0547796
6105	0	- 0.1484003	0.0304091	0.2497976	0.2244716	0.0560725
6105.5	0	- 0.1640997	0.0266866	0.2375073	0.2442773	0.0580176
6106	0	- 0.1406002	0	0.3020954	0.1938188	0.0585518

Appendix A – log database

6106.5	0	- 0.1406002	0	0.530356	0.1105058	0.0586074
6107	0.0311355	- 0.1484003	0	1	0.0357815	0.0357815
6107.5	0	- 0.1718998	0	0.9403417	0.0606159	0.0569996
6108	0	- 0.2031002	0.022001	0.4180346	0.1326051	0.0554335
6108.5	0	- 0.2031002	0.0437786	0.2664077	0.2080644	0.0554299
6109	0	- 0.2031002	0.0222813	0.2447024	0.2267746	0.0554923
6109.5	0	- 0.1796999	0.0037811	0.2629918	0.2096629	0.0551396
6110	0	- 0.1953001	0	0.2942668	0.1822712	0.0536364
6110.5	0	- 0.1093998	0	0.3073985	0.1629005	0.0500754
6111	0	- 0.1093998	0	0.3469442	0.130089	0.0451336
6111.5	0.0488433	- 0.1093998	-999.25	-999.25	-999.25	-999.25
6112	0	- 0.1171999	-999.25	-999.25	-999.25	-999.25
6112.5	0	- 0.1093998	-999.25	-999.25	-999.25	-999.25
6113	0	- 0.1093998	-999.25	-999.25	-999.25	-999.25
6113.5	0	- 0.1093998	-999.25	-999.25	-999.25	-999.25
6114	0	- 0.1093998	-999.25	-999.25	-999.25	-999.25
6114.5	0	- 0.1093998	-999.25	-999.25	-999.25	-999.25
6115	0	- 0.1015997	-999.25	-999.25	-999.25	-999.25
6115.5	0	- 0.1015997	-999.25	-999.25	-999.25	-999.25
6116	0	- 0.1015997	-999.25	-999.25	-999.25	-999.25
6116.5	0	- 0.1015997	-999.25	-999.25	-999.25	-999.25
6117	0	- 0.1015997	-999.25	-999.25	-999.25	-999.25
6117.5	0.0042373	- 0.1171999	-999.25	-999.25	-999.25	-999.25
6118	0.0461493	- 0.1718998	-999.25	-999.25	-999.25	-999.25
6118.5	0	-	0.0184969	0.2770142	0.1897635	0.0525672

Appendix A – log database

		0.1640997				
6119	0	- 0.1484003	0.0353487	0.2241243	0.2485036	0.0556957
6119.5	0	- 0.1640997	0.0090414	0.2248154	0.2642469	0.0594068
6120	0	- 0.1640997	0.0136892	0.2317656	0.2722194	0.0630911
6120.5	0	- 0.1484003	0.0161912	0.2383905	0.2725106	0.0649639
6121	0	- 0.1328001	0.0104774	0.2407728	0.2630613	0.063338
6121.5	0	- 0.0859003	0.0254564	0.2293411	0.2668345	0.0611961
6122	0	- 0.0859003	0.028125	0.2210448	0.2757556	0.0609543
6122.5	0	- 0.0859003	0.0325319	0.219602	0.2839826	0.0623632
6123	0	- 0.0468998	0.0096499	0.2542769	0.2549564	0.0648295
6123.5	0	- 0.0703001	0	0.2898687	0.2304062	0.0667875
6124	0	- 0.0234003	0.0043025	0.2977792	0.2275378	0.067756
6124.5	0	- 0.0703001	0.0323785	0.2722433	0.2556138	0.0695891
6125	0	- 0.0703001	0.0218065	0.2703057	0.2607941	0.0704941
6125.5	0	0.0234003	0.0152549	0.2758999	0.2542425	0.0701455
6126	0	- 0.0781002	0.0186583	0.2722123	0.2564411	0.0698064
6126.5	0	- 0.0859003	0.018961	0.2698699	0.2567437	0.0692874
6127	0	- 0.0390997	0.022759	0.2718138	0.2510863	0.0682487
6127.5	0	- 0.0390997	0.0084342	0.2948835	0.2273396	0.0670387
6128	0	- 0.0234003	0	0.3098792	0.2078742	0.0644159
6128.5	0	- 0.0234003	0	0.3307101	0.1884932	0.0623366
6129	0	- 0.0390997	0	0.3806634	0.1650651	0.0628342
6129.5	0	- 0.0468998	0	0.4415602	0.1484649	0.0655562
6130	0	- 0.0859003	0	0.4676771	0.1460558	0.068307
6130.5	0	- 0.1015997	0.0084763	0.3740006	0.1896186	0.0709175
6131	0	-	0.0441103	0.2988629	0.2410617	0.0720444

Appendix A – log database

		0.1015997				
6131.5	0	- 0.1015997	0.0595223	0.2638071	0.2740167	0.0722876
6132	0	- 0.0859003	0.0440866	0.2640103	0.2778063	0.0733437
6132.5	0	- 0.0546999	0.0217243	0.2883484	0.2582957	0.0744791
6133	0	0.0078001	0.0235627	0.308199	0.2424681	0.0747284
6133.5	0	0.0078001	0.0174676	0.3497493	0.2129788	0.0744892
6134	0	0.0078001	0.0048048	0.3880153	0.187725	0.0728402
6134.5	0	0.0078001	0.0061867	0.4261002	0.1671867	0.0712383
6135	0	0.0078001	0	0.4429802	0.1625283	0.0719968
6135.5	0	0.0078001	0	0.4442544	0.1685939	0.0748986
6136	0	- 0.0078001	0	0.4704068	0.167402	0.078747
6136.5	0	- 0.0390997	0	0.4914678	0.169369	0.0832394
6137	0	- 0.0468998	0	0.4627152	0.1905013	0.0881479
6137.5	0	- 0.0703001	0.005048	0.4447732	0.2095413	0.0931983
6138	0	- 0.0859003	0.0244868	0.3995853	0.2477221	0.0989861
6138.5	0	- 0.0859003	0.0242549	0.4009372	0.2608264	0.104575
6139	0	- 0.0781002	0.0356164	0.3941126	0.2769945	0.109167
6139.5	0	- 0.1015997	0.0183765	0.4238058	0.2660071	0.1127354
6140	0	- 0.0781002	0.0058585	0.4484219	0.2561701	0.1148723
6140.5	0	- 0.0703001	0	0.4637811	0.2491599	0.1155557
6141	0	- 0.0703001	0	0.4643765	0.2491791	0.1157129
6141.5	0	- 0.0703001	0	0.4522489	0.2540928	0.1149132
6142	0	- 0.0781002	0.005279	0.426331	0.2627066	0.112
6142.5	0	- 0.0703001	0.0010173	0.3973074	0.2678173	0.1064058
6143	0	- 0.0234003	0.0198497	0.3534349	0.2830934	0.1000551
6143.5	0	- 0.0390997	0.0388566	0.3076642	0.3056566	0.0940396
6144	0	- 0.0390997	0.042197	0.28199	0.3131871	0.0883156
6144.5	0	-	0.0508621	0.256368	0.3187174	0.081709

Appendix A – log database

		0.0234003				
6145	0	- 0.0156002	0.0181917	0.2623112	0.2814354	0.0738237
6145.5	0	0.0078001	0	0.3091997	0.2096923	0.0648368
6146	0.0954206	0.0078001	0	0.7933849	0.0530994	0.0421283
6146.5	0	0.0078001	-999.25	-999.25	-999.25	-999.25
6147	0	0.0078001	-999.25	-999.25	-999.25	-999.25
6147.5	0	- 0.0156002	-999.25	-999.25	-999.25	-999.25
6148	0	- 0.0156002	-999.25	-999.25	-999.25	-999.25
6148.5	0	- 0.0234003	-999.25	-999.25	-999.25	-999.25
6149	0	- 0.0234003	-999.25	-999.25	-999.25	-999.25
6149.5	0	- 0.0234003	-999.25	-999.25	-999.25	-999.25
6150	0.054814	- 0.0546999	-999.25	-999.25	-999.25	-999.25
6150.5	0	- 0.0703001	0	0.5874298	0.1158345	0.0680447
6151	0	- 0.0703001	0.0178732	0.4234655	0.1769371	0.0749268
6151.5	0	- 0.1015997	0.0145906	0.4049008	0.202276	0.0819017
6152	0	- 0.0859003	0.0127408	0.4239601	0.208252	0.0882906
6152.5	0	- 0.1015997	0.0120502	0.4574682	0.2061127	0.09429
6153	0	- 0.0781002	0.010114	0.4755031	0.2084974	0.0991411
6153.5	0	- 0.0546999	0.0226782	0.4833201	0.2135721	0.1032237
6154	0	- 0.0546999	0.0139563	0.5388749	0.2001468	0.1078541
6154.5	0	- 0.0781002	0	0.5907487	0.1910145	0.1128416
6155	0	- 0.0781002	0.0045272	0.5481356	0.2163351	0.118581
6155.5	0	- 0.0781002	0.0036378	0.5205026	0.238584	0.1241836
6156	0	- 0.1015997	0.0130014	0.5448524	0.2332142	0.1270673
6156.5	0	- 0.1171999	0	0.6434317	0.1973609	0.1269883
6157	0	- 0.1328001	0	0.6755209	0.184423	0.1245816
6157.5	0	- 0.1406002	0	0.5962811	0.2035628	0.1213806

Appendix A – log database

6158	0	- 0.1640997	0.0155285	0.4597355	0.2569065	0.1181091
6158.5	0	- 0.1953001	0.0249473	0.4028551	0.2823749	0.1137562
6159	0	- 0.2109003	0.0311978	0.3806267	0.2826485	0.1075836
6159.5	0	- 0.1640997	0.0078233	0.4330144	0.232342	0.1006075
6160	0	- 0.1640997	0	0.5421529	0.1734703	0.0940474
6160.5	0	- 0.1718998	0	0.6601809	0.1352818	0.0893104
6161	0	- 0.2109003	0	0.6582586	0.1315662	0.0866046
6161.5	0	- 0.2109003	0	0.498301	0.1720954	0.0857553
6162	0	- 0.2109003	0.007648	0.4249521	0.2031592	0.0863329
6162.5	0	- 0.2265997	0.0177126	0.3937609	0.2208095	0.0869461
6163	0	- 0.2343998	0.0012273	0.4319757	0.2010342	0.0868419
6163.5	0	- 0.2343998	0	0.5185568	0.1662708	0.0862208
6164	0	- 0.2031002	0	0.6462024	0.1318531	0.0852038
6164.5	0	- 0.2031002	0	0.8196207	0.1027579	0.0842225
6165	0	- 0.2031002	0	0.8271802	0.100457	0.083096
6165.5	0	- 0.2031002	0	0.8173659	0.1003188	0.0819971
6166	0	- 0.1953001	0	0.8993421	0.0906841	0.0815561
6166.5	0	- 0.2031002	0	1	0.0691301	0.0691301
6167	0.0064736	- 0.2031002	0	1	0.0438924	0.0438924
6167.5	0	- 0.1953001	0	1	0.0469772	0.0469772
6168	0	- 0.2031002	0	1	0.0586011	0.0586011
6168.5	0	- 0.2031002	0	1	0.0833698	0.0833698
6169	0.1052563	- 0.1953001	0	1	0.0544785	0.0544785
6169.5	0.1307107	- 0.1953001	0	1	0.0525206	0.0525206
6170	0.1028306	-	0	1	0.0577344	0.0577344

Appendix A – log database

		0.1953001				
6170.5	0.0098909	- 0.1328001	0	1	0.0991606	0.0991606
6171	0	- 0.0468998	0	0.8761892	0.1275232	0.1117344
6171.5	0	- 0.1640997	0.0037967	0.7726787	0.1521002	0.1175246
6172	0	- 0.1796999	0.0044727	0.7721142	0.1582109	0.1221569
6172.5	0	- 0.1796999	0.0016786	0.796487	0.1571102	0.1251362
6173	0	- 0.1796999	0.001437	0.7968939	0.1588303	0.1265709
6173.5	0	- 0.1796999	0	0.8209677	0.153434	0.1259643
6174	0	- 0.1953001	0	0.8361529	0.1479827	0.1237361
6174.5	0	- 0.1953001	0	0.825834	0.1461577	0.120702
6175	0	- 0.2343998	0.003707	0.684243	0.171506	0.1173518
6175.5	0	- 0.2343998	0.0150679	0.5606272	0.2042395	0.1145022
6176	0	- 0.2109003	0.0217796	0.4992302	0.2248765	0.1122651
6176.5	0	- 0.1796999	0.0200052	0.4873454	0.225887	0.110085
6177	0	- 0.1953001	0.008289	0.4963964	0.2200969	0.1092553
6177.5	0	- 0.1640997	0.0143877	0.5197031	0.2113391	0.1098336
6178	0	- 0.1718998	0.0247786	0.5415508	0.2043866	0.1106857
6178.5	0	- 0.1718998	0.01151	0.574307	0.1926523	0.1106415
6179	0	- 0.1718998	0.0073457	0.5326146	0.2042971	0.1088116
6179.5	0	- 0.1796999	0.0139591	0.5000296	0.2094702	0.1047413
6180	0	- 0.1640997	0	0.5277427	0.1870727	0.0987262
6180.5	0	- 0.1640997	0	0.6079348	0.1500406	0.0912149
6181	0	- 0.2421999	0	0.6087176	0.1358094	0.0826696
6181.5	0	- 0.2578001	0.0350881	0.388593	0.1905197	0.0740346
6182	0	- 0.2265997	0.0543368	0.2916989	0.2290244	0.0668062

Appendix A – log database

6182.5	0	- 0.2265997	0.0463171	0.218811	0.2403796	0.0525977
6183	0	- 0.2343998	0.0055194	0.223194	0.2173274	0.0485062
6183.5	0	- 0.2031002	0	0.2135826	0.2142799	0.0457665
6184	0	- 0.2734003	0.0279342	0.1882504	0.233816	0.044016
6184.5	0	- 0.2656002	0.0491524	0.1671762	0.2582434	0.0431722
6185	0	- 0.2656002	0.0849272	0.1490449	0.2866195	0.0427192
6185.5	0	- 0.2578001	0.0902639	0.1431189	0.2947572	0.0421853
6186	0	- 0.2109003	0.0521686	0.1505955	0.2766874	0.0416679
6186.5	0	- 0.2109003	0.0309116	0.1721019	0.2400025	0.0413049
6187	0	- 0.1718998	0.0359564	0.1859839	0.2203911	0.0409892
6187.5	0	- 0.1953001	0.0768949	0.1666374	0.2481615	0.041353
6188	0	- 0.2421999	0.0974246	0.1604858	0.2584246	0.0414735
6188.5	0	- 0.2421999	0.0900761	0.1543201	0.2696842	0.0416177
6189	0	- 0.2343998	0.0478959	0.1619377	0.2551583	0.0413197
6189.5	0	- 0.1640997	0.0446459	0.1517731	0.2717106	0.0412384
6190	0	- 0.1015997	0.0442745	0.1430192	0.2832621	0.0405119
6190.5	0	- 0.0546999	0.0377748	0.1422927	0.2779608	0.0395518
6191	0	- 0.0234003	0.0176502	0.1463146	0.2617854	0.038303
6191.5	0	- 0.1484003	0.0085286	0.1466019	0.2576953	0.0377786
6192	0	- 0.1953001	0.0315447	0.1504428	0.25478	0.0383298
6192.5	0	- 0.1718998	0.0318996	0.1646234	0.2437076	0.04012
6193	0	- 0.1015997	0	0.1997001	0.211217	0.0421801
6193.5	0	- 0.1093998	0	0.2201025	0.2022192	0.0445089
6194	0	- 0.1640997	0.0926481	0.2021551	0.2315461	0.0468082
6194.5	0	-	0.0643411	0.1954937	0.2472614	0.048338

Appendix A – log database

		0.2343998				
6195	0	- 0.2734003	0.0679593	0.1885101	0.2620218	0.0493937
6195.5	0	- 0.2734003	0.0411698	0.199964	0.2484321	0.0496775
6196	0	- 0.2734003	0.0528281	0.193807	0.2587099	0.0501398
6196.5	0	- 0.2343998	0.0382907	0.1904911	0.2628095	0.0500629
6197	0	- 0.2109003	0.0239222	0.1862893	0.2629098	0.0489773
6197.5	0	- 0.1953001	0.0175619	0.1857113	0.2512816	0.0466658
6198	0	- 0.1718998	0.0398255	0.1843418	0.2415178	0.0445218
6198.5	0	- 0.1640997	0.043934	0.1859907	0.2316194	0.0430791
6199	0	- 0.1718998	0.0400813	0.1866897	0.2309753	0.0431207
6199.5	0	- 0.1484003	0.0581276	0.1892815	0.2343791	0.0443636
6200	0	- 0.1640997	0.0456563	0.1865745	0.2426077	0.0452644
6200.5	0	- 0.2109003	0.0547235	0.187631	0.242409	0.0454834
6201	0	- 0.2890997	0.0566688	0.1811022	0.2564758	0.0464483
6201.5	0	- 0.2734003	0.0532142	0.1795292	0.2636674	0.047336
6202	0	- 0.2578001	0.0538459	0.180699	0.2642992	0.0477586
6202.5	0	- 0.2578001	0.0279686	0.2012042	0.235231	0.0473295
6203	0	- 0.1718998	0.0476566	0.1989228	0.2338471	0.0465175
6203.5	0	- 0.1640997	0.0594386	0.1850383	0.2438732	0.0451259
6204	0	- 0.1171999	0.0707734	0.1751665	0.2488379	0.0435881
6204.5	0	- 0.0859003	0.0326582	0.1951395	0.2122663	0.0414215
6205	0	0.0390997	0	0.2467009	0.1578232	0.0389351
6205.5	0	0.1093998	0	0.3262888	0.1150018	0.0375238
6206	0	- 0.0156002	0	0.3376745	0.1116489	0.037701
6206.5	0	- 0.1406002	0	0.2945796	0.1345511	0.039636
6207	0	- 0.0781002	0.029772	0.2808745	0.148844	0.0418065

Appendix A – log database

6207.5	0	- 0.1093998	0.0044307	0.2724724	0.1598623	0.0435581
6208	0	0.0078001	0	0.2655976	0.1711835	0.0454659
6208.5	0	- 0.1640997	0.0384707	0.2357984	0.2046539	0.0482571
6209	0	- 0.2578001	0.0777251	0.2166928	0.236789	0.0513105
6209.5	0	- 0.2031002	0.1055391	0.2182034	0.2500611	0.0545642
6210	0	- 0.2265997	0.0897975	0.2173211	0.2644851	0.0574782
6210.5	0	- 0.0859003	0.0536101	0.2279641	0.2594919	0.0591548
6211	0	- 0.0859003	0	0.2374456	0.2551263	0.0605786
6211.5	0	- 0.1953001	0	0.2525681	0.2442561	0.0616913
6212	0	- 0.1796999	0	0.2665523	0.2336095	0.0622691
6212.5	0	- 0.1640997	0	0.269324	0.2344723	0.063149
6213	0	- 0.1484003	0.0137393	0.2732155	0.2369746	0.0647451
6213.5	0	- 0.1406002	0.0483051	0.2726261	0.2466885	0.0672537
6214	0	- 0.1093998	0.0342438	0.2940177	0.2415061	0.0710071
6214.5	0	- 0.0859003	0.037089	0.3578186	0.2117766	0.0757776
6215	0	- 0.0859003	0.0004913	0.4743014	0.1717579	0.081465
6215.5	0	- 0.1171999	0.0133398	0.7411395	0.144352	0.106985
6216	0	- 0.1015997	0.0237846	0.7689655	0.1529448	0.1176093
6216.5	0	- 0.0703001	0.0244701	0.7578407	0.1689921	0.1280691
6217	0	- 0.0703001	0.039248	0.6888666	0.200248	0.1379441
6217.5	0	- 0.0546999	0.002643	0.7188511	0.2043354	0.1468867
6218	0	- 0.0781002	0.0183557	0.7265254	0.2124182	0.1543272
6218.5	0	- 0.0781002	0.0223575	0.7449696	0.2147187	0.1599589
6219	0	- 0.0703001	0.0373161	0.7018067	0.2328273	0.1633998
6219.5	0	- 0.0703001	0.0476357	0.6621717	0.2493281	0.165098

Appendix A – log database

6220	0	- 0.0781002	0.0376034	0.6429208	0.2565088	0.1649148
6220.5	0	- 0.0234003	0.0280106	0.6566117	0.2482234	0.1629864
6221	0	- 0.0156002	0.0160581	0.6761873	0.2362708	0.1597633
6221.5	0	0.0390997	0.0172749	0.6633824	0.2348655	0.1558057
6222	0	0.0234003	0.0209651	0.6552843	0.2314183	0.1516448
6222.5	0	0.0234003	0.0264916	0.6336915	0.2337539	0.1481279
6223	0	0.1015997	0.0012988	0.7201874	0.2029911	0.1461916
6223.5	0	0.1015997	0	0.876049	0.1668401	0.1461601
6224	0	0.0703001	0	1	0.1332134	0.1332134
6224.5	0	0.0156002	0	1	0.1390805	0.1390805
6225	0	0.0703001	0.0295544	0.8099816	0.1905544	0.1543456
6225.5	0	0.0859003	0.0477585	0.7305475	0.2190251	0.1600083
6226	0	0.1171999	0.0397038	0.719592	0.232065	0.1669921
6226.5	0	0.1640997	0.0193993	0.7626511	0.2284902	0.1742583
6227	0	0.1640997	0.0221212	0.7767814	0.2325744	0.1806595
6227.5	0	0.1640997	0.0336899	0.7481671	0.2481843	0.1856833
6228	0	0.1640997	0.0261066	0.7675143	0.2463193	0.1890536
6228.5	0	0.1718998	0.0272643	0.7686093	0.2487772	0.1912125
6229	0	0.1718998	0.0164417	0.8132511	0.2366545	0.1924595
6229.5	0	0.1484003	0.0121664	0.8246357	0.2336793	0.1927003
6230	0	0.1640997	0.0081726	0.8395271	0.2283853	0.1917357
6230.5	0	0.1640997	0.0051719	0.8460478	0.2240773	0.1895801
6231	0	0.1406002	0.0073268	0.8113745	0.230562	0.1870722
6231.5	0	0.0859003	0.0216643	0.7599825	0.2431773	0.1848105
6232	0	0.0234003	0.0298456	0.717773	0.2543643	0.1825759
6232.5	0	- 0.0703001	0.0274647	0.7145705	0.2519835	0.1800599
6233	0	- 0.0156002	0.0305203	0.68354	0.2588476	0.1769327
6233.5	0	0.0546999	0.0384405	0.6494489	0.2667678	0.173252
6234	0	0.0546999	0.0332499	0.6490434	0.2615772	0.1697749
6234.5	0	0.0546999	0.018488	0.6890195	0.2417233	0.166552
6235	0	0.0390997	0.0089617	0.738155	0.2207696	0.1629622
6235.5	0	- 0.0234003	0.0156557	0.7283148	0.217348	0.1582977
6236	0	- 0.2265997	0.035007	0.651489	0.2333903	0.1520512
6236.5	0	- 0.1718998	0.0367853	0.5912303	0.2440477	0.1442884
6237	0	- 0.1171999	0.0423061	0.526364	0.2585748	0.1361045
6237.5	0	- 0.0546999	0.0201285	0.5290079	0.2433638	0.1287414

Appendix A – log database

6238	0	- 0.0468998	0.0041877	0.5636131	0.2173426	0.1224972
6238.5	0	- 0.0546999	0	0.6728565	0.173988	0.1170689
6239	0	- 0.0546999	0	0.7777181	0.1448427	0.1126468
6239.5	0	- 0.0703001	0	0.8782665	0.1245681	0.109404
6240	0	- 0.0703001	0	0.9258562	0.115656	0.1070808
6240.5	0	- 0.0859003	0	0.9365853	0.1132109	0.1060317
6241	0	- 0.1093998	0	0.8204663	0.1295889	0.1063233
6241.5	0	- 0.1093998	0	0.7287934	0.1469863	0.1071227
6242	0	- 0.1328001	0	0.6970303	0.1541129	0.1074214
6242.5	0	- 0.1328001	0	0.6780725	0.1568611	0.1063632
6243	0	- 0.1406002	0	0.6409579	0.1624214	0.1041053
6243.5	0	- 0.1484003	0	0.6194487	0.1632425	0.1011204
6244	0	- 0.1484003	0	0.6612375	0.1490962	0.098588
6244.5	0	- 0.1406002	0	0.7672107	0.1261589	0.0967905
6245	0	0.0390997	0	0.8872703	0.1076844	0.0955451
6245.5	0	0.2421999	0.0076959	0.9550655	0.098828	0.0943872
6246	0	0.0390997	0	0.9580295	0.0980057	0.0938923
6246.5	0	0.0234003	0.0149756	0.8586796	0.1103152	0.0947254
6247	0	- 0.0078001	0.0083599	0.8039609	0.121269	0.0974955
6247.5	0	- 0.0703001	0.0036731	0.7756594	0.1306576	0.1013458
6248	0	- 0.0781002	0	0.7339401	0.1436057	0.105398
6248.5	0	- 0.0468998	0.0107786	0.5609708	0.1608101	0.0902098
6249	0	- 0.1093998	0.0381805	0.4948123	0.1882119	0.0931296
6249.5	0	- 0.2578001	0.0582702	0.4510771	0.2103041	0.0948634
6250	0	- 0.1328001	0.0681072	0.4320485	0.2201411	0.0951116
6250.5	0	- 0.0859003	0.0566116	0.4473264	0.2086455	0.0933327
6251	0	0.1484003	0.0154958	0.5314689	0.1692339	0.0899426

Appendix A – log database

6251.5	0	0.2734003	0	0.6452981	0.1342595	0.0866374
6252	0	0.0781002	0	0.7645888	0.1090557	0.0833827
6252.5	0	- 0.0781002	0	0.7343152	0.1111108	0.0815883
6253	0	- 0.0781002	0	0.7086852	0.1128229	0.0799559
6253.5	0	- 0.1484003	0	0.6324506	0.1245597	0.0787778
6254	0	- 0.0390997	0	0.6084201	0.1270821	0.0773193
6254.5	0	- 0.1171999	0	0.590976	0.1293034	0.0764152
6255	0	- 0.0781002	0	0.6165873	0.1210684	0.0746492
6255.5	0	- 0.1406002	0	0.5858445	0.1251234	0.0733029
6256	0	- 0.1953001	0.0015419	0.5447081	0.1325541	0.0722033
6256.5	0	- 0.0703001	0.0120152	0.4984659	0.1430274	0.0712943
6257	0.1170238	- 0.1484003	0	0.5144781	0.1156806	0.0595152
6257.5	0.1170238	- 0.0468998	0	0.5169575	0.1156806	0.059802
6258	0.1170238	0.0234003	0	0.5155566	0.1156806	0.0596399
6258.5	0	- 0.2031002	0	0.8428198	0.1010358	0.085155
6259	0	- 0.2109003	0	0.9001377	0.0926766	0.0834217
6259.5	0	- 0.2109003	0	1	0.0760564	0.0760564
6260	0	- 0.2109003	0	1	0.0629703	0.0629703
6260.5	0	- 0.1796999	0	1	0.0587625	0.0587625
6261	0	- 0.1484003	0	1	0.0704141	0.0704141
6261.5	0	- 0.1328001	0	0.8859468	0.0928447	0.0822555
6262	0	- 0.0859003	0	0.7169806	0.1095815	0.0785678
6262.5	0	- 0.0859003	0	0.6766087	0.109772	0.0742727
6263	0	- 0.0859003	0	0.6503464	0.1116329	0.0726
6263.5	0	- 0.1015997	0	0.6724007	0.1071537	0.0720502
6264	0	- 0.1171999	0	0.7008279	0.1015127	0.0711429

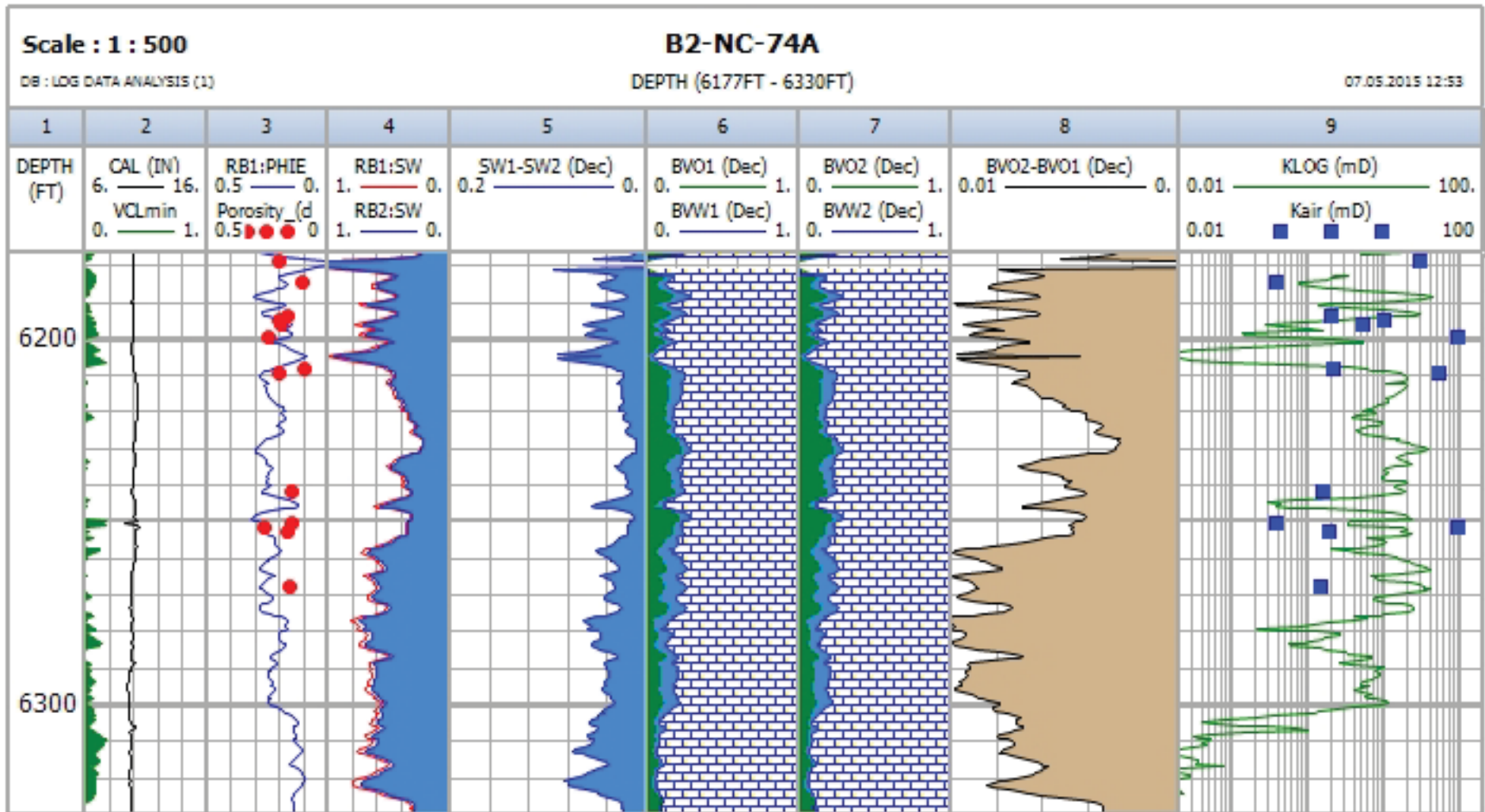


Figure 7.1 Log plot Well B2-NC-74A

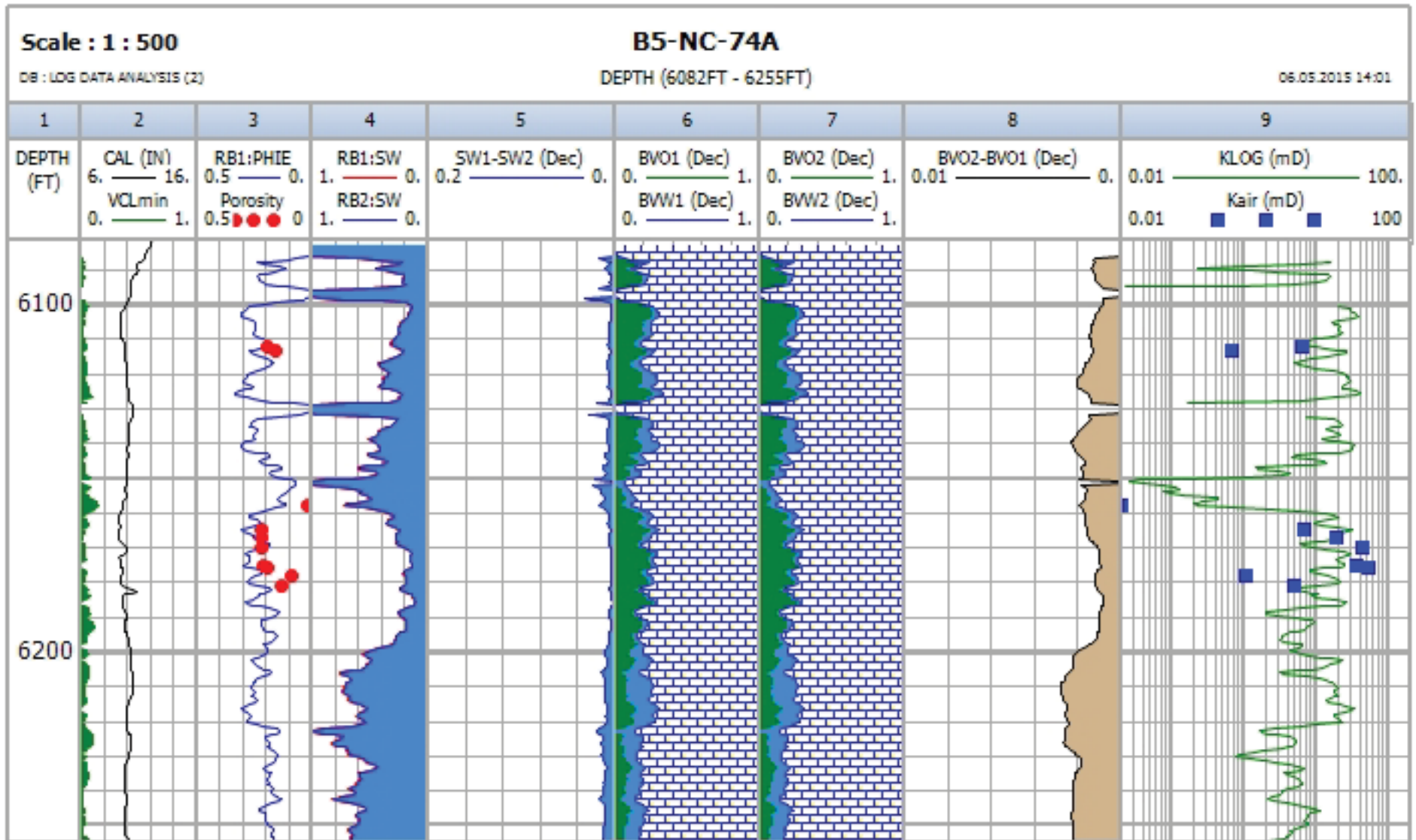


Figure 7.2 Log plot Well B5-NC-74A

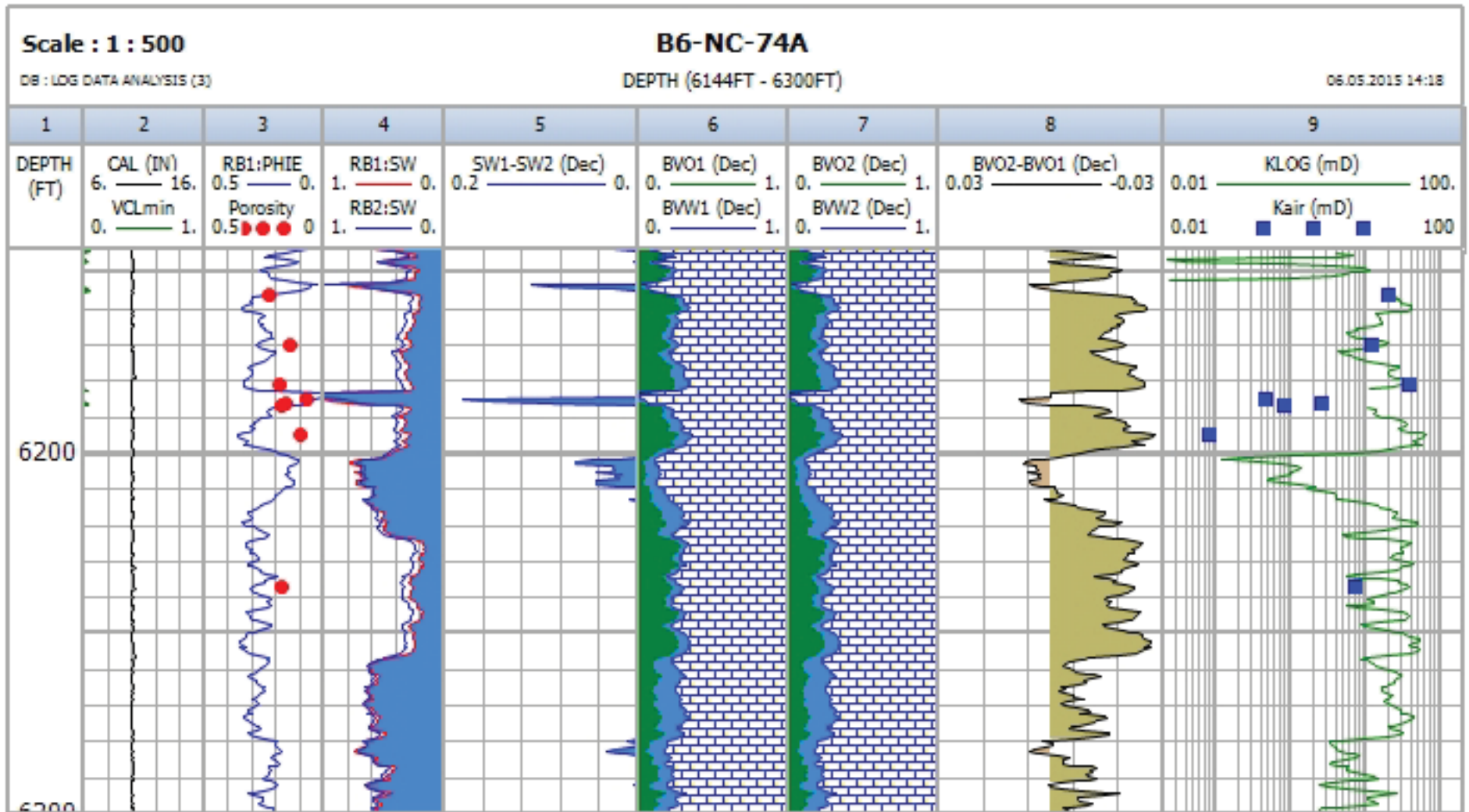


Figure 7.3 Log plot Well B6-NC-74A

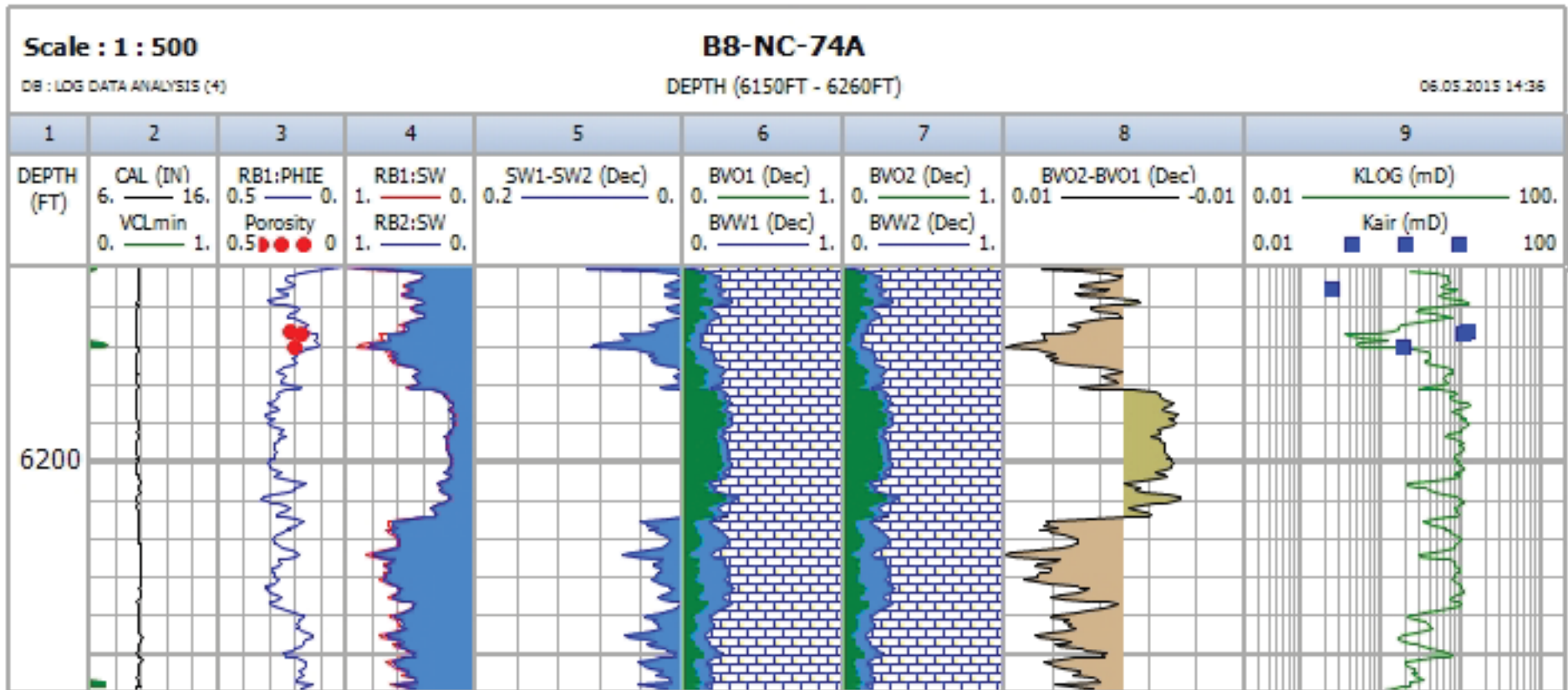


Figure 7.4 Log plot Well B8-NC-74A